Release of organic compounds from polyethylene pipes to drinking water

Laurent Coron

Technical University of Denmark

Release of organic compounds from polyethylene pipes to drinking water

Master Thesis by Laurent Coron

July 2008

DTU Environment

Department of Environmental Engineering

Preface

The present Master Thesis project has been carried out at the Department of Environmental Engineering at the Technical University of Denmark. The study was made from February to July 2008 under the supervision of Erik Arvin and Ph.D. student Martin Denberg. It accounts for a total of 30 ECTS credits.

From a personal point of view, I found this study appealing because the contamination investigated in this project is not usual, since it is not caused by the contamination of the source but by the way of distributing the water. Besides, this pollution risk has not been widely recognized yet, while the use of PE pipes (source of the problem) is becoming a standard practice nowadays. Therefore, there is a real need for a general impact assessment of PE pipes use for drinking water distribution. Although the project lasts only 5 months, I see it as a first step in this impact assessment, centred on the quantification of the contamination.

I would like to thank my supervisors Erik Arvin and Martin Denberg for their help and support along this project, as well as the employees from the Farum Waterworks and Margrethe Sørensen for their help during the collection of samples. I also would like to thank my girlfriend Laura for her support along these five months of project and my friends for taking the time of reading and correcting the present report.

_____

Laurent CORON
s060680

Abstract

Polyethylene (PE) pipes are becoming nowadays a standard way to transport and distribute drinking water. However, the use of PE pipes in distribution networks and household installations causes a contamination of the drinking water. A modelling work of this contamination in distribution networks was conducted using EPANET. Since the original version of the program was not able to model properly the release of compounds from the pipe material to the water, EPANET source code was modified and a new version was developed, which could compute the concentration in the water of these migrants released from the pipe material. Three network case studies were investigated using this modelling tool: a small network under construction (400 consumers), a middle-sized network with simple geometry (30,000 consumers) and a large network with complex geometry (370,000 consumers). The study focuses on the release from the pipe of the antioxidants Irganox 1010 and Irgafos 168, which have a saturation concentration in the water of about 310 μg/L. Two diffusion coefficients in the water of the compounds released ($D_{w,i}$) were modelled: 10^{-10} and 10^{-9} m^2/s. The simulations showed that the transport distance of the water in the network is a key parameter governing the degree of contamination. Profiles of migrant concentration increasing from the closest to the furthest locations from the source(s) were particularly observed for the middle-sized and the large network cases. Saturation levels in migrant were computed to reach 50% when $D_{w,i} = 10^{-10}$ m^2/s and up to almost 100% when $D_{w,i} = 10^{-9}$ m^2/s in the areas the furthest from the source(s). The residence time of the water in the network was not found to be a major reason for contamination, except in cases with significantly over-dimensioned pipes (e.g. network under construction). The modelling work also showed that the existence of elevated tank(s) in a network affect the variations of the contamination level along the day. Different half-lives of the migrants were investigated but no clear conclusion was made because of the high uncertainties on the actual degradation rate of these migrants. Finally, no validation of the model with field measurements was possible during the study work, although it was tried based on Non Volatile Organic Carbon measurements.

Key words: antioxidants, diffusion, drinking water, EPANET, polyethylene (PE) pipes

Table of contents

List of figures and tables

List of figures

List of tables

Chapter 1.
Introduction

1.1. Project background

Polyethylene (PE) pipes are becoming nowadays a standard way to transport drinking water. However, the use of PE pipes in distribution networks and household installations causes a contamination of drinking water. The polymer materials contain indeed a range of organic and inorganic additives, some of which have been found to migrate to water. Several papers have already been published regarding the diffusion of compounds from PE pipes. However there has been apparently only little research yet on the use of programs meant to model distribution systems to compute this diffusion. That is why this project was initiated. Hopefully, the theory on the migration of the compounds can be combined with the transport models that exist in the distribution modelling programs. Thus it would enable us to estimate the migrant concentration at the consumers' taps, taking into account the dynamic of real world piping systems.

1.2. Problem formulation

The main objective of this project is to model the release of compounds from PE pipes to drinking water inside distribution systems. A very first question can thus be raised: Can this modelling be done at all with a program for distribution systems, without inducing advanced modifications of the program code? The answer being hopefully positive, the migration of species from PE pipes into drinking water will be investigated in this project for different network models. Various simulations should enable us to answer the following questions about this contamination problem: What level of migrants released from PE pipes can be expected in the drinking water of typical distribution networks? Does this level vary

significantly depending on the network characteristics (size, geometry, flow regime conditions, water residence time…)? Is this level strongly governed by the characteristics of the migrants themselves (concentration inside the pipe material, partition coefficient at the interface, diffusion coefficient in the water…)? Besides, among the simulations made along the project, a study should be done on a real network, where modelling would be coupled with a sampling work. It should enable us to see whether the release of compounds from PE pipes to the water can be detected by Non Volatile Organic Compounds (NVOC) measurements. Additionally, some processes of migrant degradation should be modelled to assess roughly whether degradation can have a relevant decreasing impact on the contamination degree of the water. Finally, the study should show if grab sampling, which is currently used, is in the end a valid approach to estimate the contamination potential of PE pipes use to distribute drinking water.

1.3. Methodology

This project aims at studying the release of compounds from PE pipes to the water in distribution networks. This will be achieved through a modelling work using EPANET. This program is meant to model the hydraulic and water quality characteristics of distribution systems. It combines tools for computation of chemical reactions in the water with a transport model of the water within the network pipes. Using EPANET is advantageous in the sense that the program is in the public domain meaning that it is free and the source code is available and can thus be modified to implement new calculation possibilities.

The water quality modules currently existing in EPANET is studied and modified if the migration of compounds cannot be modelled properly with the available tools. These modifications should be validated by comparison of the model outputs with direct computations from the migration theory. Once proper modelling has been made possible, series of simulations are carried out to answer the different questions enumerated in the project objectives. Namely, three network case studies are investigated.

The first case investigated concerns a small network under construction. It is a real distribution system located in Farum (Denmark). The area is particularly suitable for the project since this new network is entirely composed of polyethylene pipes and only supplied with water from a single source. A model of the network is built in EPANET and used to assess the amount of migrants released from the pipes' material. In parallel water samples are taken at several locations of the system to measure the NVOC and oxygen contents. Differences in these contents between the locations in the network and the waterworks outlet, may illustrate that compounds are actually released from the PE pipes and reveal whether some degradation processes are taking place in the pipes. Conclusions are then be made on

the suitability of using NVOC measurements to detect the release of compounds from PE pipes to drinking water.

The second and third cases investigated in this project are models of theoretical networks. Both of them are model-examples provided with the current version of EPANET. These network models are used for this study because they represent two different configurations of systems that can be found in reality. The first of them is of middle size and has a relatively simple geometry with one water source, one elevated tank and a dozen of pipes. The second one represents a much larger and more complex network with two water sources, three elevated tanks and more than a hundred pipes. Contrary to the case investigated in Farum, the two models studied here correspond in fact to the networks skeletons only. Indeed, only the biggest pipes are in the model, used for transportation rather than distribution of water. This should ease the computations and results handling but still give a fair picture of the quality conditions in the networks.

During the modelling work on these three cases, a particular focus is kept on the objective of determining the influence that the network characteristics may have on the contamination degree of the water. Besides, a series of simulations is made to assess if degradation of the compounds can have a relevant impact on the level of pollution. Due to the uncertainties on the half-lives of the migrants, various degradation rates will be investigated. More generally, this project leads to a good overview of the contamination potential of the use of PE pipes for distribution networks and household installations for drinking water. The aspects that are determining on the contamination level are pointed out, and suggestions are be made on points to investigate further.

1.4. Report Structure

The remaining of this report is structured as follow:

Chapter 2: Drinking water distribution systems
This chapter provides some background information on the water supply service. It starts with a description of piping distribution systems and continues with a presentation of the modelling computer programs, which are nowadays used for the design and operation of such systems.

Chapter 3: Contamination of drinking water by compounds released from PE pipes
This chapter presents a review of several papers studying the release of compounds from PE pipes into drinking water. It then gives the mathematical equations of the migration theory, which govern the release of compounds from a tubular pipe to the water it conveys.

Chapter 4: Use of EPANET to model the release of compounds from PE pipes
This chapter starts with a description of EPANET, which is the program used to model the release of compounds from PE pipes in distribution systems. It then gives details on the required modifications that were made to enable the modelling of this release. The chapter ends with the presentation of simulations on a single pipe, some of which are used to validate the modifications made on EPANET during the project.

Chapter 5: Modelling results on three network case studies
The modified version of EPANET is used to investigate the contamination induced by PE pipes use in three configurations of networks. This chapter presents the simulation results corresponding to these three cases: a small network under construction, a network of middle size and simple geometry and a large network of complex geometry. For one of the network cases, a parallel is tried between the modelling results and the NVOC contents observed in the real network. Then, the influence of degradation phenomena is roughly assessed. Finally, the chapter ends with a general discussion on the aspects governing the most the level of water contamination in distribution systems where PE pipes are used.

Chapter 6: Project conclusions
This last chapter presents the main conclusions of the thesis project, including the answers to the questions listed in the project objectives. It includes some suggestions of points to investigate further.

Chapter 2.
Drinking water distribution systems

This chapter tries to present a comprehensive overview of water distribution systems, with a focus on the engineering of the water supply service first, and then on the computer tools for the design and operation of distribution networks. This chapter seems to be a logical preliminary step before entering in the detail of the migration of compounds from PE pipes to water (Chapter 3) and studying the possibilities to model this migration (Chapter 4).

2.1. Engineering of the water supply

2.1.1. The water supply service

A water distribution system is a set of structures aiming at distributing water from one or several sources to consumers. Although this general aim is valid for all distribution systems, the means involved to achieve it may vary significantly from a network to another. From the point of view of a developed country, a distribution system is considered to work properly if it provides drinking water, with sufficient flow conditions, at any location of the system and at any time. However, ensuring such a service can be as easy in some cases as it is complex in others, because it is highly dependent on the water source(s), on the number of consumers to supply and on their geographical locations from the source(s) in terms of elevation and distance.

To illustrate that water supply can be complex, let us decompose the definition of “good water supply”, stated in the previous paragraph, into the three criteria it induces: 1) Ensuring sufficient flow conditions for all users involves requirements on pipe sizes and pressure conditions, which may become complex for large networks. 2) Supplying consumers with water at any time may also be a difficult task. For most sources it is indeed impossible to

adjust in real-time the water withdrawal and treatment on water demands that change significantly along a day. Building storage facilities of water is then crucial. 3) Supplying drinkable water can be complex as well depending on source quality and on the legal regulations that apply to define what "drinkable" stands for. For example, fulfilling today's requirements for European Union may involve a simple aeration of the water in some cases, or a succession of advanced treatments in others (e.g. clarification, filtration, pH adjustment, disinfection…).

2.1.2. Short history of material use in water distribution systems

Collecting and transporting water for human consumption is a practice that has been around for several millenniums. The water distribution technology has dramatically evolved from the first pipe networks in Crete to today's complex networks operated via computer models. This part of the report tries to gather some key elements in the history of water supply, with a focus on the material used to convey water, since it is directly related to the subject of this project.

Devices for collection and storage of water have been used for a very long time. Indeed, rock cisterns were found in Jordan and Syria dating from the fourth millennium BC and 2350 BC, respectively. Nevertheless when looking at water transport, probably the first distribution pipes for water were used by the Minoan civilization in Crete as early as 1500 BC. Tunnels conveying water from reservoirs to consumers were also found in Iran, Palestine and Greece, dating from the same period, but the techniques used by the Minoan were one technological level ahead. To supply their palaces, this civilization used a network of tubular conduits composed of aqueducts and even underground pipes in terra cotta (ceramic). They also had advanced storm drainage and sewer systems, sometimes linked to their palaces to create a system of flushing toilets not so different from those of today. (Mays et al., 2007, Salzman, 2006 and Walski et al., 2003)

It is only numerous centuries later that the famous Roman aqueducts were built. Rome's first aqueduct was built in 312 BC followed by ten others, all constructed from over approximately 550 years. Only a portion of the aqueduct system was composed of elevated stone arches, while the rest consisted of conduits below ground mostly made of pipes in stone and terra cotta, but also sometimes of wood, leather, lead, and bronze. Interestingly the construction of the aqueducts was not originally motivated by the lack of drinking water, since local wells were usually sufficient sources, but rather by social reasons, since large amounts of water were needed for bath houses. Once reaching the city, the aqueducts were thus connected to three distinct piping networks, each of them corresponding to a special use: one for the city's basins and fountains, one for private users and one for bath houses. (Roman aqueducts, 2008 and Salzman, 2006)

While water pipes were mostly made so far of ceramic or enclosed rock canals, the first cast iron pipe was used in 1455 at Dillenburg Castle (Germany). From this date, iron piping systems were gradually installed to provide European castles and palaces with water. In 1664, Louis XIV, king of France, ordered the construction of a 24-km cast iron pipe to supply the fountains of the Palace of Versailles. It constituted the longest pipeline ever constructed at this time and some portions are still in service even today. However, it is only in the 18th century that distribution systems for main cities started to really develop. The early pumps were horses driven or using river current, later replaced by steam driven pumps. This period is also marked by significant advancements in hydraulic, with scientists such as Bernoulli, St. Venant, Darcy and others. (Walski et al., 2003)

Over the 19th and 20th centuries, the already existing municipal networks were progressively extended while new networks were built for smaller towns. At the same time, the materials used to transport drinking water were improved. From the 1920s, cement lining was introduced for iron pipes to minimize corrosion and tuberculation. The technology of metal pipes greatly evolved from the early cast iron pipes to ductile iron pipes and then to today's pipes in galvanized steel or other alloys. In the second half of the 20th century, plastic was introduced as a material for drinking water pipes. Polyvinyl chloride (PVC) pipes were used from the 1960s followed a few years later by the first polyethylene (PE) pipes. (Walski et al., 2003)

In the recent years the main advances in water supply technology were actually made in the management of distribution systems and on the treatment capacities. The accumulated knowledge in hydraulic has permit a better design of network structures and the development of today's computer tools for the modelling of piping systems. At the same time, combined progresses in domains ranging from chemistry to membrane manufacturing enabled today's extreme treatment capacities of water, with for example the latest desalinization technologies.

2.2. Computer models for water distribution systems

2.2.1. General definition

Computer programs for modelling are broadly used in all engineering domains. However, their role may be perceived differently depending on the user. If researchers see mathematical models as help for better understanding of real-world processes, engineers would see them as an efficient calculation tool for solving equations, while managers may primarily see them as a tool for decision making (Wurbs, 1995). In the domain of water distribution systems, the current urban growth creates a constant need for municipal networks expansions. This leads to bigger and more complex networks to operate, while at the same time the legal requirements

on water quality become stricter. In addition, the distribution systems of major cities, built in the beginning of the 20th century, are now ageing and need to be renovated. Consequently, modelling tools are more needed than ever, and are used to assist the operation of drinking water networks and the planning of new facilities.

The expression “modelling programs” is broadly used in this report and its meaning should be clarified before going further. In this report, “modelling programs” stands for what Wurbs (1995) calls “generalized operational models”. It corresponds to models dealing with a range of problems and configurations, while being documented enough to be used by other than the actual developers. Such programs can be contrasted with modelling tools specifically created for one site or designed to solve one particular problem, as it may be done in some research studies.

2.2.2. Historical development of water systems modelling

Computer programs for drinking water networks first appeared in the 1960s and were, at this time, meant to assist engineers in planning and dimensioning new distribution and extraction facilities for water. The increasing computer performances over the decades permitted the development of more and more advanced modelling tools. Transport model, pressure computations, pump and valve operation are among the features progressively developed over time. The 1970s-1980s marked a change with the arrival of tools mainly oriented on water resources management and operation of existing distribution systems. Even though the sizing of new facilities remained important, water resource management and network operation have since become the main focus of modelling programs. The use of computer models dramatically increased in this period thanks to the advent of micro-computer at affordable prices. The new environmental concerns of the 1990s were logically accompanied by new modelling capabilities. Major developments in water quality modelling were indeed made in this period, while tools for network optimization and economical management were added to the existing modules concerning network operation. The recent years were strongly marked by easy and affordable communication means, namely the Internet and mobile phone networks, which permitted the development of real-time modelling. Today, water network modelling can even be combined with the powerful GIS technology (geographic information system). (Walski et al., 2003 and Wurbs, 1995)

2.2.3. Main tools existing in today’s programs

A range of programs are available nowadays for the modelling of water distribution systems. Some programs might offer more modelling possibilities or nicer interface than others, but a list of the main modules common to almost all programs can be established. This list, which is

presented below, constitutes in a way the specifications of today's programs for the modelling of water networks.

The hydraulic module is the main and most essential computation tool in any software. From the definition of water demands and a range of boundary conditions, it computes flows, velocities, headlosses and pressure conditions at all points in the network. Changes over time in supply or demand can also be included in the model to perform long term simulations. Nevertheless, the calibration of the model with real-world data is required to ensure outputs in accordance with reality. Additional packages may be combined with this module such as optimization tools for pipe sizing and pressure conditions. This hydraulic module may be a significant help for water managers since simulations can be done for the current situation but also for any hypothetical scenarios, such as new residential developments or pipe breakages.

The water quality module is the second main component of the modelling program, and works in combination with the hydraulic module. It enables the users to obtain information on the water quality, such as the water age in the pipes and storage facilities and its variation over time. Simulations of a contamination may also be run and the spread in the network tracked. Finally, chemical reactions can also be modelled in the water within the network pipes. This latter tool is primarily used to see the fate of chlorine, which decays in the network but whose concentration should be maintained high enough to ensure proper disinfection of the water.

Other modules exist to assist the economical management of the water supply. Expenses from system operation and maintenance can thus be computed and compared with receipts from the water sale. Combined with scenarios on future consumptions or network developments, these tools assist managers in their planning of investments or water pricing.

More recently, real-time network modelling has been developed. This tool requires that a range of sensors measure continuously the conditions (mainly pressure and flow) at relevant points in the network and transmit them to an operational centre. Once this tool is implemented, the computer model of the distribution system is continuously updated with real-world data, that is to say it is always calibrated. While there is a limited number of sensors, simulation outputs give in real time the conditions at all points of the network and can also forecast future conditions. Some programs even propose to generate alarms via e-mail or mobile phone in case of violations of specific constraints in the network. Consequently, operational problems are identified earlier, even sometimes before they occur, and the different correction alternatives can be tested before implementation via model simulations. In a way, real-time modelling is the ultimate tool to assist water managers in their decision making.

Chapter 3.
Contamination of drinking water by compounds released from PE pipes

This section presents the contamination problem induced by PE pipes use in distribution systems for drinking water. A presentation of the case is first made, based on several scientific papers on the subject. The theory concerning this release of compounds from tubular pipes to water constitutes the second part of this chapter. It presents the equations governing the release of compounds, which have been implemented in EPANET to compute the results presented further in Chapter 5.

3.1. Presentation of the contamination problem

Plastic pipes are becoming a standard way to transport drinking water, particularly polyethylene (PE) pipes, which are the focus of this project. PE pipes are commonly used nowadays for renovation of existing networks, or complete building of new networks. PE polymer can exist under different forms, several of which are used for pipe manufacturing: low density polyethylene (PEL), medium density polyethylene (PEM), high density polyethylene (HDPE) and cross-linked polyethylene (PEX), although mainly the two latter types are used today. PE pipes in general are available in a wide range of diameters, namely from 20 to 630 mm (Wavin, 2008). Commonly, HDPE is used for network distribution pipes while PEX is reserved for hot and cold water installations inside the households (Denberg et al., 2007).

3.1.1. Types of compounds released

Polymer materials contain a range of organic and inorganic additives, which aim usually at increasing the materials life time, easing the manufacturing process, or simply changing the

polymer's colour. Ensuring good physical properties of the pipes is essential since they should last many decades but maintaining the quality of the water transported must also be a priority. Several studies have shown that the additives contained in the polymer, or their by-product, may migrate during the pipe use, which causes a contamination of the drinking water. (Brocca et al., 2002, Denberg et al., 2007 and Skjevrak et al., 2003)

The release of compounds from PE materials has been investigated in several studies, particularly in the case of a static contact between the water and materials such as HDPE and PEX. As a consequence, it was established that a release of compounds can be observed, in the laboratory as well as in real distribution network, and that the corresponding migrants are esters, aldehydes, ketones, aromatic hydrocarbons or terpenoids (Brocca et al., 2002 and Skjevrak et al., 2003). More generally, it was found that the compounds released can be classified in three categories: additives like antioxidants, degradation products of these additives, and broken PE chains usually having a functional polar oxygen group (Denberg et al., 2007).

Throughout this study, the focus is put in particular on the compounds Irganox 1010 and Irgafos 168. These two antioxidants are broadly used as additives in the manufacturing process of PE pipes. References of the release of these two compounds from PE pipes to water are found in the literature, especially in the articles quoted in this chapter. The migration theory, which is detailed in the next section, tells us that the maximum concentration of a migrant in water flowing in a PE pipe can be computed as the product of the migrant's partition coefficient at the interface polymer/water and its concentration in the polymer matrix. For the cases of Irganox 1010 and Irgafos 168, it corresponds to a maximum concentration between 0.2 and 0.3 mg/L for drinking water exposed to PE pipes (Denberg et al., 2007). This is valid if no reaction of the antioxidant takes place in the pipe extrusion step. The molecular structures of Irganox 1010 and Irgafos 168 are presented in Figure 1 and Figure 2, respectively.

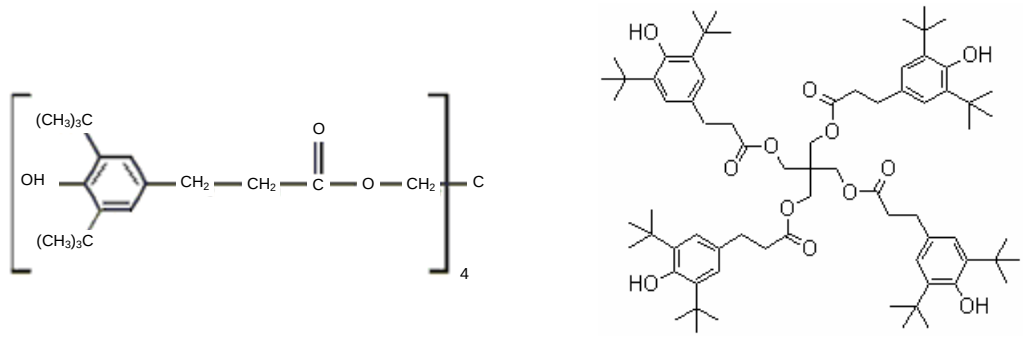

Figure 1 Molecular structure of the antioxidant Irganox 1010
From left to right, the displays are from Water Panel (2004) and ChemBlink (2008), respectively.
Compound's chemical name: Tetrakis(3-(3,5-di-tert-butyl-4-hydroxyphenyl)propionate)
Compound's CAS number: 6683-19-8

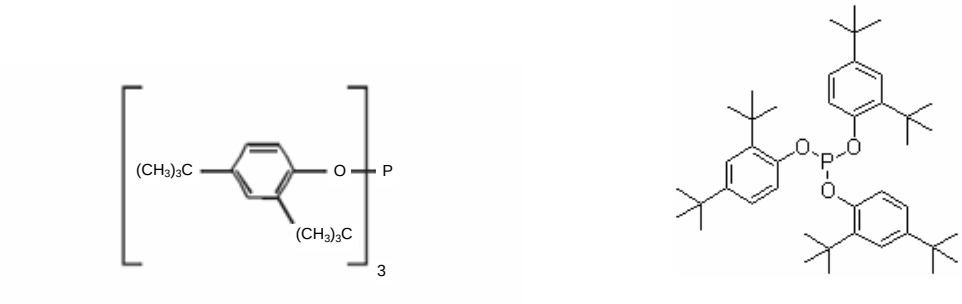

Figure 2 Molecular structure of the antioxidant Irgafos 168
From left to right, the displays are from Water Panel (2004) and ChemBlink (2008), respectively.
Compound's chemical name: Tris(2,4-ditert-butylphenyl)phosphite
Compound's CAS number: 31570-04-4

3.1.2. Particularity of the compounds' release in piping systems

This study focuses on the contamination caused by the use of polyethylene (PE) as a pipe material to transport water. The dynamic contact between the water and the PE pipe wherein it flows makes the situation complex since it induces a rate of compounds' release that is dependent on many parameters as it will be seen.

Several studies have shown that the release of compounds from plastic pipes depends on six parameters, which can be grouped in two categories: the chemical and the physical parameters. The chemical parameters are the concentration in the pipe material of the compound that migrates, its diffusion coefficient in the water and its partition coefficient at the interface between the water and the polymer. The three physical parameters are the pipe length, the pipe diameter and the flow rate of the water in the pipe. Among these, the pipe length and the flow regime (related to the flow rate) seem to be in practice the parameters governing the most the release of compounds. Variations in water velocity or pipe diameter also affect the rate of release rate, but to a lower magnitude. The reason for the length to be a determinant parameter is quite logical: if the pipe is longer, the water is more in contact with the PE during its transport, hence it receives more migrants. The dependency of the contamination on the flow regime is more complex. It is linked with the thickness of the film-layer located at the interface between the polymer and the water. With higher mixing of the water, the thickness of this film-layer decreases, which enhances the migration of compounds. Therefore, when the flow is turbulent, the release of compounds to the water is much higher that in laminar flow conditions. (Denberg et al., 2007)

As most of the physical problems, the migration of compounds from a tubular pipe into the water it conveys can be translated into mathematical equations. These equations are presented in the next section and constitute the so-called migration theory that can then be applied to any pipe, to compute the amount of compounds released in the water during its transport.

3.2. Migration theory in tubular pipes

This section presents an overview of the migration theory for compounds diffusing from a tubular pipe to the water it conveys. In order to keep this section easily readable, only the main principles and equations are presented here. More information about this migration theory can be found in the literature, particularly in the sources used to write this section: Denberg et al. (2007) and Wesselinger and Krishna (2000).

The migration theory must be expressed for a particular type of migrants. Therefore, the equations presented in this section are written for the compounds "*i*", to which corresponds the subscript "*i*".

3.2.1. Nomenclature

A	Area of inner surface of the pipe [m^2]
$c_{w,i}$	Mass concentration of compounds *i* in the water [$kg.m^{-3}$]
$c_{w,i,int}$	Mass concentration of compounds *i* at the water interface [$kg.m^{-3}$]
$c_{w,in,i}$	Mass concentration of compounds *i* in the inlet of the pipe [$kg.m^{-3}$]
$c_{w,out,i}$	Mass concentration of compounds *i* in the inlet of the pipe [$kg.m^{-3}$]
$c_{p,i}$	Mass concentration of compounds *i* in the polymer [$kg.m^{-3}$]
$c_{p,i,int}$	Mass concentration of compounds *i* at the polymer interface [$kg.m^{-3}$]
d_{inner}	Inner pipe diameter [m]
$D_{p,i}$	Diffusion coefficient of compounds *i* in the polymer [$m^2.s^{-1}$]
$D_{w,i}$	Diffusion coefficient of compounds *i* in the water [$m^2.s^{-1}$]
J_i	Mass flux of compounds *i* through the interface [$kg.m^{-2}.s^{-1}$]
k_i	Mass transfer coefficient of compounds *i* [$m.s^{-1}$]
$K_{w/p,i}$	Partition coefficient of compounds *i* at the interface between water and polymer [-]
L	Pipe length [m]
Q	Volume flow rate [$m^3.s^{-1}$]
Re	Reynolds number [-]
Sh_i	Sherwood number for compounds *i* [-]
Sc_i	Schmidt number for compounds *i* [-]
t	Time [s]
v	Flow velocity [$m.s^{-1}$]
x	Longitudinal coordinate along a pipe [m]
Δr_p	Thickness of the film-layer in the polymer [m]
Δr_w	Thickness of the film-layer in the water [m]
ρ	Density of water [$kg.m^{-3}$]
μ	Viscosity of water [$kg.m^{-1}.s^{-1}$]

3.2.2. Mass flux of species through the interface

The migration of compounds from the pipe material to the water is expressed as a flux of compounds *i* through the contact interface. When Fick's first law of diffusion is applied on each side of this interface, it gives two expressions of this flux, namely equations (1) and (2).

$$J_i = D_{w,i} \cdot \left.\frac{\partial C_{w,i}}{\partial r_w}\right|_{\text{int}} \approx \frac{D_{w,i}}{\Delta r_w}\left(c_{w,i,\text{int}} - c_{w,i}\right) \tag{1}$$

$$J_i = D_{p,i} \cdot \left.\frac{\partial C_{p,i}}{\partial r_p}\right|_{\text{int}} \approx \frac{D_{p,i}}{\Delta r_p}\left(c_{p,i} - c_{p,\text{int}}\right) \tag{2}$$

For common antioxidants migrating from PE pipes, the diffusion coefficient in the water ($D_{w,i}$) ranges typically between 10^{-10} and 10^{-9} m^2/s. The concentration of the compounds in the polymer ($c_{p,i}$) changes from one additive to another. For the compounds Irganox 1010 and Irgafos 168, investigated here, it corresponds to about 2 g/kg. (Denberg et al., 2007 and Water Panel, 2004)

If the mass transfer coefficient $k_i = D_{w,i} / \Delta r_w$ is introduced, equation (1) can be expressed as:

$$J_i = k_i \left(c_{w,i,\text{int}} - c_{w,i}\right) \tag{3}$$

Besides, every compound migrating from a media to another can be characterized by a partition coefficient at the interface between these two media. In our case of compounds release from the pipe material to the water, this coefficient ($K_{w/p,i}$) is defined according to equation (4). For antioxidants diffusing from PE pipes to water, $K_{w/p,i}$ was found to be between 10^{-5} and 10^{-3} with an average of $1.55*10^{-4}$ (Denberg et al. 2007).

$$K_{w/p,i} = \frac{c_{w,i,\text{int}}}{c_{p,i,\text{int}}} \tag{4}$$

From the combination of equations (2), (3) and (4), the equation (5) is derived:

$$J_i = \frac{k_i \cdot \frac{D_{p,i}}{\Delta r_p}\left(K_{w/p,i} \cdot c_{p,i} - c_{w,i}\right)}{\frac{D_{p,i}}{\Delta r_p} + k_i \cdot K_{w/p,i}} \tag{5}$$

It was shown that the level of mixing in the water is of importance in the migration rate of compounds released from a polymer material to water. This means that the magnitude of $k_i.K_{w/p,i}$ is usually equal to or smaller than $D_{p,i}/\Delta r_p$. For new pipes Δr_p is even extremely small and it can thus be considered that $D_{p,i}/\Delta r_p >> k_i.K_{w/p,i}$. As a consequence, equation (5) can be

simplified in equation (6), though its validity is reduced with the aging of the pipe (change in Δr_p). (Denberg et al. 2007)

$$J_i = k_i \left(K_{w/p,i} \cdot c_{p,i} - c_{w,i} \right) \tag{6}$$

The flux of compounds *i* from the pipe to the water has with equation (6) a convenient formulation. However, the mass transfer coefficient k_i is still expressed from the thickness of the film layer in the water Δr_w, which may be difficult to calculate. k_i thus needs to be expressed differently, as it can be done from the Sherwood number.

Sherwood number	Reynolds number	Schmidt number
$Sh_i = \frac{k_i \cdot d_{inner}}{D_{w,i}}$	$Re = \frac{\rho \cdot v \cdot d_{inner}}{\mu}$	$Sc_i = \frac{\mu}{\rho \cdot D_{w,i}}$

(7)

The objective being to express k_i as a function of Sh_i, the Sherwood number must be calculated. However, the experimental expressions to compute Sh_i depend greatly on the flow conditions and different versions can be found in the literature. The ones presented below seemed the most relevant for our case of compounds migrating from tubular plastic pipes to water. They are from Denberg et al. (2007), and are very similar to what can be found in Bird et al., (2007) and Wesselinger and Krishna (2000).

Stagnant flow	$Sh_{loc,i} = 2$	(local)
Laminar flow not fully developed:	$Sh_{\ln,i} = 1.86 \left(Sc_i \cdot \frac{\rho \cdot d_{inner}^2}{\mu \cdot t} \right)^{1/3}$	(logarithmic mean)
Laminar flow fully developed	$Sh_{loc,i} = 3.657$	(local)
Turbulent flow with $L/d_{inner} > 60$	$Sh_{\ln,i} = 0.026 \cdot \mathrm{Re}^{0.8} \cdot Sc_i^{1/3}$	(logarithmic mean)

Within laminar flow conditions, the velocity profile is considered fully developed when $t > 0.035 \cdot d_{inner}^2 \cdot \rho / \mu$ or when the fluid has flown $L > 0.035 \cdot d_{inner} \cdot Re$. Besides, if the flow is turbulent but $L / d_{inner} < 60$, the expression presented above looses its validity. The explanation for having local or logarithmic mean values is complex and is not given here to simplify the presentation of the migration theory, but more information can be found in the literature quoted previously.

3.2.3. Theory solving for one pipe

The mass balance of compounds *i* applied on a pipe gives equation (8), where $J_{ln,i}$ is the logarithmic mean of J_i, corresponding to the overall mass flux of the compounds *i* from the pipe material to the water. Denberg et al. (2007) provide us with an other expression of $J_{ln,i}$ given in equation (9).

$$c_{w,out,i} - c_{w,in,i} = J_{\ln,i} \cdot \frac{A}{Q} \tag{8}$$

$$J_{\ln,i} = k_{\ln,i} \cdot \frac{\left(K_{w/p,i} \cdot c_{p,i} - c_{w,in,i}\right) - \left(K_{w/p,i} \cdot c_{p,i} - c_{w,out,i}\right)}{\ln\left(K_{w/p,i} \cdot c_{p,i} - c_{w,in,i}\right) - \ln\left(K_{w/p,i} \cdot c_{p,i} - c_{w,out,i}\right)} \tag{9}$$

By combining equation (8) with equation (9) and considering $A = \pi \cdot d_{inner} \cdot L$, equation (10) is obtained. The concentration of migrants *i* at the pipe outlet can now be computed, being a function of the pipe length, its inner diameter and the flow conditions.

$$\frac{K_{w/p,i} \cdot c_{p,i} - c_{w,out,i}}{K_{w/p,i} \cdot c_{p,i} - c_{w,in,i}} = \exp\left(-k_{\ln,i} \frac{\pi \cdot d_{inner} \cdot L}{Q}\right) \tag{10}$$

The maximum obtainable concentration of migrants in the water is derived from equation (6) with $J_i = 0$, meaning that the water is saturated with migrants. It gives equation (11), which can then be combined with equation (10) to express a saturation ratio of contaminant. If we assume that the inlet concentration is zero, this saturation ratio can be written as equation (12).

$$c_{w,\max,i} = K_{w/p,i} \cdot c_{p,i} \tag{11}$$

$$\frac{c_{w,i}}{c_{w,\max,i}} = 1 - \exp\left(-k_{\ln,i} \cdot \frac{\pi \cdot d_{inner} \cdot L}{Q}\right) \tag{12}$$

3.2.4. Determinant parameters in the migration rate

As mentioned previously, several parameters are determinant in the migration rate of a compound from a tubular pipe to the water (cf. section 3.1.2). The chemical parameters are the compounds' concentration in the pipe material ($c_{p,i}$), its diffusion coefficient in water ($D_{w,i}$), its partition coefficient at the interface between the water and the PE ($K_{w/p,i}$). The physical parameters are the pipe length (L), the pipe diameter (d_{inner}) and the flow rate of the water in the pipe (Q). The dependency on these parameters is directly visible in equation (10).

Before going further, it is important to note that the limit between laminar and turbulent flow conditions is based on the Reynolds number (*Re*) and is set in this study to *Re*=2300. However, the transition is not at all so strict in reality. Commonly, one can affirm to have a laminar flow for *Re* below 2000 and a turbulent flow for *Re* above 4000 (Walski et al., 2003). In between, the flow is called transitional and can be either laminar or turbulent but it is really complex to mathematically find the actual regime. To ease the calculations this transitional zone is neglected, though this assumption should be kept in mind from now on.

A series of computations is done to see the impact that changes in these parameters will have on the migrant concentration at the outlet of a single pipe. Since this release of compounds from the PE pipe must be investigated for particular species, the chemical parameters are fixed here. The characteristics of the common antioxidants Irganox 1010 and Irgafos 168 are thus used, being $c_{p,i}$ = 2 g/kg and $K_{w/p,i} = 1.55 \cdot 10^{-4}$. In this particular case $D_{w,i}$ is set to be 10^{-9} m^2/s, although in the actual modelling work two values should be studied: 10^{-10} and 10^{-9} m^2/s. Assuming that $c_{w,in,i}$ equals zero, the saturation level of migrants is thus calculated using equation (12) for various configurations of flow, pipe length and diameter. The results are displayed on Figure 3.

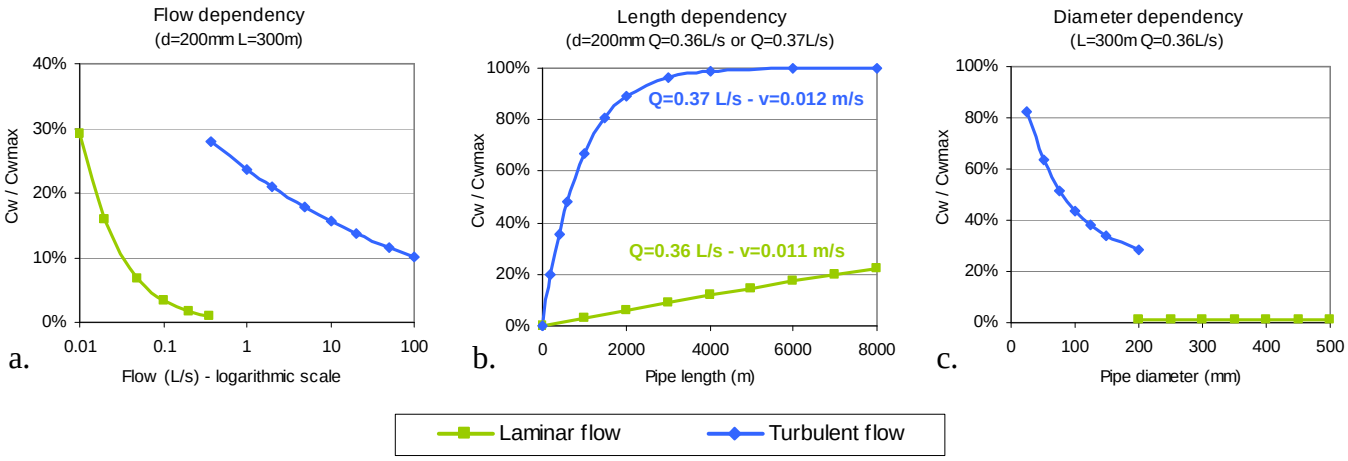

Figure 3 Dependency of the compounds' release on the physical parameters
The figure presents the saturation level of antioxidant in the water at the outlet of a PE pipe. Graphs a, b and c illustrate the dependency on flow, length and diameter, respectively. The particular conditions applied are indicated in each chart title. The diffusion coefficient of the compounds in the water is set at 10^{-9} m^2/s. If one considers antioxidants such as Irganox 1010 or Irgafos 168, the concentration of migrants in the PE matrix is about 2 g/kg and their partition coefficient at the interface around $1.55*10^{-4}$, leading to a saturation concentration of 310 µg/L.

It was stated previously that a switch from laminar to turbulent flow conditions induces a significant increase in the release rate of compounds from the pipe. This is clearly visible on the Graph a from Figure 3, where the outlet saturation level in migrants jumps from 1% to

28% when the flow rate reaches about 0.37 L/s. This flow rate marks indeed for these particular conditions the transition between laminar and turbulent flow regime. Nevertheless, one can observe that within each flow regime domain, the migrant concentration in the outlet decreases with increasing flow. This second phenomenon is in accordance with common pollution cases: “longer contact time of the water with the pipe leads to higher contamination”, but it is only valid within each flow regime. It is worth noting that for almost stagnant water (very low flow and high residence time) the outlet concentration may become significantly high. In such cases indeed, even though the migration rate is much lower than when conditions are turbulent, the contact between the water and the pipe lasts for so long than the amount of compounds released may eventually be high.

In Figure 3 Graph b, it can be seen that when the migrants concentration in the water is far from saturation (roughly <60%), the concentration profile is relatively proportional to the pipe length. When the conditions are closer to saturation, the migration rate slows down until equilibrium is reached between the migrant concentration in the water and in the PE (cf. equation (6)).

Finally, Graph c illustrates graphically the diameter dependency of the migration. In accordance with equation (12), it is observed that at constant flow rate, a higher diameter leads to a smaller migration of compounds. After a certain increase in diameter, the flow conditions may switch from turbulent to laminar, leading to a drop of the migrant content at the pipe outlet. Once laminar flow domain is reached, no variation in the level of compounds is observed within the range of reasonable diameters. Additional computations have shown that even at very low flow rate, when the outlet saturation in antioxidant is not close to zero as it is here, changes in diameter still do not affect the amount of migrants released.

3.2.5. Migration rate expressed as a production rate

To model the diffusion of compounds from pipe to water more easily, it is interesting to express the migration rate of compounds to the water as a production rate of compounds in the water, in the zone closed to the interface with the pipe.

The mass balance of species along a pipe given by equation (8) can be written as:

$$c_{w,out,i} - c_{w,in,i} = J_{\ln,i} \cdot \frac{4 \cdot L}{d_{inner} \cdot v} \tag{13}$$

The same mass balance can be made for a very small displacement ∂x, where x represents the longitudinal coordinate in the pipe. The change in concentration is therefore very small as well and should be written $\partial c_{w,x,i}$. Hence equation (14):

$$c_{w,x+dx,i} - c_{w,x,i} = \partial c_{w,x,i} = J_{\ln,i} \cdot \frac{4 \cdot \partial x}{d_{inner} \cdot v} \tag{14}$$

Besides, x can also be expressed as $x = v \cdot t$ (v being the velocity and t the transport time from the pipe inlet. This gives $\partial x = v \cdot \partial t + \partial v \cdot t$. If it is now assumed that the water velocity in the pipe is constant along the very small length ∂x, then ∂x expression can be simplified as $\partial x \approx v \cdot \partial t$. Equation (14) is thus derived into equation (15)

$$\partial c_{w,x,i} = J_{\ln,i} \cdot \frac{4 \cdot \partial t}{d_{inner}} \tag{15}$$

If equation (15) is now generalized as a derivative to time and combined with equation (6), it gives equation (16), which is the production rate of compounds i at the interface pipe/water. This production rate reflects the migration of the compounds that occurs in reality.

$$\frac{dc_w}{dt} = \frac{4}{d_{inner}} \cdot k_i \left(K_{w/p,i} \cdot c_{p,i} - c_{w,i} \right) \tag{15}$$

Chapter 4.
Use of EPANET to model the release of compounds from PE pipes

This chapter starts with a description of EPANET, which is the program used to model the release of compounds from PE pipes inside distribution systems. It then gives details on the modifications that were made on EPANET to enable this modelling. The chapter ends with the presentation of simulations on a single pipe, some of which are used to validate the modified version of EPANET developed during the project.

4.1. Presentation of EPANET

EPANET is a simulation-software developed by the United States Environmental Protection Agency to help water utilities in the maintenance and operation of distribution systems. First released in the early 1990s, its current version runs under Windows 95/98/NT/XP.

EPANET can be used to compute various hydraulic or water quality properties such as: flows, pressure conditions, water levels in tanks, water age, chlorine concentration or contaminant propagation. EPANET integrates a computer environment for creating and editing models of distribution systems. The model of a system is defined through links (pipes), nodes (pipe junctions), elevated tanks, reservoirs, pumps or valves. Demands at nodes, diurnal variations in demand or control-rules for pumps working can also be set up using the built-in interface. EPANET computations results may be displayed using various formats such as colour-coded network maps, data tables or time series graphs.

Once a network model has been set up, EPANET becomes a powerful tool to obtain hydraulic and water quality properties at all points in space and time of a network. It can also be used for hydraulic optimization purposes, for example pumps placement and sizing or fire flow analysis. EPANET may as well assist water quality management through the evaluation of alternative strategies such as modifying the filing/emptying schedules of tanks to reduce water age or using booster disinfection facilities to balance chlorine losses.

When released in the early 1990s, EPANET received a warm welcome because it was free and included what some people consider to be the industry-standard-computational-engine for hydraulic modelling. More than being free, EPANET is in the public domain, which means that is can be freely copied, distributed but also that its source code is available. As a consequence, institutions or companies can modify EPANET for their use or even develop new modelling programs based on EPANET computational engine.

More information can be found on the US-EPA webpage on EPANET (2008).

4.2. Existing water quality tools in EPANET

EPANET is not originally designed to simulate the migration of substances from the pipes' material to the water. It is therefore necessary to modify the program to enable the modelling of compounds' release from PE pipes. However, the water quality module of EPANET 2.0 already includes the possibility to set both bulk reactions and wall reactions, which minimizes the modifications required to model the compounds' release. The elements presented in this section come from Rossman L.A. (2000), which is the user manual for EPANET 2.

EPANET 2.0 permits computing reactions in the bulk water of any kinetic order, as far as it is expressed according to equation (17). Additionally, the bulk reactions can be computed considering a limiting concentration, as shown on equations (18) and (19).

$$R = K_b \cdot C^n \tag{17}$$

$$R = K_b \cdot (C_L - C)^{(n-1)} \qquad \text{for n > 0, Kb > 0} \tag{18}$$

$$R = K_b \cdot (C - C_L)^{(n-1)} \qquad \text{for n > 0, Kb < 0} \tag{19}$$

with R Instantaneous reaction rate [$kg.m^{-3}.s^{-1}$]
K_b Bulk reaction rate coefficient [$(kg.m^{-3})^{(1-n)}.s^{-1}$]
C Reactant concentration in bulk [$kg.m^{-3}$]
C_L Limiting concentration [$kg.m^{-3}$]
n Reaction order [-]

A wall reaction can be modelled in parallel, with a dependency on the concentration in the bulk, as shown in equation (20). However, its kinetic order is limited to either 0 or 1.

$$R = (A/V) \cdot K_w \cdot C^n \tag{20}$$

with A/V Surface area per unit volume within the pipe (equals $4/d_{inner}$) [m^{-1}]
K_w Wall reaction rate coefficient [$kg.m^{-2}.s^{-1}$] if n=0 or [$m.s^{-1}$] if n=1

In order to set up these reactions in EPANET, the user must supply K_b, K_w and their corresponding kinetic orders. These coefficient rates can be either defined once, and be valid throughout the entire model, or each of them can be set differently for each pipe. This particular possibility is crucial to enable the computation of the release of organic compounds from PE pipes to water, as it will be seen later.

Figure 4 illustrates the differentiation between a bulk reaction and a wall reaction. As it can be seen, these tools for water quality reactions were mainly designed to simulate the action of chlorine on the pipes' material. The reason for separating a wall reaction from a bulk reaction is that it permits the computation of two main that may occur when chlorine is added into water: the desired disinfection reaction in the bulk and the undesired corrosion of the pipe inner surface if this one is in steel.

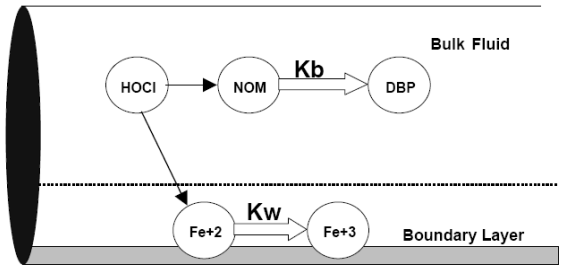

Figure 4 EPANET model: scheme of the reactions zones within a pipe

4.3. Modifications of EPANET to enable the release modelling

Before going further in the explanation of the modifications made to EPANET 2.0, one should state that these modifications remove the possibility for the program to compute other water quality issues than the actual migration of compounds from the pipes. Therefore with these modifications a new version of EPANET is created. Nevertheless, the same model file of a network (e.g. "model_example.net") can be opened either in the original version or the modified version. The user therefore chooses which version to use depending on the water quality computations wished. Since the modified version of EPANET created during the

project is delivered along with this report (cf. digital appendix), any reader has the possibility to compute the release of compounds from PE pipes on its own network model.

The reader may know that a "multi-species extension" has been developed for EPANET. It appears that this extension could also have been used to compute the migration of compounds. However, after assessing the modelling objectives, it appeared that using this "multi-species extension" was too complex when compared to the relatively few modifications that were necessary on the source code directly. The choice was thus made not to investigate further the use of this extension, but to make the modifications described in the following.

Modifications of EPANET source code

In order to model the release of organic compounds from PE pipe into drinking water, the wall reactions tools, already built in the EPANET, are used. To keep the report as clear as possible, only a description of the source code modifications is given in this section, while the corresponding parts of the actual code are given in Appendix 1.

As demonstrated in the migration theory, the release of compounds from the pipe can be expressed as a production rate of these compounds in the boundary layer between the pipe and the water. Therefore, EPANET source code is changed and the initial wall reaction rate formula is replaced by equation (16) (cf. section 3.2), repeated below.

$$\frac{dc_w}{dt} = \frac{4}{d_{inner}} \cdot k_i \left(K_{w/p,i} \cdot c_{p,i} - c_{w,i} \right) \qquad (16)$$

with
- $c_{w,i}$ Mass concentration of compounds *i* in the water [kg.m-3]
- d_{inner} Inner pipe diameter [m]
- k_i Mass transfer coefficient of compounds *i* [m.s-1]
- $K_{w/p,i}$ Partition coefficient of compounds *i* at the interface between water and polymer
- $c_{p,i}$ Mass concentration of compounds *i* in the polymer [kg.m-3]

The mass transfer coefficient k_i is computed from the Sherwood number as presented previously with equation (7), also repeated below to facilitate the reading.

$$Sh_i = \frac{k_i \cdot d_{inner}}{D_{w,i}} \qquad \mathrm{Re} = \frac{\rho \cdot v \cdot d_{inner}}{\mu} \qquad Sc_i = \frac{\mu}{\rho \cdot D_{w,i}} \qquad (7)$$

with
- Sh_i Sherwood number for compounds *i* [-]
- Re Reynolds number [-]
- Sc_i Schmidt number for compounds *i* [-]
- d_{inner} inner pipe diameter [m]
- $D_{w,i}$ Diffusion coefficient of compounds *i* in the water [$m^2.s^{-1}$]
- ρ Density of water [$kg.m^{-3}$]
- μ Dynamic viscosity of water [$kg.m^{-1}.s^{-1}$]

As described in the migration theory (cf. section 3.2), Sh_i has different expression depending on the water flow rate. EPANET code is again modified here, though the theory was simplified to ease the programming as well as the computations. A justification of these simplifications is presented in a further section.

- for $Re < 1$, the flow is considered stagnant, hence $Sh_i = 2$
- for $1 < Re < 2300$, the flow is considered laminar and fully developed, hence $Sh_i = 3.657$
- for $Re \geq 2300$, the flow is considered turbulent, hence $Sh_i = 0.026 \cdot \mathrm{Re}^{0.8} \cdot Sc_i^{1/3}$

In order to minimize the modifications of the program, a crucial aspect is to try to keep the existing interface of EPANET. While the diffusion coefficient $D_{w,i}$ can be set up with the existing interface (cf. print screens in Appendix 1), it is not the case for the concentration of migrants in the polymer ($c_{p,i}$) and their partition coefficient at the interface water/polymer ($K_{w/p,i}$). However, these parameters cannot be entered directly in the code because their values depend on the type of migrants. It would be thus be a big disadvantage of the modelling tool to have these values unchangeable. In addition, $c_{p,i}$ can be different from one pipe to another. Firstly, for PE pipes, this concentration is likely to decrease with the pipe aging. Secondly, one could want to compute the release of compounds in networks not only composed of PE pipes. In such cases, it would be necessary to define $c_{p,i}$ at 0 for the pipes that are not is PE. Therefore, it would be very nice if possible to be able to set $c_{p,i}$ separately for each pipe.

The parameters accessible for the user through the interface are of course limited. As a consequence, an advanced analysis of the code concerning water quality has been carried out to find a way to use the existing interface to input $c_{p,i}$ and $K_{w/p,i}$ in model, without taking the place of a parameter that is crucial for other computations. This analysis was successful since it has enabled us to point out that the boxes meant for the wall coefficients (K_w) could be used as an input access to the program. As mentioned before, K_w presents a great advantage since it can be defined either generally, in the “Reactions Options” menu, or differently for each pipe, in the “Pipe” menu (cf. EPANET print screens in Appendix 1). It has of course been carefully checked that the impacts of using this box, for other purposes than the initial ones, were not inhibiting the proper computing of the compounds’ release. Nevertheless, it should be precised that these modifications remove the possibility to use the wall reaction tool for other purposes than the migration of compounds from the pipes’ material to the water, such as the modelling of corrosion.

EPANET source code has thus been modified in such a way that, the boxes meant for the wall coefficients (K_w) is used to enter the value of the product $K_{w/p,i} \cdot c_{p,i}$. This allows having at the same time an easy way to define $K_{w/p,i}$, which depends on the migrant type, and to define $c_{p,i}$, which depends on the migrant type but also on the pipe material and age. However, K_w unit in

the interface is day^{-1} and before it reaches the code of the quality module, it has already been converted in s^{-1}. Besides, the calculations in the program are all made in US-units and conversions are made is the interface display is set up for SI-units. In the code, all concentrations are thus expressed in g/ft^3. Therefore, some opposite unit conversions are required. These conversions have already been inserted in the source code so that via the interface, the product $K_{w/p,i} \cdot c_{p,i}$ should be entered in µg/kg, which would lead to outputs of $c_{w,i}$ expressed in µg/L. The detail of the code corresponding to these changes is in Appendix 1.

The rest of EPANET source code has been unchanged since the few modifications just described are sufficient to ensure a correct modelling of the compounds' release from pipes to water. It is worth noting that the bulk reaction tools were not modified at all, giving the possibility to compute some reactions of the migrants in the bulk water (typically degradation processes).

Input data required to ensure a proper computation of the release

Various input data are required to compute the release of the compound *i* from the pipe to the water. Each of them is presented below, with its corresponding way of definition in EPANET:

- $c_{p,i}$ is the mass concentration of compound *i* in the polymer, which may vary from one pipe to another. As mentioned before, EPANET code was modified to enable the setting up of $c_{p,i}$ differently for each pipe through the user interface. The user must enter the $K_{w/p,i} \cdot c_{p,i}$ value expressed in µg/kg, in the boxes meant for the wall coefficients K_w.
- d_{inner} is the pipe inner diameter, defined for each pipe through the software user interface.
- $D_{w,i}$ is the diffusion coefficient of compound *i*. It must be defined through the EPANET user interface as a relative diffusion compared to the chlorine one ($D_{w,i}/D_{w,Cl}$). It was set for this project to 0.083 and 0.830, corresponding to a diffusion coefficient of 10^{-10} and 10^{-9} $m^2.s^{-1}$, respectively (taken from Denberg et al. 2007).
- $K_{w/p,i}$ is the partition coefficient of compound *i* at the interface water/polymer. It is a constant defined in the program by entering the value of the product $K_{w/p,i} \cdot c_{p,i}$, in the box meant for the wall reaction rate K_w. In this project, $K_{w/p,i}$ was set to its average value of $1.55*10^{-4}$ (taken from Denberg et al. 2007).
- μ is the dynamic viscosity of water. It must be defined through the EPANET user interface as a relative viscosity to the standard at 20°C. It was unchanged (kept to 1), corresponding to the value of 10^{-3} $kg.m^{-1}.s^{-1}$.
- ρ is the water density. It must be defined through EPANET user interface as a relative density to the standard at 4°C. It was unchanged (kept to 1), corresponding to the value of 1000 $kg.m^{-3}$.

Assumptions in the migration modelling

The assumptions of the computation method used to model the release of compounds from pipes' material to water are presented in this section. These assumptions should always be kept in mind by modellers when analysing simulations results. It is however important to say here that these assumptions were already in the initial EPANET model and have not been introduced with the modifications made for this study.

- In the code, a strict boundary is defined between laminar and turbulent regime (here defined for Re=2300). As discussed previously (cf. section 3.2.4) this does not exactly reflect the reality but simplifies greatly both programming and model computations. The simulations made in the present project show that the cases where the Reynolds number is within the transition layer (from 2000 to 4000) occur rarely and do not last over time when they occur.

- Again to simplify computations, it is assumed that if the flow is laminar, it is always fully developed. The error induced by this assumption being most likely negligible in practice, the existence of a transitional stage between stagnant and fully developed laminar conditions is thus neglected.

- According to the theory, the condition $L/d > 60$ is required for the expression of Sh_i for turbulent flow to be valid. In practice, cases where $L/d < 60$ are almost never met, except for very specific cases where two pipe junctions are very close to each other. It is thus neglected.

Moreover, all computations in this report are made with particular values of $K_{w/p,i}$ and $c_{p,i}$. They correspond to what was found in the literature for the antioxidants Irganox 1010 and Irgafos 168. However the modelling results of the migrant concentration in the water are expressed throughout this report as a percentage in saturation. This gives an independency of the results to $K_{w/p,i}$ and $c_{p,i}$ input values. Indeed if a user wants to study another type of antioxidants, which has for example the same partition coefficient ($K_{w/p,i}$) but a concentration in the polymer ($c_{p,i}$) only half as high, then all the results in percentage would still be valid and only the saturation concentration, which equals the product $K_{w/p,i} \cdot c_{p,i}$, would be changed (in this case halved).

4.4. Validation and first modelling work on a single pipe

Before handling a real distribution system, simulations are done on a single pipe. This way, the right behaviour of the model computations under static and dynamic conditions can easily be checked.

Presentation of the single pipe model

Figure 5 shows the single pipe model built in EPANET. It is composed of a source node, a pump and four nodes. The pipe inlet and outlet are nodes 1 and 4, respectively. The pipe is divided into three sections in order to see the concentration profile along the pipe. The water demand is set at node 4. For the simulations described in this section, the pipe diameter is 200 mm, while the pipe length is 300 m (100 m between each node).

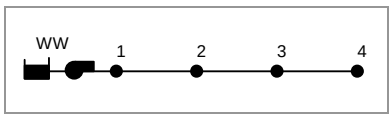

Figure 5 Scheme of the single pipe model used in EPANET

Modelling for static flow conditions and validation of the results

A first round of simulations is done with static flow conditions to validate the model computations. They are meant to reflect the release of antioxidants such as Irganox 1010 or Irgafos 168 (cf. section 3.1.1). As a consequence, the concentration of migrants in the PE matrix is set to 2 g/kg and their partition coefficient at the interface is $1.55*10^{-4}$, leading to a saturation concentration of 310 µg/L. Since the diffusion coefficient ($D_{w,i}$) of the species in water is of relevance, two values are modelled here: 10^{-10} m^2/s and 10^{-9} m^2/s. The modified version of EPANET (cf. section 4.3) is thus run for various flow demands at node 4. The inlet concentration of species in the water is assumed to be 0 µg/L and no degradation reactions in the bulk are set for these first simulations. In parallel to these simulations, equation (10) from the migration theory (cf. section 3.2) is solved for similar conditions. The comparison in made in Table 1.

Table 1 clearly shows that the results computed with EPANET are virtually the same as the theoretical results. This illustrates that the modifications made in the EPANET source code (cf. section 4.3) successfully enable the computing of the migration of compounds from a pipe to the water it conveys.

Table 1 Comparison between theoretical results and EPANET modelling results
This comparison is made for a pipe of 200 mm diameter. The results are presented in percentage of saturation concentration in the water. If one considers antioxidants such as Irganox 1010 or Irgafos 168 then the concentration of species in the PE matrix is about 2 g/kg and their partition coefficient at the interface around $1.55*10^{-4}$, leading to a saturation concentration of 310 µg/L.

Flow [L/s]	Velocity [m/s]	Flow regime	For Dw,i = 10^{-10} m^2/s			For Dw,i = 10^{-9} m^2/s		
			Cw/Cmax after 300 m [ug/L]		Standard Deviation between the two computation methods	Cw/Cmax after 300 m [ug/L]		Standard Deviation between the two computation methods
			Formula solving	EPANET computations		Formula solving	EPANET computations	
0.1	0.003	laminar	0.3%	0.3%	0.02%	3.4%	3.1%	0.19%
0.2	0.006		0.2%	0.2%	0.00%	1.7%	1.7%	0.00%
0.3	0.010		0.1%	0.1%	0.00%	1.1%	1.1%	0.00%
0.4	0.013	turbulent	6.7%	6.7%	0.04%	27.7%	27.5%	0.14%
0.5	0.016		6.5%	6.4%	0.04%	26.7%	26.5%	0.14%
1	0.032		5.6%	5.6%	0.03%	23.7%	23.5%	0.12%
5	0.159		4.1%	4.1%	0.02%	17.8%	17.6%	0.09%
10	0.318		3.6%	3.6%	0.02%	15.7%	15.6%	0.08%
20	0.637		3.1%	3.1%	0.02%	13.8%	13.7%	0.06%
30	0.955		2.9%	2.9%	0.02%	12.8%	12.7%	0.05%
40	1.273		2.7%	2.7%	0.02%	12.1%	12.0%	0.05%
50	1.592		2.6%	2.6%	0.01%	11.6%	11.6%	0.04%
100	3.183		2.5%	2.3%	0.18%	10.2%	10.2%	0.02%
Average standard deviation =					**0.03%**			**0.08%**

EPANET computes the concentration of organic compounds at the 4 nodes, which can then be derived into a concentration profile along the pipe as presented on Figure 6. The two graphs show the results for the values of $D_{w,i}$ investigated here: 10^{-10} and 10^{-9} m^2/s.

At first, it is clearly visible that the diffusion coefficient ($D_{w,i}$) greatly affects the degree of contamination. Roughly, one can say here that the saturation level in the water is four times higher when $D_{w,i} = 10^{-9}$ m^2/s, than when $D_{w,i} = 10^{-10}$ m^2/s. Since the migrant concentration in the water is in these cases far from saturation, the concentration profile appears proportional to length on Figure 6, though for longer pipes this apparent proportionality is not valid (cf. Figure 3). The significant effect of the flow regime on the migration rate that was observed on Figure 3 is visible again here, since the outlet saturation concentration of species jumps from 0.1% to 7% on chart a and from 1% to 28% on chart b when the regime changes. Besides, it is also illustrated here that, within each regime type, an increasing flow leads a decreasing outlet concentration.

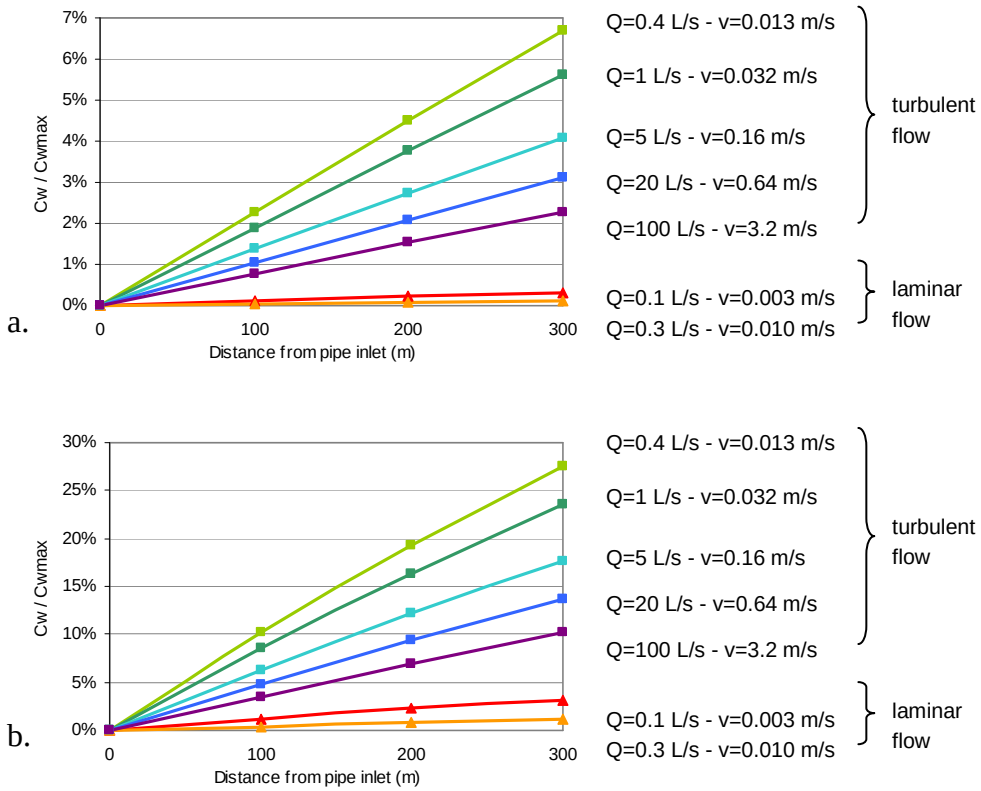

Figure 6 EPANET static simulations on a single pipe model
The figure presents the migrant saturation level in the water computed along a pipe of 200 mm diameter. The charts illustrate the distribution along the pipe and the flow dependency. Chart a and b correspond to a diffusion coefficient of the species in the water of 10^{-10} m^2/s and 10^{-9} m^2/s, respectively. It should be noted that the ordinate scale is different between the two charts. If one considers antioxidants such as Irganox 1010 or Irgafos 168 then the concentration of species in the PE matrix is about 2 g/kg and their partition coefficient at the interface around $1.55*10^{-4}$, leading to a saturation concentration of 310 µg/L.

As mentioned previously, a fixed transition between laminar and turbulent regime is used (set for *Re*=2300), which does not really reflect the reality. The use of this fixed transition affects the results given in Figure 6 but has not been found to affect the results of simulations on network models reflecting real world conditions. Indeed, the cases where the Reynolds number is within the transition layer (from 2000 to 4000) occur rarely in practice and do not last over time when they occur.

There is a real uncertainty on the actual values of the diffusion coefficient in the water of the compounds we are looking at. To date the literature does not provide a single and trustable value for $D_{w,i}$ for each migrant type. The fact that a change from 10^{-10} to 10^{-9} m^2/s affects so much the migrant level in the water confirms the necessity to always model both cases throughout this study. This way, a range of contamination degree will be established.

Although this range may be quite wide, it appears more suitable than taking an average value of the diffusion coefficient and maybe being really far from reality.

Modelling for dynamic flow conditions

The results presented for static conditions (cf. Figure 6) could also have been obtained by solving the theoretical equation (10) for the same pipe (cf. section 3.2.3). However, no real dynamic simulations would have been possible without a more advanced computer program. Indeed, once the flow conditions become dynamic (i.e. change over time), the release of species must be combined with a transport model to compute the migrant concentration in the water at anytime. Such a tool is precisely what is created with the modifications of EPANET source code (cf. section 4.3). As a consequence, it becomes possible to see the effect that diurnal variations in demand have on the contamination degree of water. Figure 7 presents the pattern that is set up in EPANET to reflect these variations in demand. This pattern is used for all the dynamic simulations made along this project.

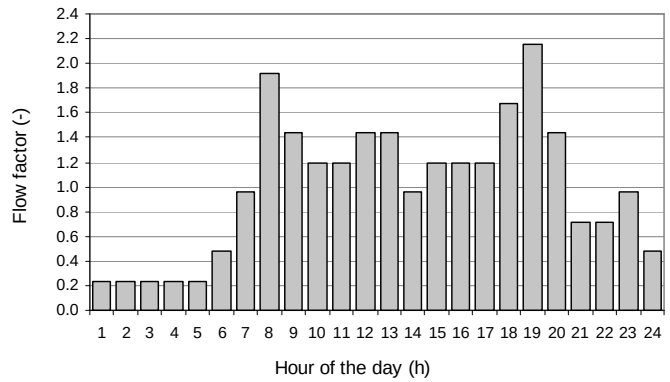

Figure 7 Flow factors used in EPANET to simulate diurnal variations in demand
At every time step, the actual demand is obtained by multiplying the base demand by the corresponding multiplier.

Dynamic simulations are done on the single pipe model presented in Figure 4. In order to avoid the effect of initial conditions, the model is run for 4 days and only the simulation results of days 3 and 4 are considered. A range of simulations are carried out for several base flow demands at node 4. The most relevant outputs from these simulations are displayed in Figure 8.

Here again, two cases are studied ($D_{w,i} = 10^{-10}$ and 10^{-9} m^2/s) and lead to results significantly different. Much flatter variations of the migrant concentration are observed along the day. However, this flattening effect is caused by the graph scale and the variance of the concentration around the average is in fact almost identical between the two cases.

In accordance with the results obtained under static conditions, the influence of the flow regime on the migration rate is obvious, particularly for cases b and c in Figure 8 where both laminar and turbulent conditions occur in a daily period. When looking at Graph c where it is the most obvious, it can be seen that as soon as the flow becomes laminar (around 0h), the saturation drops by 2.5% and 10% for cases with $D_{w,i} = 10^{-10}$ and 10^{-9} m^2/s, respectively. Besides, when a turbulent regime is established and lasts over some time, similarities between the flow and the saturation degree become obvious. Since the saturation profile behaves inversely to the flow profile, it was chosen to represent the flow with a reversed axis in Figure 8, to ease the comparison. It can be established that the greater the flow is, the stronger the analogy is. Finally, one can say that significant changes in base flow affect quite little the outlet concentration of species, except when the flow conditions become laminar. Indeed, when Graphs c and d are compared, the saturation of species in the water remains in average around 15% to 20% µg/L while the flow varies from 1 to 20 L/s.

The results presented here are to be balanced with the simulations made on network models which reflect real world conditions. Indeed, from the results presented so far, it is hard to tell if the phenomena observed here are still relevant in a large branching system composed of numerous pipes. These results are however not pointless at all since they allow us to understand what may happen on a localised scale.

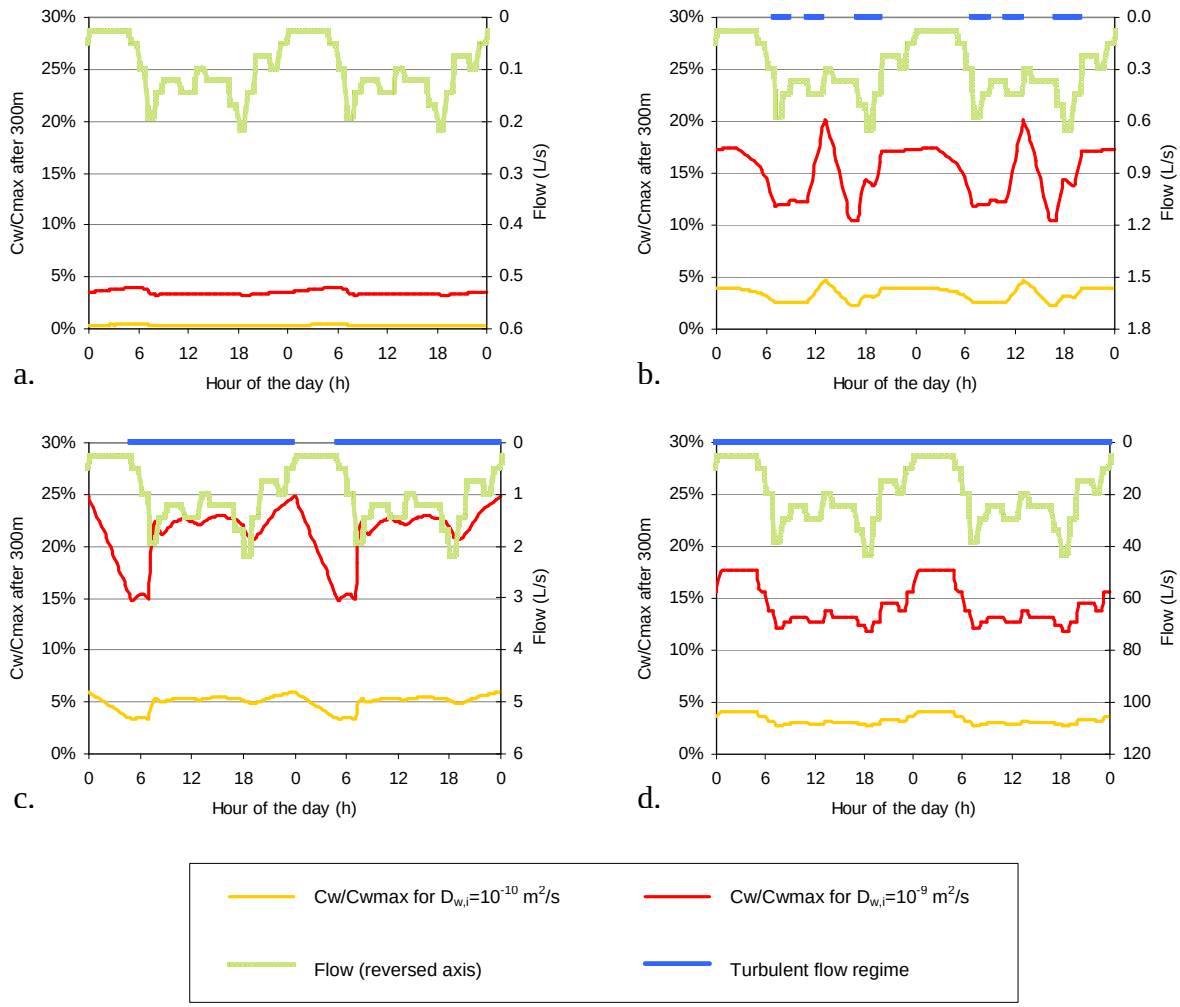

Figure 8 EPANET dynamic simulations on a single pipe

Graph a, b, c, d represent simulation results for a base flow of 0.1 L/s, 0.3 L/s, 1 L/s, and 20 L/s, respectively. Each graph displays the computed saturation level in migrant at the outlet of a pipe of 200 mm diameter and 300 m length. The flow is shown using a secondary axis which has been reversed to highlight similarities between flow and migrants content. A binary representation is used to display the flow regime: if there is a blue line the flow is turbulent, otherwise it is laminar. Simulations are made for two cases of migrant's diffusion coefficient in the water: 10^{-10} and 10^{-9} m²/s. If one considers antioxidants such as Irganox 1010 or Irgafos 168 then the concentration of species in the PE matrix is about 2 g/kg and their partition coefficient at the interface around $1.55*10^{-4}$, leading to a saturation concentration of 310 µg/L.

Chapter 5.
Modelling results on three network case studies

The release of organic compounds from polyethylene pipes to water is now investigated on three network case studies. The first case concerns a small network under construction. It is a real distribution system located in Farum (Denmark). The area is particularly suitable for the project since this new network is entirely composed of polyethylene pipes and only supplied with water from a single source. The modelling results are then compared with the NVOC content measured on site to determine whether NVOC is a suitable indicator of the release of organic compounds from PE pipes. The second and third cases investigated are models of theoretical networks. Both of them are model-examples provided with EPANET, and are thus assumed to reflect real world conditions. The first of them is of middle size and has a relatively simple geometry with one water source, one elevated tank and a dozen pipes. The second one represents a quite bigger network with two water sources, three elevated tanks and more than a hundred pipes. Contrary to the case investigated in Farum, the two models studied here are in fact models of the skeleton of the network only. Indeed, only the biggest pipes that are used for transportation, rather than distribution of the water are in the model. This should ease the computations and results handling but still give a fair picture of the quality conditions in the networks.

During the modelling work on these three cases, the focus is kept on the project objectives listed in the section 1.2. These objectives are mainly centred on determining the effects that the migrant characteristics, the network characteristics, or some degradation processes may have on the level of the contamination caused by PE pipes. The computations presented here were only made possible by modifying the EPANET source code, as described in the previous chapter.

5.1. Case of a small network under construction (new network in Farum)

5.1.1. Presentation of the area

The area investigated is a residential area under construction located in Farum (North-Zealand, Denmark). A complete new network is built to supply the new buildings and houses that will be developed in the years to come. Figure 9 gives an overview of the location of the site in Denmark and a sketch of the accommodations already inhabited at the time of the sampling. The site is particularly interesting because the area has its own waterworks and only PE pipes are used in the network. This relatively simple configuration of the site was suitable to make some sampling work and compare the observations on site with modelling predictions. Moreover, the pipes of the network, already in use today, are dimensioned to cope with further developments of the area. As a consequence they are significantly over-dimensioned compared to the current water demands in the area.

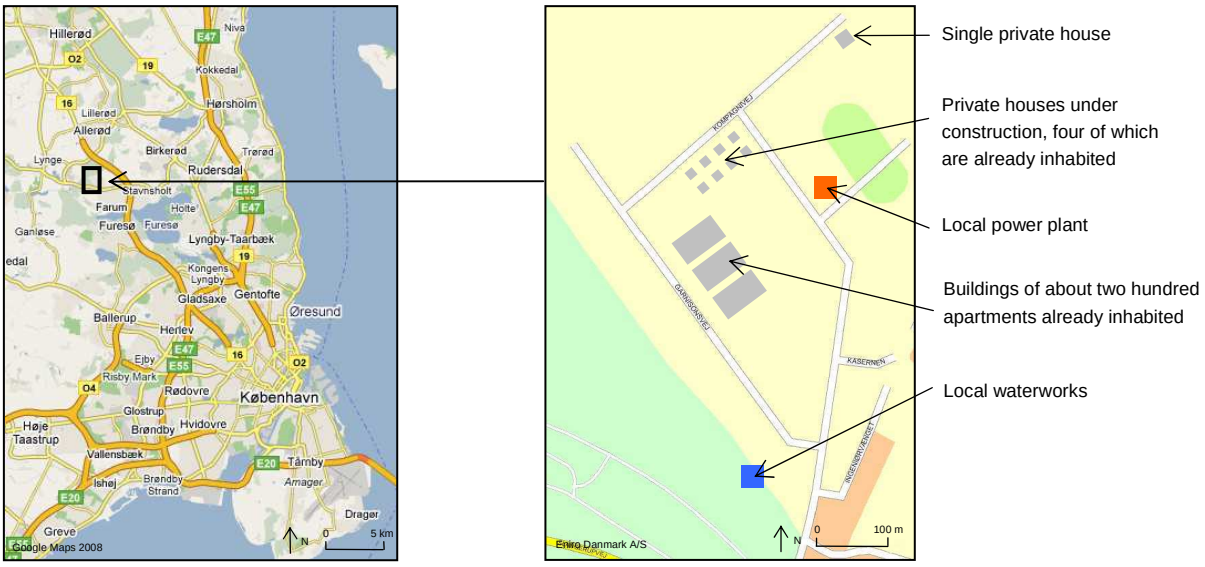

Figure 9 Map of the construction area in Farum
The maps on the left and right were obtained from Google Maps and Eniro Danmark, respectively.

A model of the current water network is built in EPANET. A sketch of this network model is presented in Figure 10. It is important to say that this model was not calibrated with actual data. Nevertheless, it was developed based on data provided by the Farum Waterworks, which organizes the construction of this new network and manages the water supply service for the people already living in the area. It is thus assumed that the uncertainties induced in the model are acceptable for the context of this study. It is estimated that about 400 people live in the apartment buildings (node 2), 12 people live in the group of houses under construction (node 11) and 3 people live in the house located in the northern limit of the site (node 12). Additionally, containers for workers are located next to the power plant (node 6), the

cumulative consumptions of the workers are assumed to correspond to the demand generated by 2 people living there. To model the water demands generated by these inhabitants, it is assumed that their consumption is equal to the Danish average of 160 L/day/person. Tables in Appendix 2 give the network characteristics, namely the pipes length and diameter, as well as the demands modelled at each node (based on the assumptions presented here).

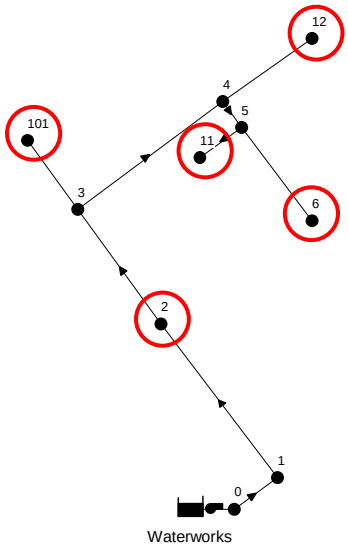

Figure 10 Sketch of the EPANET water network model of the construction area in Farum
The red circles indicate the locations that were considered relevant to give an overview of the pollution level. At these locations, the detailed migrant concentration is analysed.

5.1.2. Simulation conditions

The pattern presented in Figure 7 is used in order to model diurnal variations in demand. Since no elevated tank exists in the network, the water flow provided by the waterworks to the network (cf. Figure 11) exactly follows the variations in demand. Since the pipes are over-dimensioned for the current number of inhabitants, the residence time of the water is quite high in most parts of the network. Indeed, the water is a week old when it reaches the group of private houses in node 11 and three weeks old when it is consumed at the power plant. Figure 12 displays the variations of the water age along the day at four of the five locations investigated in the network. These variations are directly induced by the variations in demand, which create changes in water flow in the pipes. No data is given for node 101 because it is basically the outlet of an unused pipe. This pipe is filled with water but since there is no real demand at node 101, the water is stagnant. The water age is then basically equal to the time elapsed since the last flushing of the pipe.

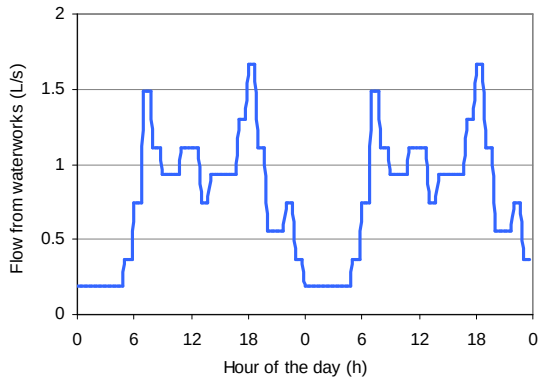

Figure 11 Computation of the flow sent from the waterworks to the Farum network

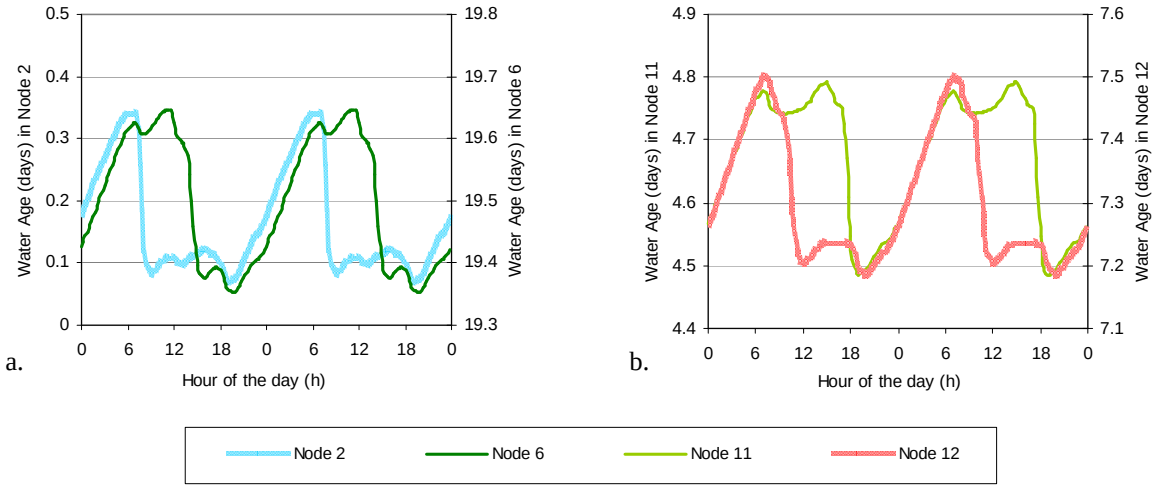

Figure 12 Computation of the water age in the Farum network
Due to big differences in age between the different locations, each curve has its own Y-axis, otherwise it would not be possible to see the variations along the day.

The original version of EPANET is not made to make "network map plots" of the Reynolds number. However, such plots are quite interesting because they permit highlighting the network characteristics clearly in terms of flow conditions (laminar or turbulent). Therefore, the program has been modified and a new version of EPANET has been created to enable this preview. The modifications were simpler than what was required for the compounds' release modelling. It was not considered relevant to give the details of these modifications in the report content. Nevertheless, in case the reader wants more detail, the coding parts are given in Appendix 1.

Figure 13 below presents two "network map plots" of the Reynolds number in the pipes at two times of the day that seemed relevant: a night time at 4:30 a.m. and a time of peak in demand at 7:30 p.m. The particularity of this network case is clearly emphasized in this figure:

laminar flow is the dominant regime in the network. Even during the peak in demand of the dinner time, the flow regime is only turbulent between the waterworks and the node 2, corresponding to the apartment buildings. Further in the network, the demands are much lower and the flow always remains laminar, with the high water age observed on the previous figure. These results also show that the Reynolds number ranges over a large range of values, which confirms that the conditions never stay long within the transition zone for *Re* between 2000 and 4000. In other words there is little incertitude in practice on telling whether the flow is laminar or turbulent.

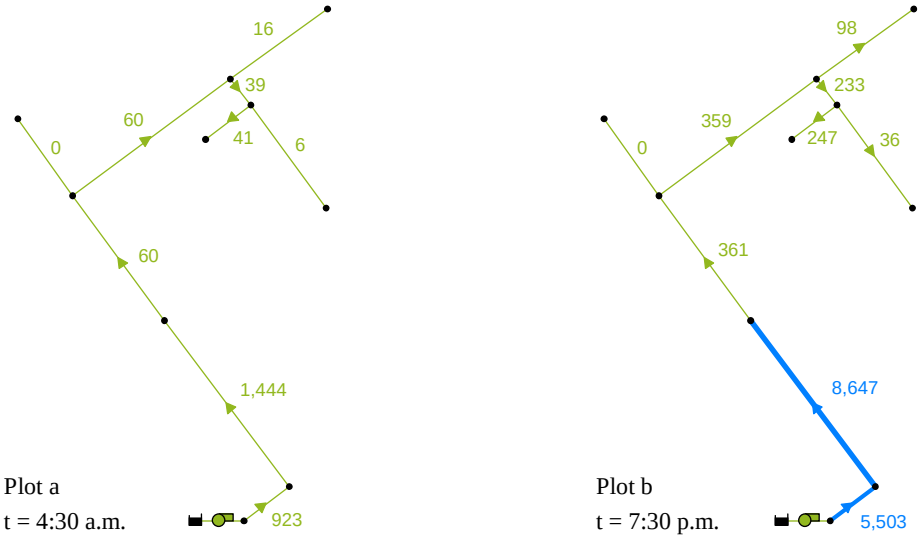

Figure 13 Computation of the Reynolds number in the Farum network
The numbers plotted next to the pipes are estimations of the Reynolds number. The colour code indicates the distinction between laminar (thin green line) and turbulent (thick blue line) flow conditions.

EPANET has been used to compute the release of compounds from the pipes to the water. Time steps of 5 minutes and of 30 seconds have been used in the program for the hydraulic and quality computations, respectively. Model runs show that a simulation period of at least 20 days is necessary to reach a stabilized concentration profile over a daily cycle. The reason for that is simply the very long residence time of the water in some parts of the network. Before 20 days of simulations, the network has not yet been flushed with new water from the waterworks. In order to ensure stabilized concentration profiles, the results presented below were obtained after 23 days of simulation period.

5.1.3. Migrant concentration in the network when no degradation is modelled

Figure 14 presents the saturation level in migrant at several locations in the network. These locations, highlighted on Figure 10, were considered relevant to give a fair overview of the contamination degree in the system. Results for the overall network are also displayed in Figure 15, which presents a "network map plot" of the contamination at two times of the day. After the conclusions made from the modelling on a single pipe, it is chosen to investigate two cases here, with diffusion coefficients of the migrant in water ($D_{w,i}$) of 10^{-10} and 10^{-9} m^2/s, respectively.

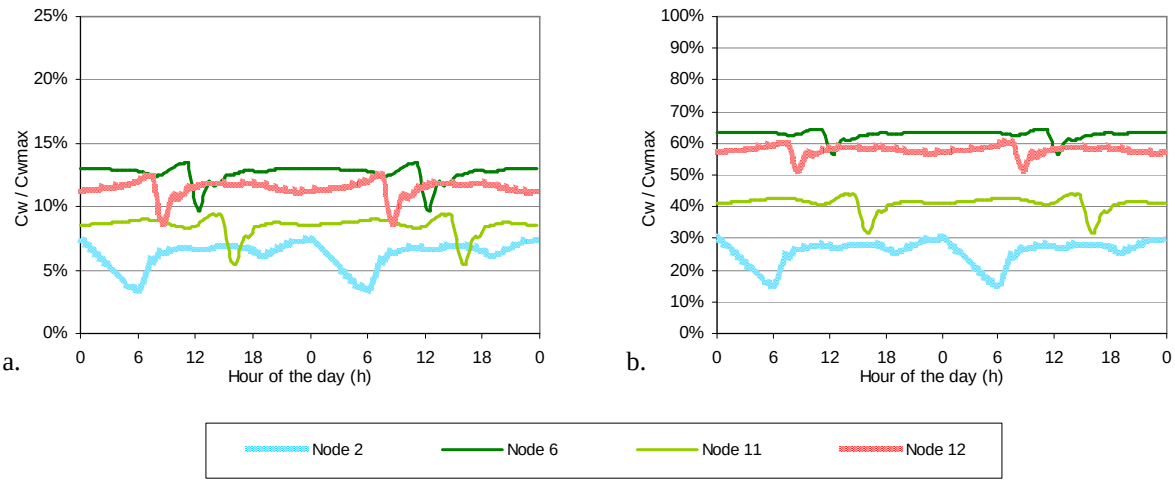

Figure 14 Simulation results for the Farum network: daily variations of the migrant concentration
The two graphs represent the saturation level of species along the day at relevant nodes of the network, for migrant's diffusion coefficient in the water of 10^{-10} m^2/s for Graph a and 10^{-9} m^2/s for Graph b. If one considers antioxidants such as Irganox 1010 or Irgafos 168 then the concentration of species in the PE matrix is about 2 g/kg and their partition coefficient at the interface around $1.55*10^{-4}$, leading to a saturation concentration of 310 µg/L.

In accordance with the simulation results for a single pipe, one of the main conclusions that can be drawn at first sight is the high influence of $D_{w,i}$. Indeed, when looking at the four locations investigated, the saturation level ranges from 3% to 14% when $D_{w,i} = 10^{-10}$ m^2/s, while it ranges from 15% to 65% when $D_{w,i} = 10^{-9}$ m^2/s (cf. Figure 14). This influence of $D_{w,i}$ is also clearly visible when comparing Graphs a and b with Graphs c and d on Figure 15.

Differences in the average migrant content in the water are also observed between different locations in the network (cf. Figure 14 and Figure 15). These differences are explained by two main aspects: the transport distance in the pipes and the residence time.

Longer transport distances always induce higher levels of migrants released, until saturation level is reached (as shown previously in Figure 3 Graph b). This is simply the consequence of

a bigger surface of contact between the water and the PE material. This effect of the transport distance is expected to be one of the main governing aspects of the degree of contamination in a network. Although it is not so much emphasized in this study case, it clearly illustrated in the next two (cf. sections 5.2 and 5.3).

The water residence time and the flow conditions in the pipes are closely linked. The theory tells us that laminar flow conditions induce a much lower migration rate of the compounds than if the conditions were turbulent (cf. section 3.1.2). In consequence, the concentration in migrants does not usually increase significantly when the water is conveyed under laminar conditions and remains at the level where it entered the pipe. Nevertheless in the case of this network under construction, the residence time of the water in the pipe is very high in some locations: up to one week at node 12 and almost three weeks at node 6 (cf. Figure 12). The water age in these parts of the network is in fact so high that a phenomenon only expected on stagnant water is observed here: the water remains for such a long time in the pipe that, in spite of a low migration rate, the level of migrants in the water becomes eventually high. This phenomenon observed in the theory for very low flow (cf. Figure 3 Graph a) is a clear indicator of over-dimensioned pipes. In this case it is explained by the fact that the network is under construction and is dimensioned in accordance with the demands expected from future constructions in the area. The current demands are thus much lower than what the network is dimensioned for, hence the very high residence times observed.

These simulations also show that at the scale of the entire network, no significant variations of the contamination degree occur along the day (cf. Figure 15, comparison of Graph a with b and c with d). The variations remain indeed relatively limited and are not significantly affected by the changes in flow demands. However, what is observed in Figure 14 is still worth some comments. A drop in the migrant content is observed once a day for each node and is for example visible between 12 p.m. and 6 a.m. for node 2, where the saturation level drops by 5% when $D_{w,i} = 10^{-10}$ m^2/s and by 15% $D_{w,i} = 10^{-9}$ m^2/s. The reason behind this decrease is the fact that during the night time, the flow between the waterworks and node 2 becomes laminar. It induces a lower migration rate and, since the conditions are far from being stagnant, causes the drops in migrant concentration observed. While the drop at node 2 is actually observed at the same time as the laminar conditions, delays are observed for other locations before a drop occurs. These delays are caused by the low travel velocity of the water in the rest of the network and correspond in fact to the water age in the network. For example, the drop in concentration observed for node 12 was generated by a switch from laminar to turbulent conditions occurring about 7 days earlier, and should not be associated with the drop for node 2observed just before in Figure 14.

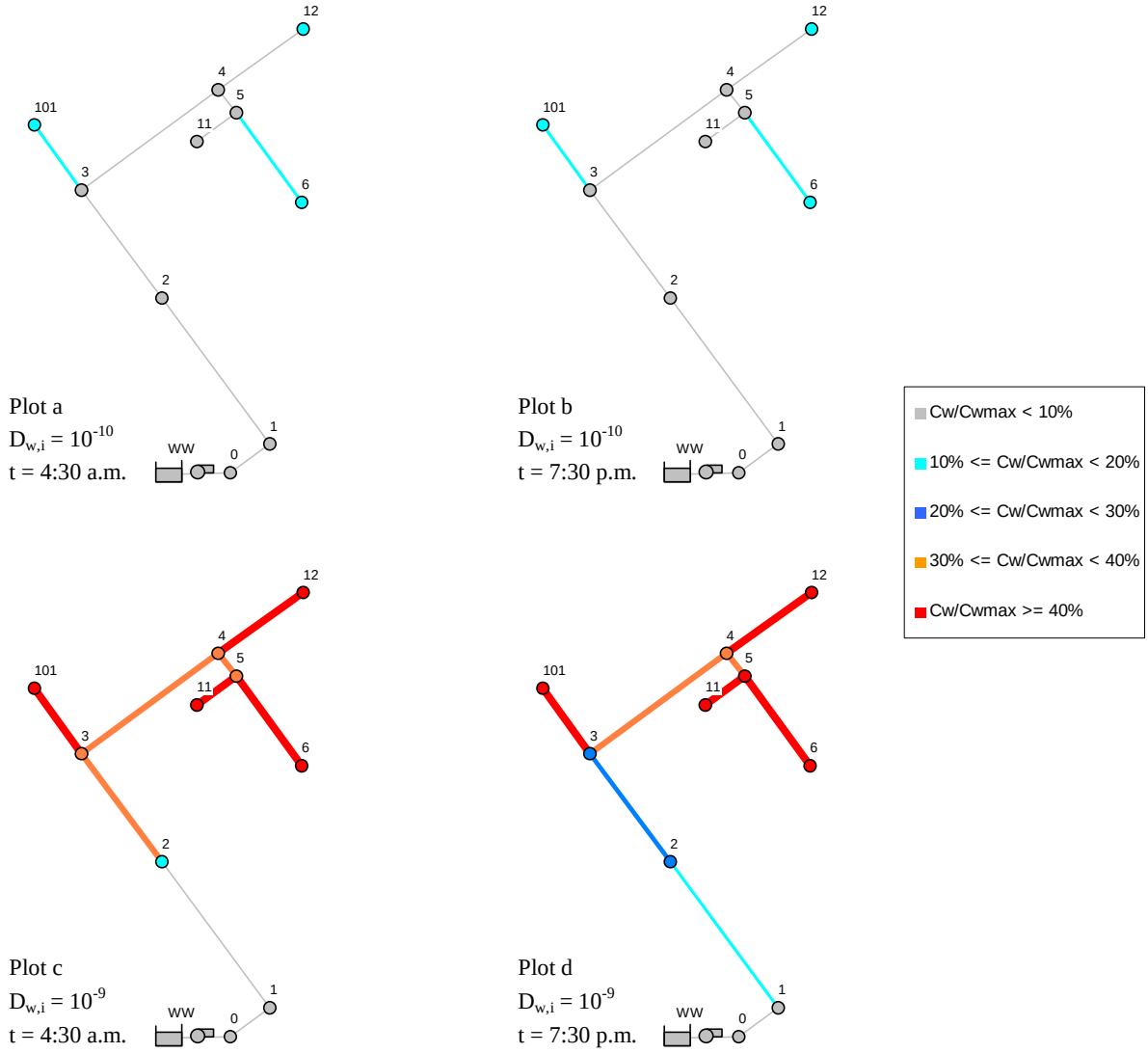

Figure 15 Simulation results for the Farum network: map-plot of the migrant concentration
The figure represents the migrant saturation level in the network when no degradation is simulated at two times of the day. Plots a and b correspond to the case where a diffusion coefficient of the migrants in the water is 10^{-10} m^2/s, and plots c and d to the case where it is 10^{-9} m^2/s. If one considers antioxidants such as Irganox 1010 or Irgafos 168 then the concentration of species in the PE matrix is about 2 g/kg and their partition coefficient at the interface around $1.55*10^{-4}$, leading to a saturation concentration of 310 µg/L.

5.1.4. Systematization of the migrant concentration profile

Figure 14 shows the daily variations of migrant content at different locations in the network. In addition to this figure, it was considered interesting to compute and plot the cumulative distribution of the migrant concentration, as it is done in Figure 16 below.

The cumulative distribution of a set of data is a statistical distribution of these data, which corresponds to the integral of the normal (Gaussian) distribution. More details about the

computation of this distribution are available in Appendix 3. In simpler terms, the cumulative distribution shows the probability that a variate will assume a value less than or equal to x (the abscissa). Thus, the plot of the cumulative distribution always starts with an ordinate at 0% and ends with an ordinate at 100%. It is the way that the curve switches from one extremity to the other that characterizes the set of data. Basically, the mean abscissa where the curve switches is the average of the data set, while the "slope" of the curve during the switch indicates the variance in the data. During this switch from 0% to 100% in ordinate, a very steep (almost vertical) curve shows than all data are very close to each others, whereas a more gentle slope shows that variations of the data around the average are occurring.

In the context of this project, the cumulative distribution curves are seen as a different way of presenting the simulation results. Figure 16 does not particularly provide a source for new interpretations compared to Figure 14 and no additional comments will be done here. However, such a display of the results should be seen as a way to systematize the concentration profiles in a network, which permits an easier comparison with other network models. This figure is used later on (cf. section 5.4) to make some general conclusions on the effect of the position in the network, the change in the migrant's diffusion coefficient, or the effect of different network configurations on the degree of contamination caused by using PE pipes.

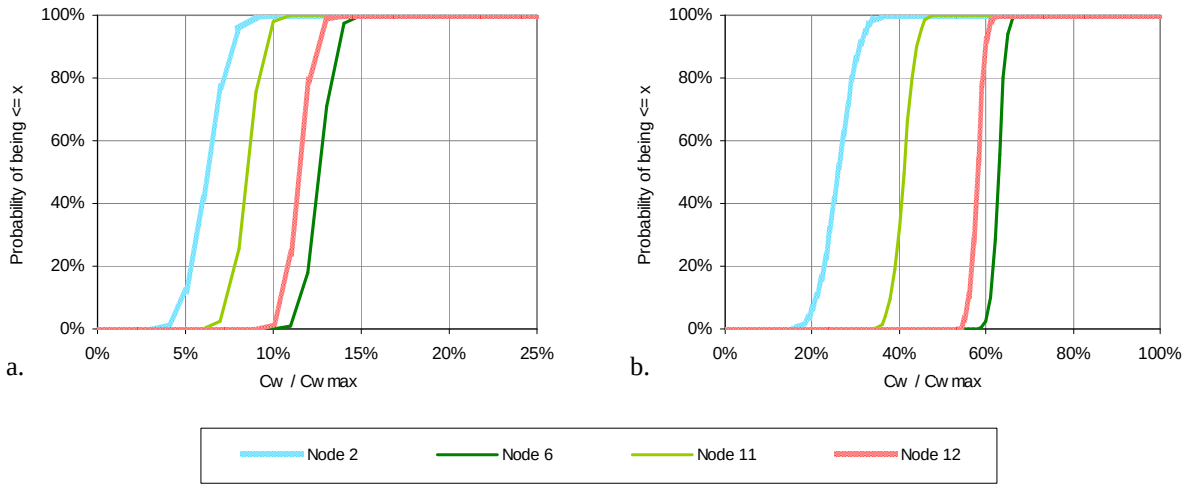

Figure 16 Simulation results for the Farum network: cumulative distribution of the migrant concentration
The two graphs represent the probability distribution that the saturation level along the day is ≤ x (the abscissa), for migrant's diffusion coefficient in the water of 10^{-10} m^2/s for Graph a and 10^{-9} m^2/s for Graph b. If one considers antioxidants such as Irganox 1010 or Irgafos 168 then the concentration of species in the PE matrix is about 2 g/kg and their partition coefficient at the interface around $1.55*10^{-4}$, leading to a saturation concentration of 310 µg/L.

5.1.5. Effect of degradation on the migrant concentration

There is a high uncertainty on the degradation of the compounds migrating from PE pipes to drinking water. It is generally assumed that their degradation is a 1st order kinetic reaction. In their work Denberg et al. (2007) give some values of half-life for migrants released from PE pipe. These half-lives are strongly dependent on the temperature and the type of migrants, and range from a few days to 30 days. As a consequence, several simulations have been made with EPANET for different rates of degradation. A total of six cases are investigated: one case with no degradation and five cases with half-lives of 28 days, 21 days, 14 days, 7 days and 1 day. The results of these various simulations are gathered in Figure 17, which shows the mean saturation level in migrants at the investigated nodes of the network. As previously in this project, two values of $D_{w,i}$ are investigated: 10^{-10} and 10^{-9} m^2/s.

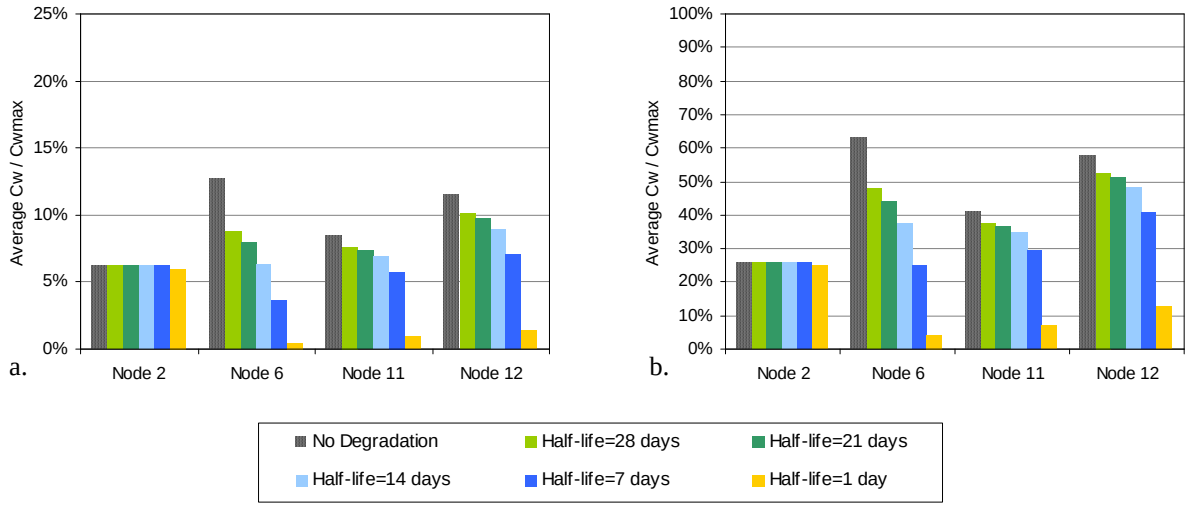

Figure 17 Simulation results for the Farum network: effect of degradation on the migrant concentration
The figure represents the daily average of the migrant saturation level at relevant nodes of the network and for different migrant half-lives. In these simulations, the migrant's diffusion coefficient in the water is 10^{-10} m^2/s for Graph a and 10^{-9} m^2/s for Graph b. If one considers antioxidants such as Irganox 1010 or Irgafos 168 then the concentration of species in the PE matrix is about 2 g/kg and their partition coefficient at the interface around $1.55*10^{-4}$, leading to a saturation concentration of 310 µg/L.

Coherently, there is a strong relation between the water age at nodes and the reduction of the migrant content in water due to degradation. For example, it is quite clear in Figure 17 that degradation processes have almost no effect at node 2 because the water age is much lower than the migrant half-life. In opposition, in the other parts of the network where the water age is much higher (cf. Figure 12), the decrease in migrant concentration caused by degradation processes is much stronger. The detailed variations of the migrant concentration along the day are not given here, not to overload the report, but are available in Appendix 2. On average, it

is observed that no particular phenomenon occurs along the day. The variations observed previously (cf. Figure 14) are indeed only translated downwards but not really affected by the fact that the overall level of migrants decreases.

These simulations highlight that degradation processes can lead to a significant decrease of the migrant concentration, in at least some parts of a network where residence times are very high. It calls for further work on the precise estimation of the half-lives of the migrants. More investigations should also be done concerning the by products resulting from the degradation of migrants in the water. If it happens that some of them are persistent, phenomena of accumulation could occur, although the concentration of migrants themselves could remain low because they are continuously degraded.

5.1.6. Comparison with experimental results

As mentioned previously, this network under construction in Farum was chosen because of its simple configuration. It permits making a reasonable comparison between modelling predictions and sampling results, without having too many uncertainties on the origin of the compounds observed. Two sampling campaigns were thus carried out on the 10th of March and 29th of April 2008, although only the results from the second campaign were considered reliable and are presented here. The sampling work aimed at measuring the Non Volatile Organic Compounds (NVOC) content in the network to see if any differences would be observed between different locations in the network. Such differences could indeed be caused by the release of organic compounds from PE pipes. Nevertheless, theses differences are expected to be small relative to the background level of NVOC in the water. As a consequence, precautions were taken to avoid any contamination from other sources of organic compounds and to have a good repeatability of the results. The idea was to try to avoid a case where small variations, if some were observed, could not be interpreted because they would stand within the uncertainty range of the measurement. In parallel to NVOC, the dissolved oxygen concentration was measured to see if some consumption is observed, which could indicate degradation processes.

In the following paragraphs, the sampling procedure is described first, followed by a presentation of the measurement results and a comparison with the model computations.

Sampling procedure

Samples of drinking water were taken at the waterworks outlet and in the network for five configurations: 1-2) the end of an unused pipe located in the North West of the area (node 101 in the model) before and after a flushing, 3-4) the junction next to the power plant (node 6 in the model) before and after a flushing, and 5) the kitchen tap of a private house in the area (node 11 in the model). For each “configuration” investigated in the field, at least 5 samples

were taken. The detail of the sampling program and the sampling procedure is presented in Appendix 4. The dissolved oxygen concentration was measured on site using the instrument HQ10 from the Hach Company, which is based on luminescent technology. The NVOC content was measured in the lab using the instrument Shimadzu TOC-Vw. More information concerning the method to measure NVOC are also available in Appendix 4. It was chosen not to give all the details of the sampling work here to lighten the report and since the general focus of the project is on modelling. However the elements appearing to be the most relevant in this context are still given below.

Although the sampling work in itself was carried out on April 29th, 2008, different operations were made on the network to prepare the sampling. The reason behind this is that three pumping wells, located in the area, can supply the network with water. Only one of them is used at a time, but a regular change of connections ensure that each well is often used, mainly to preserve the source. As a consequence, the network is supplied alternatively with waters of potentially different quality. Due to high residence time of the water in some parts of the network, it is likely that the water from one source can be found in the network several days after the use of this source has been stopped. Because the sampling results are obtained by comparing samples from the network with the waterworks outlet, it was crucial to ensure that on the sampling day, the water collected in the network was coming from the same well as the one taken at the waterworks outlet, otherwise no real comparison could be made. It is indeed likely that the background NVOC content in the water is different between the three sources. To avoid such a situation, the last switch of pumping well was made at least six days before the collection of the samples. In addition the unused pipe (leading to node 101) and the pipe leading to the power plant (node 6) were flushed five days before the collection of the samples to ensure that the water collected was indeed the same.

During the sample collection, on April, the 29th, a new flush of the unused pipe and of the pipe leading to the power plant was made. Water samples were taken before and after the flush to see whether differences could be observed. This was particularly interesting for the unused pipe where the water collected before the flushing had been stagnating for five days. When looking at the results, the situation before flushing should be considered to be the normal conditions, while results after flushing are to be considered separately. Indeed, the act of flushing the pipes induced a local demand of about 1.4 L/s, which in the case of this network is considerably higher than the normal demand at the locations investigated (0 L/s at the unused pipe outlet and 0.004 L/s at the junction next to the power plant). Thus, the disturbance generated by the flushing cannot be neglected.

Measurement results

The results obtained from the sampling work in the Farum network are summarized in Figure 18 and Figure 19 below. They present the 95% confidence interval of the NVOC and oxygen

concentrations measured in the network, respectively. The confidence interval is an expression stating that the true mean is likely to lie within a certain distance from the measured mean (Harris, 2003). It is a way to estimate the reliability of a comparison between two series of data. Practically, if the confidence intervals of two series are not overlapping, one can be 95% sure that the means of the two series are different. More details on the method to compute this confidence interval can be found in the literature, such as Harris (2003). In our case, the main idea is to look at the confidence interval for NVOC and dissolved oxygen concentrations from the different locations investigated and see if they overlap with the ones for the waterworks. If they do overlap, then one cannot conclude that the concentration measured in the network is different from the initial concentration in the water.

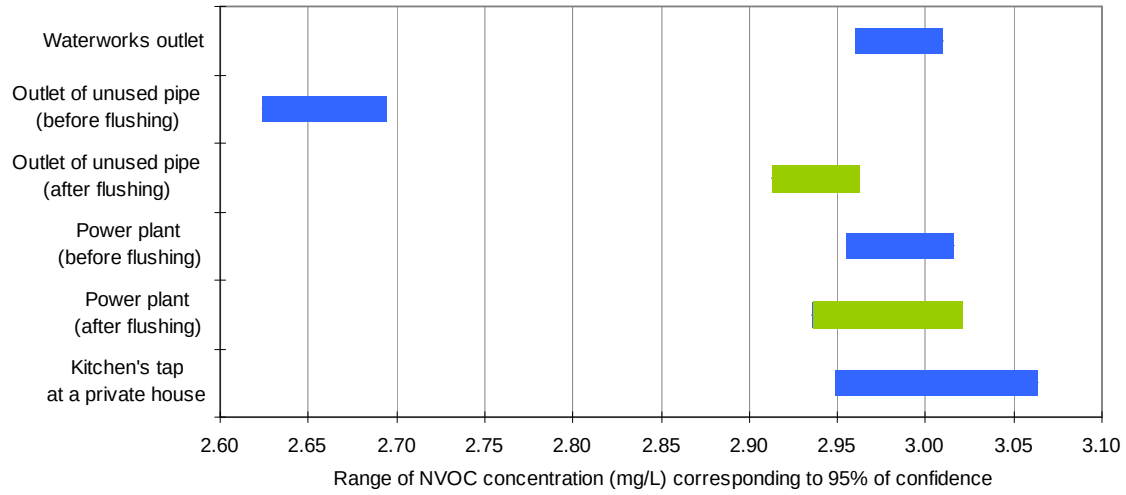

Figure 18 95% confidence interval of the NVOC concentration measured in the Farum network on 29/04/08
A colour code distinguishes the concentrations measured after flushing (light green) from the others (dark blue), which are assumed to reflect normal conditions in the network.

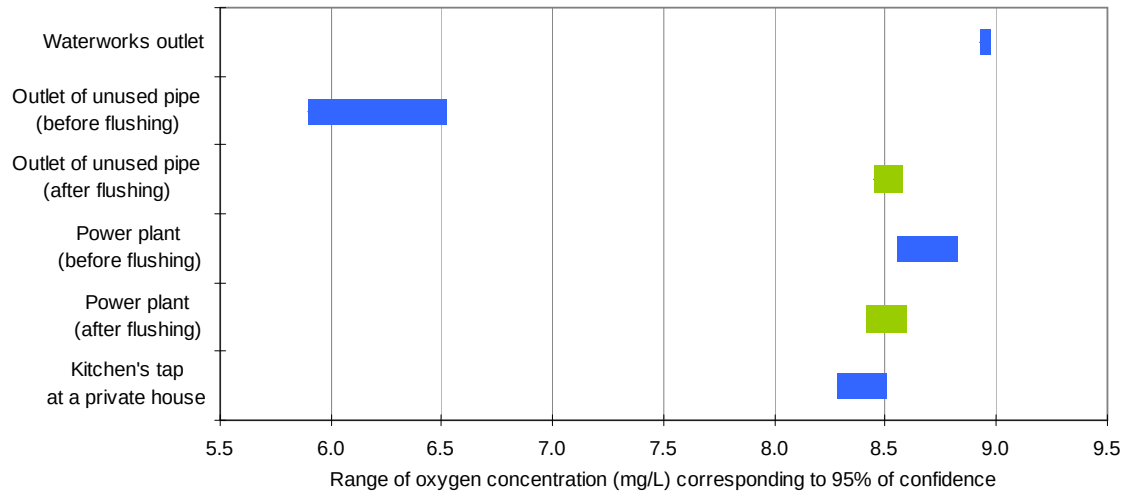

Figure 19 95% confidence interval of the oxygen concentration measured in the Farum network on 29/04/08
A colour code distinguishes the concentrations measured after flushing (light green) from the others (dark blue), which are assumed to reflect normal conditions in the network.

The results on NVOC measurements show that, considering the uncertainties, one can say that the only cases where the concentration is different from the waterworks are the outlet of the unused pipe (node 101) before and after flushing. The NVOC content in the water that has been stagnating for five days is about 0.3 mg/L lower than the background level in the water (cf. results for the unused pipe outlet before flushing in Figure 18). Concerning the concentration measured after flushing, they are harder to interpret due to the uncertainties on the actual disturbance created by the act of flushing, although some parallels with modelling computations are investigated in the next section. Finally, the small differences in NVOC content between the other locations and the waterworks are not large enough to allow us to state that the concentrations are different. Besides, it is important to note that for all the configurations investigated, no increase in NVOC content is observed, when compared to the source water.

The results on oxygen measurements illustrate first of all that the fluorescence oxygen meter provides a good repeatability of the measurements. As expected, the level of oxygen is a bit lower in the network than at the waterworks outlet (about 0.5 mg/L lower). In the particular case of the stagnant water in the unused pipe, a high oxygen consumption of more than 3 mg/L is observed. This shows clearly that some kind of oxidation or biodegradation process occurs in this pipe, most likely of ammonia or organic compounds. It is however hard to tell whether most of the compounds degraded were already in the water source or whether part of them migrated to the water during its transport in the PE pipes.

Comparison with the results from the modelling

The results from the measurements on NVOC obtained from the real network are now to be compared with the modelling work. However, the sampling results in NVOC are expressed as mg-C/L, while the modelling results are in mg/L. The first thing to do is thus to compute a molar weight ratio for the two antioxidants studied in this project: Irganox 1010 and Irgafos 168, as is done in Table 2. The results computed with EPANET can then be converted into concentration in mg-C/L in order to see the corresponding change in NVOC that should be observed if no degradation occurs.

Table 3 gives the modelling results at the locations where samples were collected, expressed both in µg/L and mg-C/L. Here again, two diffusion coefficients of the migrants in the water are investigated ($D_{w,i}$ = 10^{-10} and 10^{-9} m^2/s). However, even when $D_{w,i}$ is fixed, it is worth noting that the results presented do not all come from the same simulation. The results for the power plant before flushing and for the private house come from the simulations presented previously. Thus the values given in Table 3 can also be found in Figure 14 at 10 a.m. for nodes 6 and 11. This time of 10 a.m. was used because it is approximately the time when the samples were collected in the field. Nevertheless, it can be easily seen that once expressed as mg-C/L, the daily variations in concentration become insignificant compared to the precision

of the NVOC measurements. Concerning now the results after flushing, it was mentioned before that the act of flushing is believed to induce changes in the migration rates of the compounds to the water. A small model was thus built to compute the concentration at the unused pipe outlet and the power plant site, considering the increase of 1.4 L/s in demand created by the flushing. Finally, the concentration before flushing at the outlet of the unused pipe was also computed in EPANET. In the field, five days had elapsed between the last flush and the collection of the samples. Therefore, a pipe filled with water stagnating for five days was modelled, with an initial migrant concentration in the pipe set at the level computed for the case after flushing.

Table 2 Molar weights of the antioxidants Irganox 1010 and Irgafos 168

Migrants name	Molar weigth (g/mol)	Molar weigth (g-C/mol)	Ratio (g-C/g)
Irganox 1010	1176	876	0.745
Irgafos 168	643	504	0.784

Table 3 Modelling results for Farum network at the locations where samples were collected

Location in the network	Average concentration computed by EPANET for $D_{w,i} = 10^{-10}$ m^2/s			Average concentration computed by Epanet for $D_{w,i} = 10^{-9}$ m^2/s		
	ug/L	mg-C/L if Irganox	mg-C/L if Irgafos	ug/L	mg-C/L if Irganox	mg-C/L if Irgafos
Waterworks	0	0	0	0	0	0
Outlet of unused pipe (before flushing)	48	0.04	0.04	203	0.15	0.16
Outlet of unused pipe (after flushing)	37	0.03	0.03	146	0.11	0.11
Power plant (before flushing)	41	0.03	0.03	199	0.15	0.16
Power plant (after flushing)	36	0.03	0.03	152	0.11	0.12
Private House	26	0.02	0.02	128	0.10	0.10

Table 3 mainly illustrates that a small increase in NVOC, caused by the release of compounds from the PE pipes, should be observed in the network if no degradation occurs. The comparison with the field measurements should tell us more about it. This comparison is made in Figure 20 below, where the modelling results, for both values of $D_{w,i}$, are plotted on the same graph as the 95% confidence interval for the NVOC concentration measured in the field. In order to plot the modelling results, the increases in NVOC given in Table 3 were added to the average value measured at the waterworks, considered as the background NVOC level in the water. Due to high similarities between the results for Irganox 1010 and Irgafos 168, only the results for one of them were plotted (Irganox 1010) here.

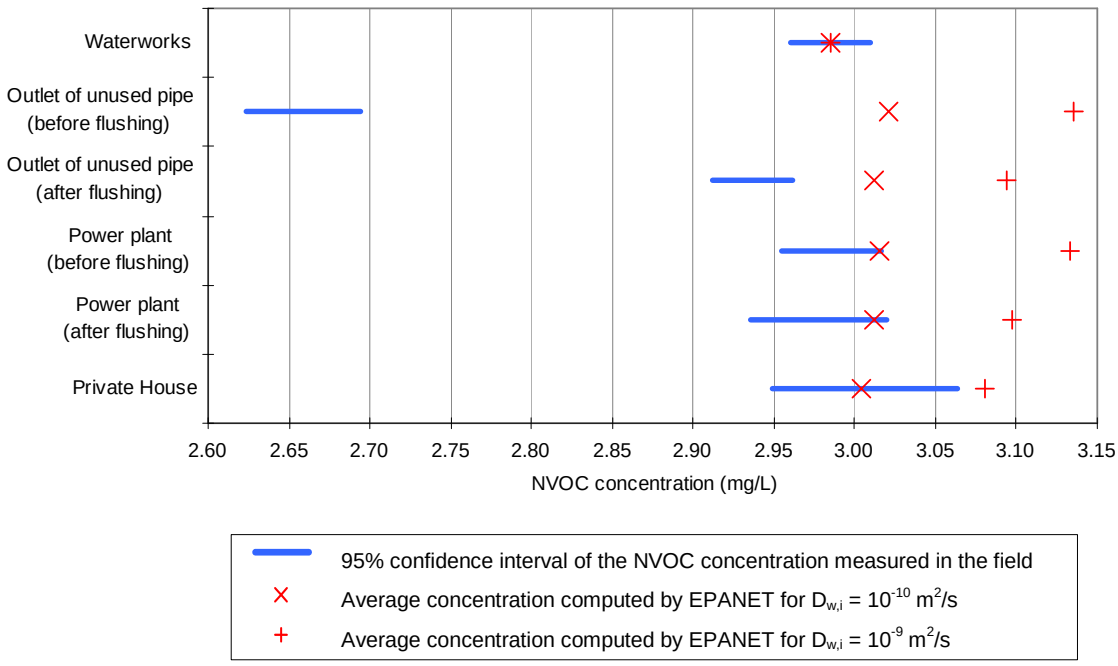

Figure 20 Comparison between modelling and sampling results for the Farum network
The modelling results correspond to the antioxidants Irganox 1010 or Irgafos 168, which have a concentration in the PE matrix of about 2 g/kg and a partition coefficient at the interface around $1.55*10^{-4}$, leading to a saturation concentration of 310 µg/L.

Discussion

No real match is observed in Figure 20 between the modelling work and the field measurements. The origins of the differences observed are probably multiple but can be traced.

Several uncertainties may exist in the modelling and could explain these differences. If one assumes that the migration theory presented in section 3.2 is correct, the level of migrants released depends on three chemical parameters: the concentration of the migrants in the pipe material ($c_{p,i}$), their diffusion coefficient in the water ($D_{w,i}$) and their partition coefficient at the interface between the water and the PE ($K_{w/p,i}$). In the modelling work, the results are always presented as percentage in saturation, which allows having identical results even when $c_{p,i}$ or $K_{w/p,i}$ are different. However, in our comparison here with field data, we look at the actual concentration and thus the values of $c_{p,i}$ or $K_{w/p,i}$ have a great impact on the results. Although the values used in the modelling were found in the literature, if it happens that in reality one of them is halved, the concentration of migrants released would also be halved of what has been computed. Similarly, two values of $D_{w,i}$ have been investigated in accordance to what was found in the literature, but the modelling results in Figure 20 clearly show how strong could be the consequences from a wrong estimation of this diffusion coefficient.

Degradation processes were not considered here but could have a significant role, especially for this Farum network where high residence times occur. The oxygen measurements made on site (cf. Figure 19) show that oxygen is consumed in the pipes, which confirms that some degradation processes occur indeed. However, it was chosen not to try to compare here the modelling results on degradation (cf. Figure 17) with field data because of too high uncertainties. Indeed, the half-life of the migrants in the water are not precisely known while at the same time, telling the origin of the oxygen consumption observed from the field results is quite complex. Many species such as ammonia or various types of organic compounds are indeed known to exist in the water can degrade. While the Farum waterworks claims that the water supplied to the network has a low content in ammonia, we do observe a decrease in NVOC on site, but it is not possible to tell which particular compounds have actually been degraded. Therefore, in the comparison of NVOC content between modelling and sampling results, even if a match was obtained for a certain migrant half-life, it would be impossible to say if the modelling is correct or completely wrong. The NVOC decrease measured on site could indeed be partly or totally due to the degradation of other compounds than the migrants.

To make the picture even more complex, not only Irganox 1010 or Irgafos 168 are expected to be found in the water but most likely both of them, as well as several other additives present in the pipe material (Brocca et al., 2002). Each migrant type would separately induce a small increase of the NVOC level in the water. Therefore, if we really want to compare the NVOC measured on site with the modelling results, all the compounds expected to migrate should be considered in the modelling. This is practically not possible yet because we simply do not know how many and which types of species could be released, and what migration characteristics they have.

The different aspects mentioned above clearly illustrate that in the case of the Farum network, NVOC is not a good indicator of the release of compounds from PE pipes. Since degradation processes occur in the pipes, no increase in NVOC can be observed and we cannot tell which of the following occurs: 1) no compounds are released from the PE pipes and the degradation observed is only due to compounds already in the source water, 2) compounds are released from the PE pipes but not degraded in the water, some species already in the source water are degraded and induce a higher NVOC decrease than the increase caused by the release of compounds from the pipes 3) compounds are released from the PE pipes and degraded in the water, but other species already in the source water are also degraded and contribute to the NVOC decrease. It is crucial to note that in each case, we can never tell the amount of migrants released from the PE pipes.

As a conclusion, one can say that the sampling work has clearly shown that NVOC is not a suitable approach for detecting the release of compounds from PE pipes. Indeed, the field measurements of NVOC were not even able to indicate whether any compounds' release or

degradation had occurred. Besides, even if an increase in NVOC had been measured, one could not have told which migrant had contributed to which part of this increase. In both cases no validation or calibration of the model from field data is thus possible. A measurement method such as Gas Chromatography-Mass Spectrometry (GC-MS) could be used instead. Indeed this method would enable the detection of very specific compounds in the water. It should thus be used to validate and maybe calibrate the modelling tool developed in this project. This GC-MS method was considered too complex to be used within the scale of the present study, but further works with this method or an equivalent should definitely be carried out on this topic.

5.2. Case of a middle-sized network with simple geometry (“Net 1”)

5.2.1. Presentation of the network

The second network case investigated is “Net 1”, which is one of the example models available with EPANET 2.0. This model is assumed to be similar to what can be found in real-world, although it only represents a network skeleton. This skeleton is composed by what can be called transportation pipes as opposed to distribution pipes. Distribution pipes would be much smaller and make the connection between the consumers and the network skeleton. This simplification reduces the computations and eases the handling of the results, but is sufficient to get a good feeling of the hydraulic and quality properties of the distribution system. This simplified system is composed one source (waterworks with its outlet pump), 12 pipes that are assumed to be in PE, 9 nodes and an elevated tank. The corresponding sketch of this network is presented in Figure 21. All input data, such as pipe lengths, diameters or water demands at nodes, were already defined in the model file provided with EPANET. Some tables in Appendix 5 give the detailed characteristics of the network. If it is assumed that this distribution system provides only water for domestic use and if the Danish average consumption of 160 L/day/person is used as a reference, this system would correspond to a town of about 35,500 inhabitants. This high number confirms that what is presented in Figure 21 is only the skeleton of the network.

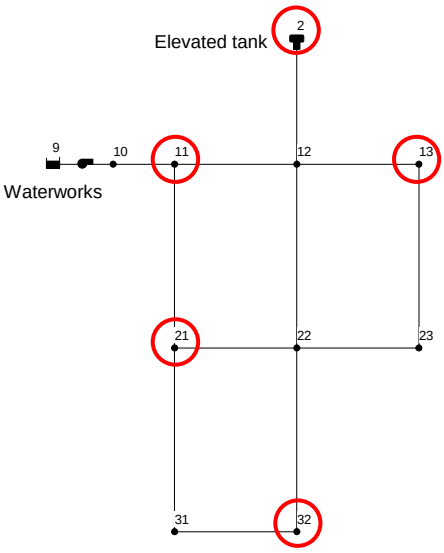

Figure 21 Sketch of the EPANET network model “Net 1”
The red circles indicate the locations that were considered relevant to give an overview of the pollution level. At these locations, the migrant concentration is analysed in detail.

5.2.2. Simulation conditions

For these simulations, the model "Net 1" is kept as the original provided with EPANET 2.0., expect for one thing: the pattern used to model diurnal variations in demand. In this study, the existing pattern was indeed replaced by the one given in Figure 7, which seemed more appropriate to reflect real conditions. With this configuration, the waterworks pump and the elevated tank work in combination to supply water to the nodes. The pump working status (i.e. on-off) is in fact controlled by the water level in the elevated tank (cf. Appendix 5). This creates a daily cycle of the pump working that is illustrated on Figure 22. Basically when the pump is on (from 9:30 a.m. to 12 p.m.), almost all the water consumed comes from the waterworks and the elevated tank is filling with water (except around 7 p.m.). Inversely, when the pump is not working (from 12 p.m. to 9:30 a.m.), the water supply is ensured by the elevated tank. As a consequence of this working cycle, the water age varies along the day and from one node to another as it can be observed on Figure 23.

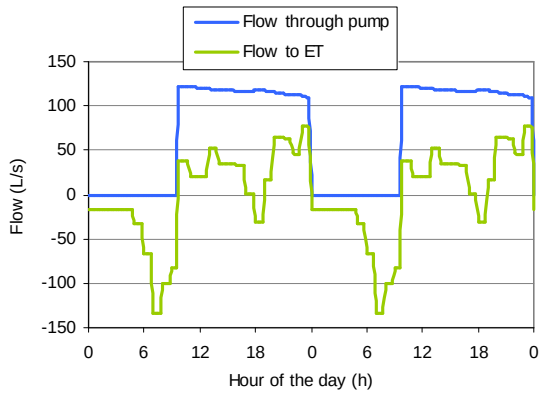

Figure 22 Computation of the waterworks pump working cycle in "Net 1"

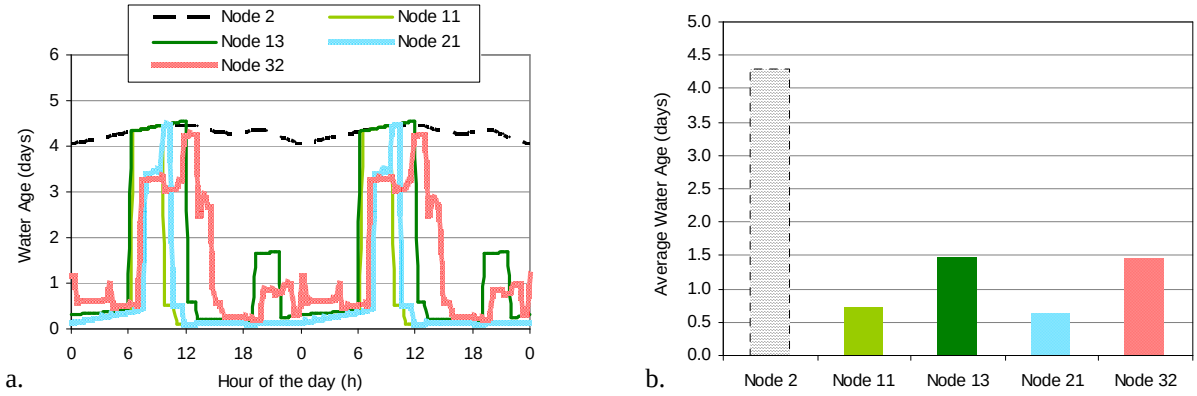

Figure 23 Computation of the water age in "Net 1"
Graphs a and b represent respectively the water age variation along the day and its average value at relevant nodes of the network.

Figure 24 below presents the network characteristics in terms of flow conditions. It shows two “network map plots” of the Reynolds number in the network pipes at two times of the day that seemed relevant: a night time at 4:30 a.m. and a time of peak in demand at 7:30 p.m. More details about the way this figure was obtained were discussed in the Farum case study. It is visible that contrary to the Farum network case, the conditions are turbulent in most of the network and most of the time (even at night). When looking at the detailed conditions along the day, laminar conditions are found to occur in three pipes of the network. Nevertheless, they are localized and last very little over time (1-2 hours), which probably makes them negligible on the scale of the overall network.

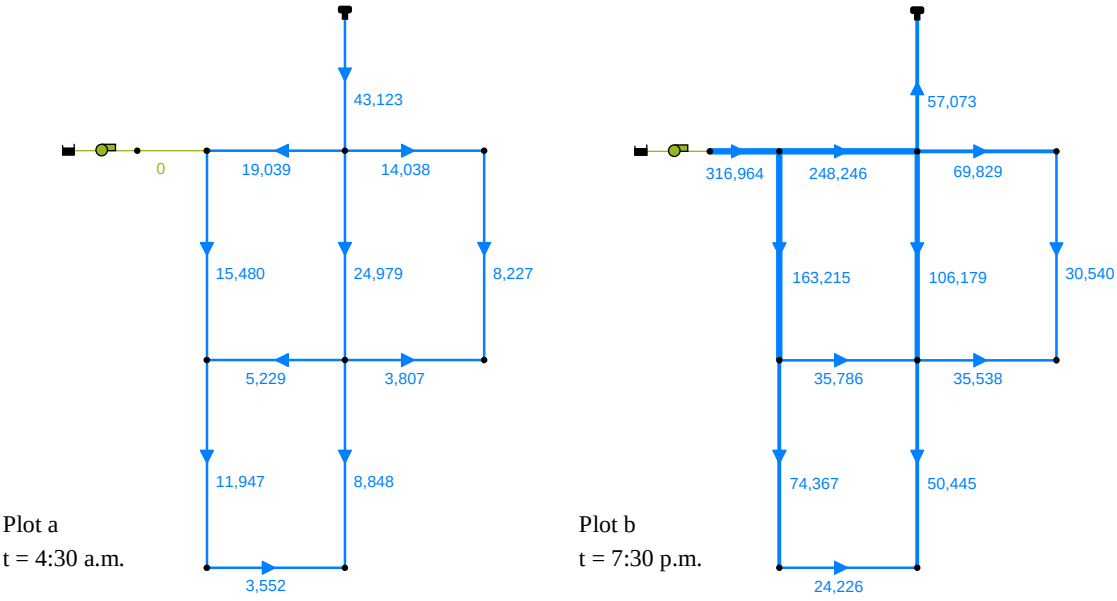

Figure 24 Computation of the Reynolds number in “Net 1”
The numbers plotted next to the pipes are estimations of the Reynolds number. The colour code indicates the distinction between laminar (thin green line) and turbulent (thick blue line) flow conditions.

EPANET has been used to compute the release of compounds from pipes to water. Time steps of 5 minutes and of 30 seconds have been used in the program for the hydraulic and quality computations, respectively. Model runs show that a simulation period of at least 30 days is necessary to reach a stabilized concentration profile over a daily cycle. This means that within this period, the initial quality that was set at 0 µg/L at all points, still has an influence on the results. This transition time corresponds to the time required to flush the entire network. Since the elevated tank has a large capacity of about 8300 m^3 and is initially full of non-contaminated water, a long period is thus required to flush it completely. In order to avoid any effect of these initial conditions, the results presented below were obtained after 38 days of simulation period.

5.2.3. Migrant concentration in the network when no degradation is modelled

Figure 25 presents the saturation profile of migrants at several locations in the network. These locations, highlighted on Figure 21, were considered relevant to give a fair overview of the contamination degree in the system. Results for the overall network are also displayed in Figure 26, which presents a "network map plot" of the contamination at two times of the day. Here again two case are investigated, with diffusion coefficient of the migrants in water ($D_{w,i}$) of 10^{-10} and 10^{-9} m^2/s, respectively.

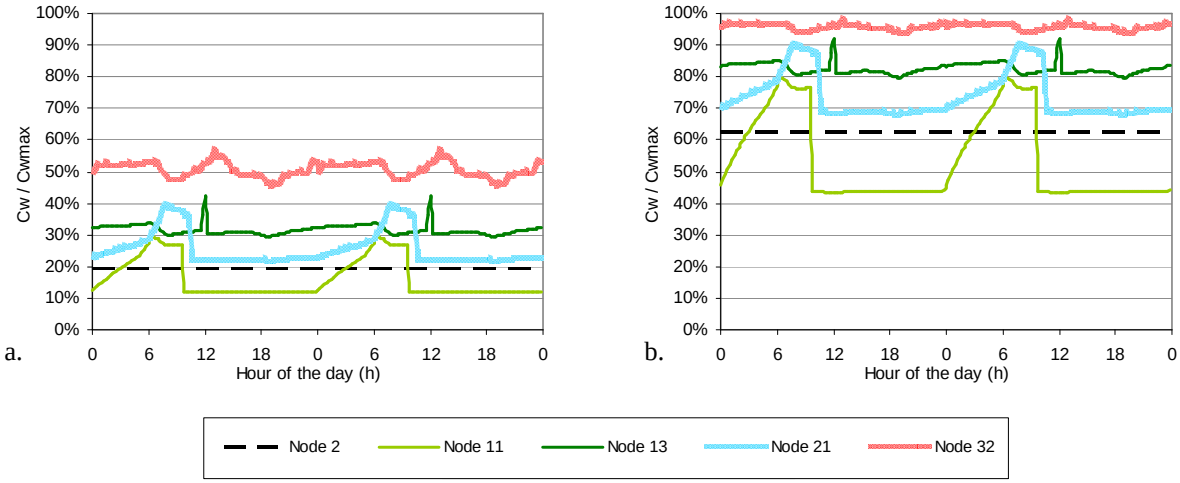

Figure 25 Simulation results for "Net 1": daily variations of the migrant concentration
The two graphs represent the saturation level of species along the day at relevant nodes of the network, for migrant's diffusion coefficient in the water of 10^{-10} m^2/s for Graph a and 10^{-9} m^2/s for Graph b. If one considers antioxidants such as Irganox 1010 or Irgafos 168 then the concentration of species in the PE matrix is about 2 g/kg and their partition coefficient at the interface around $1.55*10^{-4}$, leading to a saturation concentration of 310 µg/L.

Here again, the high influence of $D_{w,i}$ is observed. Indeed, in the simulation conditions, the saturation level ranges from 10% to 60% when $D_{w,i} = 10^{-10}$ m^2/s, while it ranges from 40% up to almost saturation when $D_{w,i} = 10^{-9}$ m^2/s. This can be clearly seen on both Figure 25 and Figure 26. Additionally, it can be noticed that there is no real link in this case between longer residence time and higher contamination of the water with migrants. A link should however be made with the pump working cycle (presented on Figure 22), as explained in the next paragraph.

The modelling results clearly emphasize that the working state of the waterworks pump has a great influence on the species' content in the network. When the pump is working (from 9:30 a.m. to 12 p.m.), there is an increasing migrant concentration from the closest to the furthest locations from the waterworks. Indeed, the water consumed at nodes far from the waterworks has travelled through more pipe length and thus received more migrants. This is for example

visible on Graph b, where the migrant's content increases gradually for nodes 11, 21, 13 and 32 with saturation levels of 45%, 70% 80% and 95%, respectively. When the pump is not working, the configuration is quite different since all the water supplied comes from the elevated tank. While the water from the waterworks contains no species at all, the water from ET is already containing migrants: about 20% and 60% in saturation level when $D_{w,i}$ equals 10^{-10} and 10^{-9} m^2/s, respectively. Starting from this basis, the concentration increases proportionally to the distance from ET (node 2). In this network case however, the elevated tank is relatively close to the rest of the network. Therefore, the fact that the water comes from ET does not, increase the total transport distance, for some locations. This can be observed in Figure 25 for nodes 13 and 32. On the contrary, for other locations in the network, the transport from the waterworks to the node is longer in distance via ET than when it is done directly. That is the reason why an increase in the migrant's content is observed for nodes 11 and 21 between 12 p.m. and 9:30 a.m. (waterworks pump off). This influence of the pump working cycle on the pollution degree in the network is also visible in Figure 26. This figure presents a "network map plot" of the contamination at two times of the day (4:30 a.m. and 7:30 p.m.), respectively corresponding to the configuration modes: pump off and pump on. The arrows indicate the flow direction and permit seeing easily whether the water is supplied by the waterworks or by ET.

Finally, a particular phenomenon occurs just after the pump starts again: peaks in migrant concentrations are observed for some locations, for example at node 13 around 12 a.m. (cf. Figure 25). The reason behind this is most probably a change in the direction of the water flow. Indeed, it is likely that the water that is on its way to supply node 11 just before the pump starts, is suddenly flushed back towards the rest of the network. When this water is eventually consumed, it has a concentration in migrant roughly equal to the concentration at node 11, when the pump is off, plus the contribution caused by the transport from node 11 back to the consumption point, hence the peaks observed.

Nevertheless, it must be pointed out that the influence of the pump cycle on the contamination level, which was observed under several forms in this network, is highly dependent on the position of ET in the network. In fact, if ET was next to the waterworks, the saturation level in ET would be close to 0% and thus almost flat profiles would be observed along the day at the other nodes. In such a case, the concentration profiles would be at about the same level than when the pump is off and probably slightly affected by the changes in demand. The question of the relevance of the variations observed here must therefore be raised in the cases of bigger networks, such as the last case study ("Net 3").

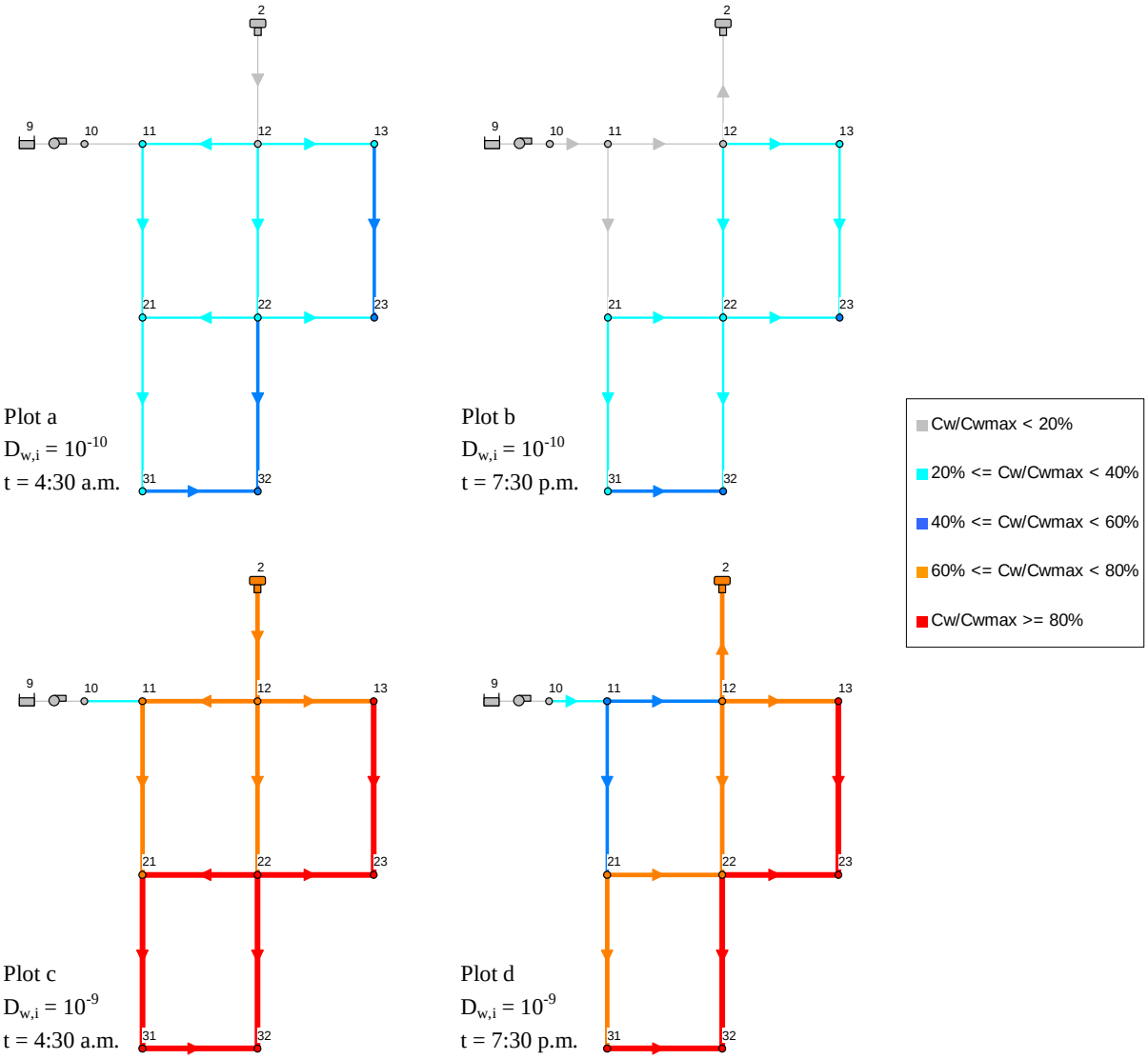

Figure 26 Simulation results for "Net 1": map-plot of the migrant concentration
The figure represents the migrant saturation level in the network when no degradation is simulated at two times of the day. Plots a and b correspond to the case where a diffusion coefficient of the migrants in the water is 10^{-10} m^2/s, and plots c and d to the case where it is 10^{-9} m^2/s. If one considers antioxidants such as Irganox 1010 or Irgafos 168 then the concentration of species in the PE matrix is about 2 g/kg and their partition coefficient at the interface around $1.55*10^{-4}$, leading to a saturation concentration of 310 µg/L.

5.2.4. Systematization of the migrant concentration profile

Similarly to what was done for the Farum study case, the cumulative distribution of the migrant concentration has been computed. The corresponding plot is given in Figure 27 below. Details about the meaning of the cumulative distribution of a data set, and the way to compute it, were presented in the section 5.1.4 and are given in Appendix 3. This cumulative distribution gives systematized information on the network behaviour with regards to contamination caused by PE pipes use. Figure 27 will especially be used further in the

discussion section (cf. section 5.4), to make a comparison between the different network cases studied in this project.

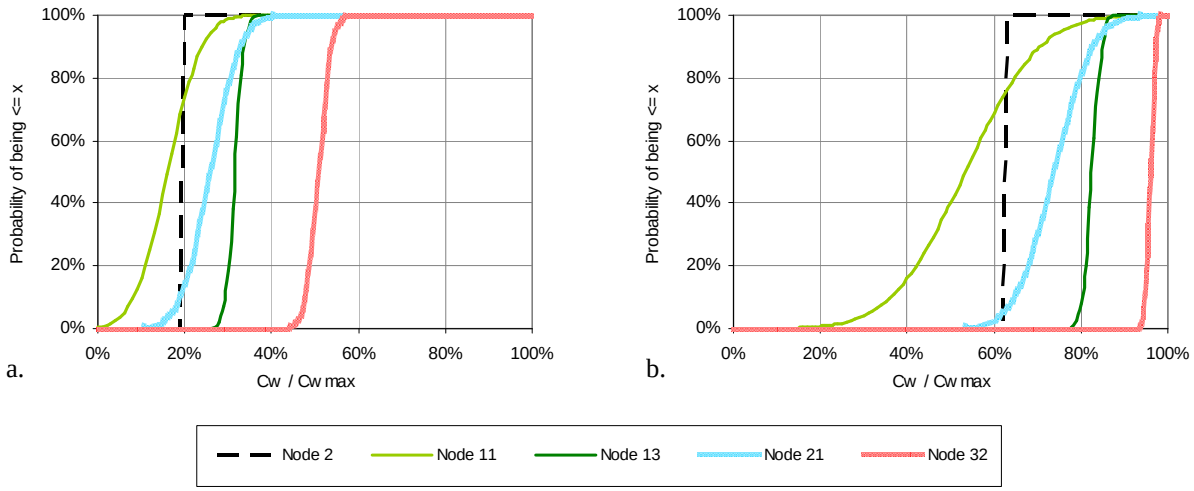

Figure 27 Simulation results for “Net 1”: cumulative distribution of the migrant concentration
The two graphs represent the probability distribution that the saturation level along the day is ≤ x (the abscissa), for migrant’s diffusion coefficient in the water of 10^{-10} m^2/s for Graph a and 10^{-9} m^2/s for Graph b. If one considers antioxidants such as Irganox 1010 or Irgafos 168 then the concentration of species in the PE matrix is about 2 g/kg and their partition coefficient at the interface around $1.55*10^{-4}$, leading to a saturation concentration of 310 µg/L.

5.2.5. Effect of degradation on the migrant concentration

Similarly to what was done for the previous network case, the effect of degradation on the concentration profile has been studied here. A total of six cases are investigated: one case with no degradation and five cases with half-lives of 28 days, 21 days, 14 days, 7 days and 1 day. The simulations results are gathered in Figure 28, which shows for each case the mean saturation level in migrants at the investigated nodes of the network. Here again, two values of $D_{w,i}$ are investigated: 10^{-10} and 10^{-9} m^2/s.

The relation between the water age at nodes and the reduction of the migrant content in water due to degradation is observed again here, similarly to the Farum network case. The decrease induced by degradation processes is indeed stronger at node 2 than at node 11 (cf. Figure 28), since the mean water ages are 4.3 and 0.7 days, respectively (cf. Figure 23). However, it is observed that the influence of degradation on the overall degree of contamination is much weaker for this network case “Net 1”, than it was for the Farum network. Indeed, for most of the half-lives investigated (7-28 days) the decrease in saturation level caused by degradation processes is less than a few percent for nodes 11, 13, 21 and 32 (cf. Figure 28). This is due to the fact that the maximum water age in the network is only about 1.5 days (cf. Figure 23) if

one excludes ET (node 2). Thus, degradation has simply not the time to occur during the transport since the water is consumed before.

The detailed variations of the migrant concentration along the day are not given here, not to overload the report, but are available in Appendix 5. Although Figure 28 summarizes the overall picture well enough, it is still interesting for this particular network case to elaborate some more on these variations. Indeed, this network is quite special for a reason already mentioned and discussed before: the network is alternatively supplied either by the elevated tank only, or by both the waterworks and the tank. Due to this cycle, the water is about 4 days older when it comes from ET than when it comes directly from the source. As a consequence, when the migrant half-life is short, degradation processes can become of importance for the contamination level. In such cases indeed, some parts of the network receive less contaminated water when is comes from ET than if it had come from the source directly. This phenomenon can be observed when looking at the variations of the migrant concentration along the day at some nodes (e.g. node 13 between 6 a.m. and 12 a.m. visible on Graphs c, d, e and f in Appendix 5).

On a general scale, these simulations emphasize that the network geometry may actually affect the influence of degradation processes on the migrant concentration, at least in some parts of a network.

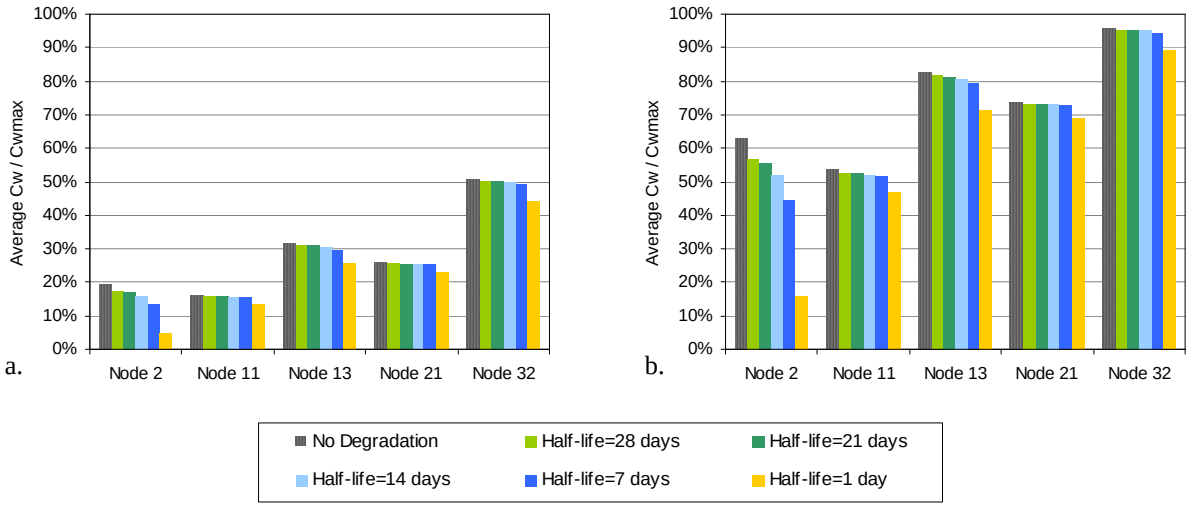

Figure 28 Simulation results for "Net 1": effect of degradation on the migrant concentration
The figure represents the daily average of the migrant saturation level at relevant nodes of the network and for different migrant half-lives. In these simulations, the migrant's diffusion coefficient in the water is 10^{-10} m^2/s for Graph a and 10^{-9} m^2/s for Graph b. If one considers antioxidants such as Irganox 1010 or Irgafos 168 then the concentration of species in the PE matrix is about 2 g/kg and their partition coefficient at the interface around $1.55*10^{-4}$, leading to a saturation concentration of 310 µg/L.

5.3. Case of a large network with complex geometry (“Net 3”)

5.3.1. Presentation of the network

The third network case investigated is “Net 3”. As “Net 1”, it is one of the example models available with EPANET 2.0. and is assumed to be similar to what can be found in real-world, although again here only a network skeleton is modelled. Compared to the previous network case, the network “Net 3” is much bigger, since the simplified system is already composed of two sources, a lake and a river with their respective pumps, 117 pipes (compared to only 12 pipes for “Net 1”), 92 nodes and 3 elevated tanks in the network. The sketch of this network is presented in Figure 29. All input data, such as pipe length, diameters or water demands at nodes were already defined in “Net 3”. Some tables in Appendix 6 give the detailed characteristics of the network.

If it is assumed that this distribution system provides only water for domestic use and if the Danish average consumption of 160 L/day/person is used as a reference, this system would correspond to a town of about 367,300 inhabitants. This confirms that this network is much larger than “Net 1” that was investigated in the previous section. Besides, it is worth repeating that here again the network modelled is only the “skeleton” of a real network. Only “transportation pipes” that are also called “water highways” are modelled here.

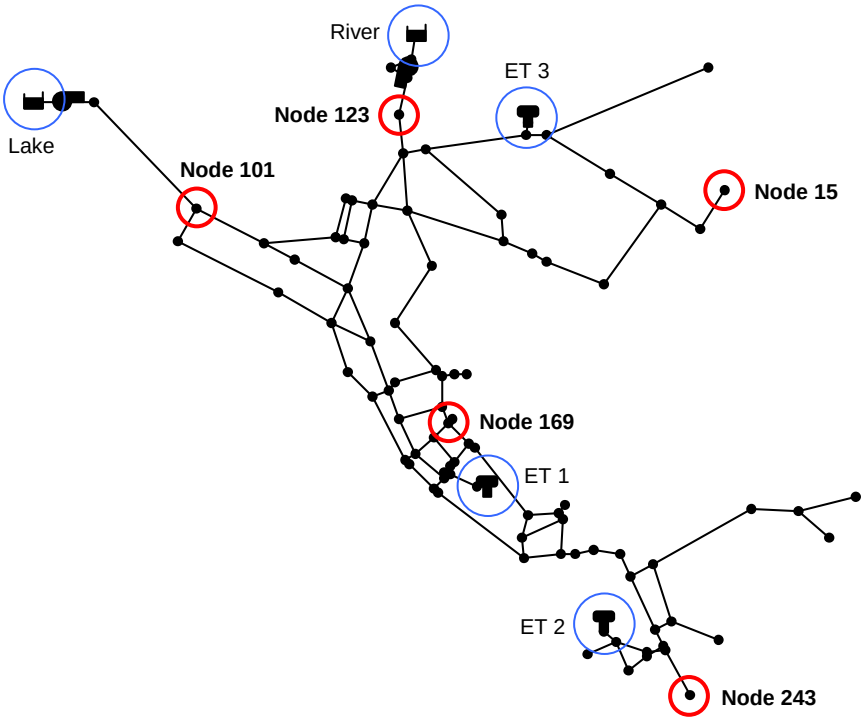

Figure 29 Sketch of the EPANET network model “Net 3”
The thick-red circles indicate the locations that were considered relevant to give an overview of the pollution level. At these locations, the migrant concentration is analysed in detail. The thin-blue circles are used to highlight the locations of the two sources and the three elevated tanks (ET).

5.3.2. Simulation conditions

For these simulations, the model "Net 3" has been kept as the original provided with EPANET 2.0., expect for two things: The first thing modified concerns the patterns used to model daily variations in demand. In the original version, 5 patterns exist in total, 4 of them being defined for 4 specific nodes. These patterns have been unchanged, but the last pattern that was used for all the other nodes (88 nodes) has been replaced by the one from Figure 7. This pattern has been changed, because the original one did not seem to reflect what we could expect from real conditions (e.g. low demands at night, peaks in demand in the morning and evening, etc.). The second modification made on the model concerns the pump connecting the lake to the network. In the original version, a rule is set up so that this pump works 15 hours at the beginning of the simulation period and then stops for the rest of the simulation. The reason behind this is that "Net 3" is a model example used to study the trace of the water coming from the lake in the network, as seen on the US-EPA webpage on EPANET (2008). In our case, was chosen to remove this control rule and keep both sources providing the network along the simulation period. It was indeed considered that this configuration was more interesting to investigate. Consequently, both the river and the lake supply the network at all time of the day. This network case is thus quite different from "Net 1", since the elevated tanks are used here as tools to handle peaks in demand but are never the only sources of water in the network.

Figure 30 illustrates the supply of water from the two sources to the network. The inflow from the river is more than twice the inflow from the lake and it is quite visible that these inflows are governed by the demands in the network (cf. comparison of Figure 30 with the demand pattern from Figure 7).

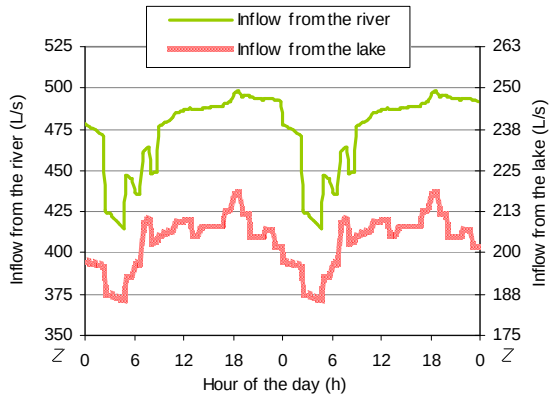

Figure 30 Computation of the inflow of water from the sources to the network in "Net 3"
It should be noted that the two curves do not have the same Y axis. The inflow from the river is indeed quite higher.

The water age in the network increases from the sources in the north-western parts of the network to the eastern and south-eastern parts, located the furthest from the network. To this must be added the impact of the three elevated tanks that act as a “booster” of the water age, since they contain large quantities of water that is renewed more slowly than the water in the network pipes. However, the influence of this “old water” on the areas surrounding the tanks depends greatly on the location, because water is anyway supplied at all time by both the river and the lake. For some locations, indeed, almost all the water comes from the tank when the demand reaches a peak, while in others, it only provides the lacking surplus in supply caused by the peak. Thus in the latter case, because the water from the tank is mixed with the water from the source(s), the overall water age in the area remains quite low and never reaches the age of the water inside the tank. These two different cases are observed at the locations that are investigated in this project, as seen in Figure 31and Figure 32 which give the average and the variations along the day of the water age at nodes 15, 101, 123, 169 and 243. For example, a very high water age is observed at node 15 during the period of the day when the node is supplied with water coming almost only from the elevated tank 3. In opposition, the water supplying nodes 169 and 243 is coming in majority from the sources directly and only partly from the near-by tank(s). Thus, peaks in water age are observed in these nodes but with a much lower magnitude than what is seen at node 15. Finally, nodes 101 and 123 are close to the source and thus never supplied by water from the tank. The water age is therefore relatively low there with almost no variations along the day.

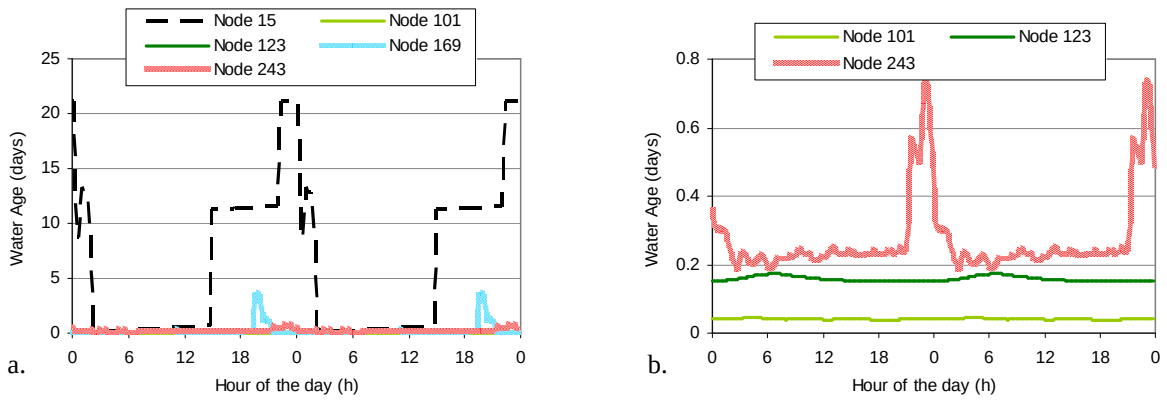

Figure 31 Computation of the water age in “Net 3”: variations along the day

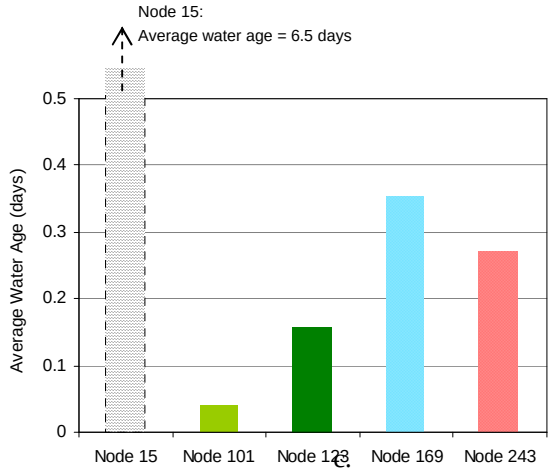

Figure 32 Computation of the water age in “Net 3”: mean age

Figure 33 presents the network characteristics in terms of flow conditions. It shows two “network map plots” of the Reynolds number in the network pipes at two times of the day that seemed relevant: a night time (4:30 a.m.) and a time of peak in demand (7:30 p.m.). More details about the way this figure was obtained were discussed in the Farum case study. Similarly to the previous case study “Net 1”, the turbulent conditions are observed in most of the network and during most of the time, although laminar conditions are found to occur in the smallest branching. These conditions seem to last some time (about 5 hours) but remain localized in the network extremities. It is interesting to see if they have any influence on the quality conditions in the network, especially in our case on the contamination caused by plastic pipes.

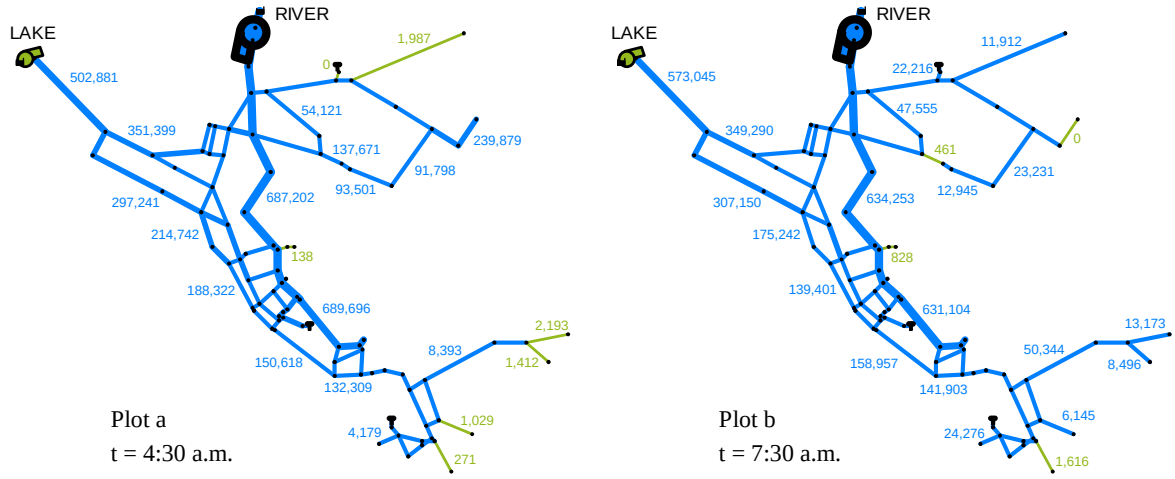

Figure 33 Computation of the Reynolds number in the “Net 3”
The numbers plotted next to the pipes are estimations of the Reynolds number. The colour code indicates the distinction between laminar (thin green line) and turbulent (thick blue line) flow conditions.

EPANET has been used to compute the release of compounds from pipes to water. Time steps of 5 minutes and of 30 seconds have been used in the program for the hydraulic and quality computations, respectively. Model runs show that a simulation period of at least 110 days is necessary to reach a stabilized concentration profile over a daily cycle. For simulation period shorter than this, the initial quality in the network (0 µg/L) still has an influence on the results. As explained for “Net 1”, this long transition time is due to the presence of tanks in the networks, which have large capacities. In order to avoid any effect of these initial conditions, the results presented below were obtained after 160 days of simulation period.

5.3.3. Migrant concentration in the network when no degradation is modelled

Figure 34 presents the saturation profile of migrants at several locations in the network. These locations, highlighted in Figure 29, were considered relevant to give a fair overview of the contamination degree in the system. Results for the overall network are also displayed in Figure 35, which presents a “network map plot” of the contamination at two times of the day. Here again two cases are investigated, with diffusion coefficient of the migrants in the water ($D_{w,i}$) of 10^{-10} and 10^{-9} m^2/s, respectively.

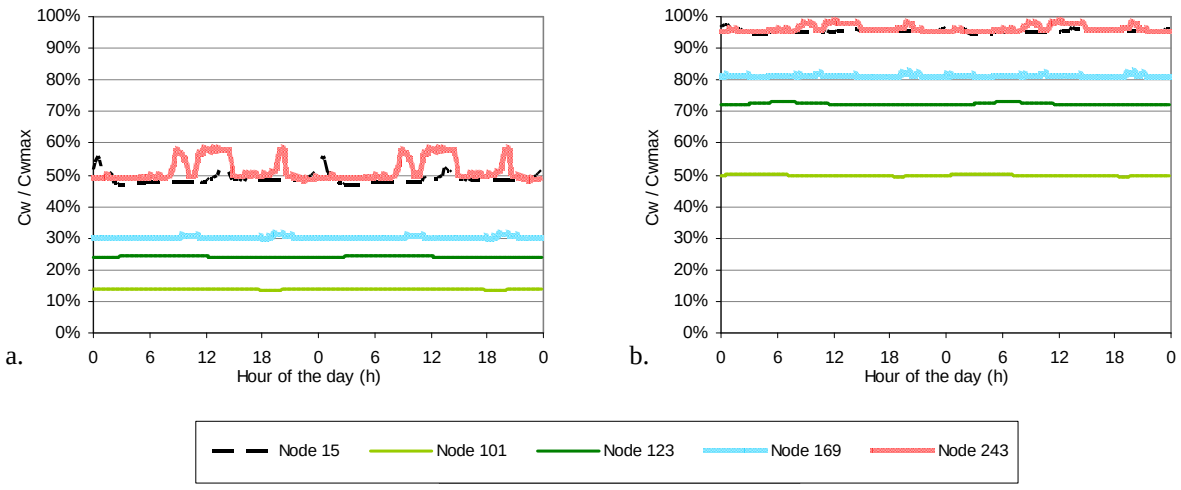

Figure 34 Simulation results for “Net 3”: daily variations of the migrant concentration
The two graphs represent the saturation level of species along the day at relevant nodes of the network, for migrant’s diffusion coefficient in the water of 10^{-10} m^2/s for Graph a and 10^{-9} m^2/s for Graph b. If one considers antioxidants such as Irganox 1010 or Irgafos 168 then the concentration of species in the PE matrix is about 2 g/kg and their partition coefficient at the interface around $1.55*10^{-4}$, leading to a saturation concentration of 310 µg/L.

For this model, it is again obvious that the diffusion coefficient of the migrants in the water ($D_{w,i}$) has a great impact on the overall degree of contamination. Indeed, in the simulation

conditions, the saturation level ranges from 10% to 60% when $D_{w,i} = 10^{-10}$ m^2/s, while it ranges from 50% up to almost saturation when $D_{w,i} = 10^{-9}$ m^2/s. Similarly to the previous network case "Net 1", the residence times in the network do not seem long enough to affect significantly the degree contamination from migrants, as well seen in the Farum case.

It can clearly be observed that the migrant concentration increases from the north-western parts to the eastern and south-eastern parts of the network (cf. Figure 35). It rigorously corresponds to the increasing in transport distance from the water sources (i.e. the river and the lake) to the network branching, and is not really varying along the day. Indeed, contrary to the "Net 1" case, the existence of elevated tanks in the network is not found to affect significantly the concentration profiles along the day. The reason behind this is a combination of the network size, the localization of the tanks and the fact that the water supply from the sources is continuous along the day. Therefore, for this network case, the tanks may act as a source of water aging but not really as a source of greater transport distance between the sources and the consumers, when compared to the scale of the network, hence not as a source of additional contamination with migrants. On a local scale, small variations are still observed, as in the case of nodes 15 and 243 (cf. Figure 34 Graph a), but on the network scale, there is nothing occurring like the two-phases-situation observed for "Net 1" (cf. Figure 26 compared with Figure 35).

Therefore, it can be established that for large networks the contamination degree is governed by the network geometry, in the sense of the transport distances in the system. These simulations also show that although the variations in demand may have real effect on the flow conditions in the system, particularly the flow regime, they have in practice little impact on the overall content of migrants in the water, which is almost steady over time.

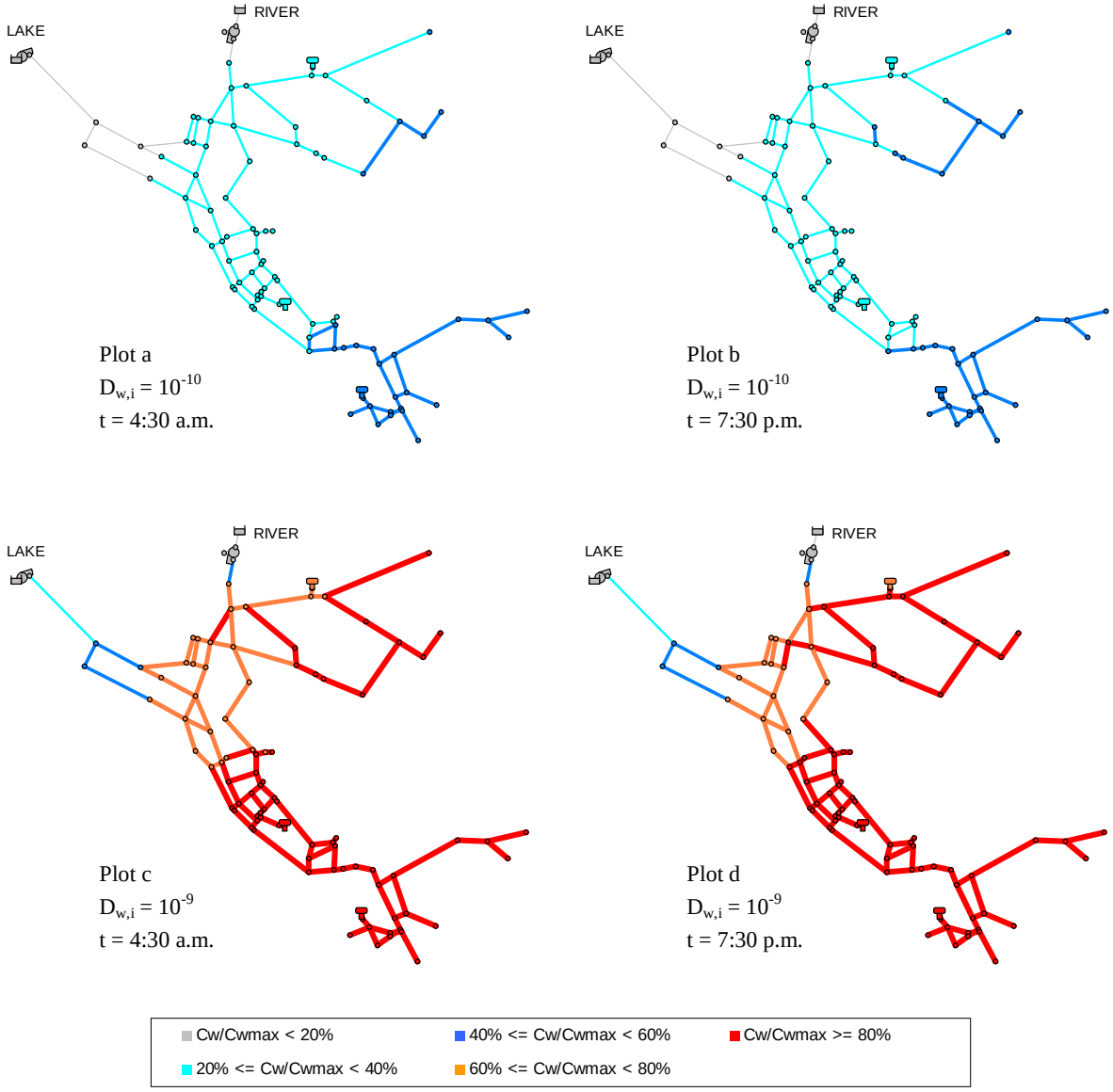

Figure 35 Simulation results for “Net 3”: map-plot of the migrant concentration
The figure represents the migrant saturation level in the network when no degradation is simulated at two times of the day. Plots a and b correspond to the case where a diffusion coefficient of the migrants in the water is 10^{-10} m^2/s, and plots c and d to the case where it is 10^{-9} m^2/s. If one considers antioxidants such as Irganox 1010 or Irgafos 168 then the concentration of species in the PE matrix is about 2 g/kg and their partition coefficient at the interface around $1.55*10^{-4}$, leading to a saturation concentration of 310 µg/L.

5.3.4. Systematization of the migrant concentration profile

Similarly to what was done for the two other network case studies, the cumulative distribution of the migrant concentration has been computed and plotted in Figure 36 below. It gives systematized information on the network behaviour with regards to contamination caused by PE pipes use, and is used in the discussion section 5.4, to make a comparison between the three network configuration investigated in this study.

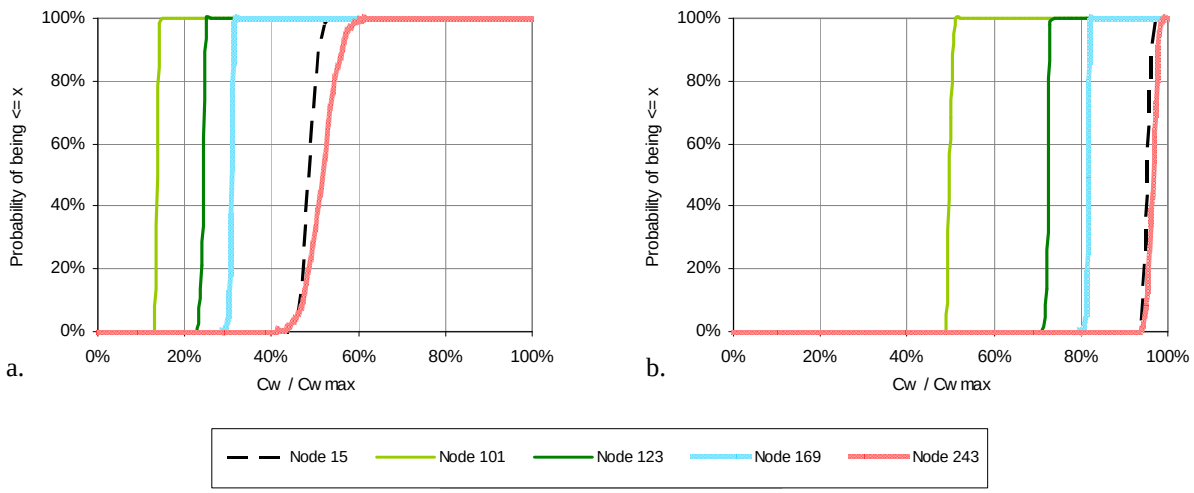

Figure 36 Simulation results for "Net 3": cumulative distribution of the migrant concentration
The two graphs represent the probability distribution that the saturation level along the day is ≤ x (the abscissa), for migrant's diffusion coefficient in the water of 10^{-10} m^2/s for Graph a and 10^{-9} m^2/s for Graph b. If one considers antioxidants such as Irganox 1010 or Irgafos 168 then the concentration of species in the PE matrix is about 2 g/kg and their partition coefficient at the interface around $1.55*10^{-4}$, leading to a saturation concentration of 310 µg/L.

5.3.5. Effect of degradation on the migrant concentration

Again, similarly to the previous network case studies, the effect of degradation on the concentration profile has been assessed. A total of six cases are investigated: one case with no degradation and five cases with half-lives of 28 days, 21 days, 14 days, 7 days and 1 day. The simulation results are gathered in Figure 37, which shows for each case the mean saturation level in migrants at the investigated nodes of the network. Here again, two values of $D_{w,i}$ have been investigated: 10^{-10} and 10^{-9} m^2/s.

Clear similarities are observed here with the results from the previous network case "Net 1". Indeed, we see again the expected relation between the water age at nodes and the reduction of the migrant content due to degradation. However this relation is slightly more complex in this case, due to the bigger size of the network. In the network parts where the water age is high mostly because of a continuous transport over long distances (e.g. nodes 101, 123, 169) should be distinguished from the network parts where the water age is high mostly because the water is "stopping" in an elevated tank on the way (e.g. nodes 15, 243). Naturally, a stronger effect of degradation on the migrant concentration is observed in the latter case (cf. Figure 37). This phenomenon is not only influencing the mean level of migrants in the water, but also the variations of their concentration along the day.
The detailed variations of the migrant concentration are not given here, not to overload the report, but are available in Appendix 6. It is observed that for locations where the water age is

governed by the long transport distances (e.g. nodes 101, 123, 169), the variations observed along the day in Figure 34 are simply shifted downwards. However, for locations whose water supply passes by an elevated tank (e.g. nodes 15, 243), these daily profiles in concentration may really be changed by degradation processes. In these cases indeed, the water coming from the tank can be less contaminated than if it had come from the source directly. Nevertheless, this phenomenon is much weaker here than in the “Net 1” case.

These simulations confirm that the network geometry may affect the influence of degradation processes on the migrant concentration, but they also emphasize that the larger the network is, the lees its geometry affects the overall picture in the network. Besides, it is confirmed with this case that in large networks this influence of degradation on the migrant concentration remains relatively low for most of the half-lives investigated (7-28 days). Nevertheless, it should be reminded that high uncertainties exist on the actual half-lives of these migrants from PE pipes.

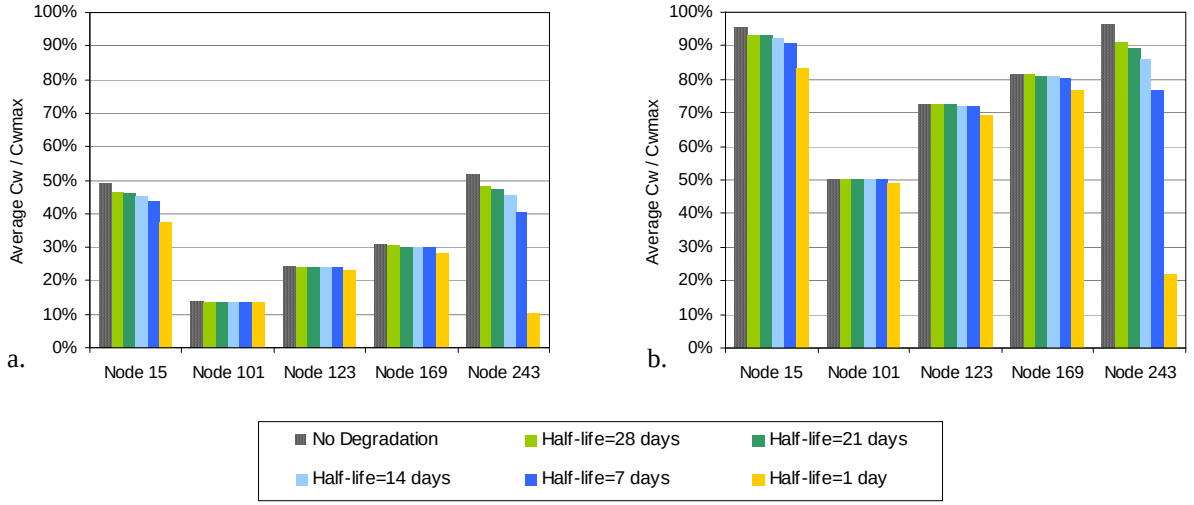

Figure 37 Simulation results for “Net 3”: effect of degradation on the migrant concentration
The figure represents the daily average of the migrant saturation level at relevant nodes of the network and for different migrant half-lives. In these simulations, the migrant’s diffusion coefficient in the water is 10^{-10} m^2/s for Graph a and 10^{-9} m^2/s for Graph b. If one considers antioxidants such as Irganox 1010 or Irgafos 168 then the concentration of species in the PE matrix is about 2 g/kg and their partition coefficient at the interface around $1.55*10^{-4}$, leading to a saturation concentration of 310 µg/L.

5.4. Discussion and conclusions on the modelling work

Elaboration of a tool to model the release of compounds from the pipe to the water

EPANET 2.0. has been modified and used in a series of simulations to study the release of compounds from PE pipes to drinking water in distribution networks. Various configurations have been investigated, centred mainly on three networks of different size or geometry. For each of them, two values of diffusion coefficient of the migrants in the water have been modelled (10^{-10} and 10^{-9} m^2/s) as well as different degradation rates of the migrants in the water (no degradation, half-lives of 28, 21, 14, 7 days and 1 day). For all these simulations, no particular problems were faced with the model and all computations are believed to be correct. As a consequence, it can be stated that the modified version of EPANET created in this project can be successfully used to compute the release of organic compounds from PE pipes into drinking water. However, no validation of this modelling tool with actual field data has been possible in this project, due to the absence of a suitable method for measuring the release of compounds for the PE pipes.

Nevertheless, the original EPANET program has been modified in such a way that the new version can be calibrated to compute the migration of any compound from the pipe material to the water. Indeed, all the migrant characteristics can be defined in the program using the existing interface of EPANET. These characteristics are the concentration of antioxidants in the pipe material ($c_{p,i}$), their diffusion coefficient in the water ($D_{w,i}$) and the partition coefficient of the antioxidants at the interface between the water and the PE ($K_{w/p,i}$). Moreover, $c_{p,i}$ can be defined separately for each pipe, which allows the user to adjust these parameters depending on the pipe age or simply the pipe material (e.g. for non-PE pipes $c_{p,i} = 0$ µg/L).

Use of NVOC measurements to detect the release of compounds from the pipe

An attempt has been made to compare modelling results with field measurements of the NVOC concentration in the Farum network case. It clearly showed that measuring NVOC is not an appropriate approach to detect the presence of compounds released from polymer pipes in the water. The reasons for this are multiple but mainly linked to the fact that the number of species that may influence the NVOC concentration is far too high. Indeed, if a decrease in the NVOC content is observed it is no possible to tell whether this indicates the migrants have been degraded or whether only the other species included in the NVOC content are degrading. Besides, each migrant released from the polymer pipe induces an increase in the NVOC concentration, but it is not possible yet to reference all the compounds that may migrate. Therefore, if an increase in NVOC is observed, one cannot distinguish the contribution of each migrant. As a conclusion, one can say that a more targeted detection method of migrants

should be used to calibrate and validate the modelling tool developed in this project. Gas chromatography-mass spectrometry is for example a possibility to investigate, among others.

Influence of chemical parameters on the release of compounds from the pipe

The release of compounds from the pipe polymer to the water depends on three chemical parameters which are the concentration of antioxidants in the pipe material ($c_{p,i}$), their partition coefficient at the interface between the water and the pipe ($K_{w/p,i}$) and their diffusion coefficient in the water ($D_{w,i}$). In the simulations made in this project, these parameters were defined to match two antioxidants broadly used: Irganox 1010 and Irgafos 168.

However, the concentration of migrants in the network was always expressed in this report as a percentage in saturation level. As a consequence, $D_{w,i}$ is the only migrant's characteristic influencing the results presented here. Indeed, other antioxidants having a different $c_{p,i}$ or $K_{w/p,i}$ would give the same relative results in percentage, although the saturation concentration (i.e. the ordinate of 100% in the graphs) would be different. Since this saturation concentration is basically defined as the product $K_{w/p,i} \cdot c_{p,i}$, if one or the other is halved, or doubled, then the migrant level in the network is also halved, or doubled, except of course when saturation is reached.

Besides, the simulations made in this project have clearly shown that $D_{w,i}$ has a great influence on the migrant concentration in the water. This is particularly visible when comparing the cumulative distribution of the migrant concentration (cf. Figure 16, Figure 27 and Figure 36). In each case indeed, the level of contamination is at least twice higher when $D_{w,i} = 10^{-9}$ m^2/s than when $D_{w,i} = 10^{-10}$ m^2/s. This large influence of $D_{w,i}$ calls for further research to determine this parameter more precisely for each migrant type.

Influence of physical parameters on the release of compounds from the pipe

The release of compounds from the pipe polymer to the water also depends on three physical parameters: the transport distance in the pipe, the pipe diameter and the water flow rate. These parameters are closely linked to the network characteristics (size, geometry, demand conditions…) and the comparison between the three cases investigated enables us to make the following conclusions:

A profile of migrant concentration is always established in the network increasing from the closest to the furthest locations from the source(s) (cf. map-plots in Figure 15, Figure 26 and Figure 35). Indeed, the simulations have shown that on the scale of a whole distribution system, the transport distance in the pipes is a major parameter which governs the migrant concentration in the network. In addition, it was observed that the variations of the migrant

concentration along the day can be caused by some changes in transport distance, themselves caused by the existence of storage tanks in the system. Indeed, the transport distance from the source(s) to the consumers is often longer when it has passed by a tank than if it had gone directly. This may induce a higher contamination of the water with migrants, although tanks also induce a higher water age, which could lead to a decrease of the migrant concentration, depending on the migrant's half-life. While the influence of storage tanks on the contamination level was clearly observed in the case "Net 1", the simulations made on "Net 3" showed that for large networks, which are continuously supplied by one or several sources, this influence becomes almost negligible.

The pipe diameter and the flow rate were shown to have, in most practical cases, only little impact on the degree of contamination caused by PE pipes. It was chosen to group the discussion about these two parameters in one paragraph because they are closely linked in practice. Indeed, if the pipes are properly dimensioned, the changes in diameter are made in accordance with the changes in flow rate. The reason for this is to ensure that water residence times in the pipes are not too high for quality reasons, but at the same time not too low, corresponding to high velocities, for reasons linked to the durability of the pipes over the years. The accordance between the pipe diameters and the flow rates is also crucial with regards to the flow regime. In most cases, the flow regime in drinking water networks is turbulent most of the time (cf. Figure 13, Figure 24 and Figure 33). Although laminar conditions are sometimes observed, they usually take place at night or locally in the smallest branching of the network, while the conditions remain turbulent in the main pipes forming the "network skeleton". Besides, even in the cases where laminar conditions occur at night in the entire network, they usually do not last long enough to make a real flush of the network under these conditions.

Concerning now the release of compound from PE pipes, the theory tells us that laminar flow conditions induce a much lower migration rate of the compounds than if the conditions were turbulent (cf. section 3.1.2). The simulations confirmed that most of the migrants found in the water were released during the transport under turbulent conditions. When laminar conditions occur in a network, the concentration in migrants almost stops increasing until turbulent conditions are established again (cf. "Net 1" and "Net 3" case studies). Nevertheless, this phenomenon can be inversed in some specific cases where the contact time between the water and the pipe lasts for so long that, even with a low migration rate, the contamination of the water eventually becomes severe. This is typically observed in areas where the pipes are over-dimensioned, such as network parts under construction (cf. Farum network case) or in areas with numerous summer houses during winter time.

Level of contamination observed in the cases investigated

The level of contamination caused by PE pipes in drinking water distribution systems greatly depends on various aspects that were discussed in the previous paragraphs. However, we will try to summarize here the levels that were computed for the different configurations investigated. The results presented in the report are expressed as a percentage in saturation level. If we consider migrants such as Irganox 1010 or Irgafos 168, the concentration of compounds in the PE matrix is about 2 g/kg and their partition coefficient at the interface around $1.55*10^{-4}$, leading to a saturation concentration of 310 µg/L.

For the new network in Farum, the migrant saturation level computed in the network ranges from 0% at the waterworks up to about 15% when $D_{w,i} = 10^{-10}$ m^2/s and up to about 70% when $D_{w,i} = 10^{-9}$ m^2/s. An average level of 6% and 26% is observed at node 2 (apartment buildings) for $D_{w,i} = 10^{-10}$ and 10^{-9} m^2/s, respectively. This level is believed to be governed mostly by the transport distance, whereas further in the network, it is most likely the very long residence times that cause the contamination. For all points investigated, the changes in migrant level along the day are limited (standard deviation around 1-3%, cf. Figure 16) and are only governed by the variations of the flow rates in the pipes. Due to the high residence time in most of the network, degradation was found to be a relevant aspect on the contamination level in the network (cf. Figure 17). Therefore, further investigations should be made concerning the by products resulting from the migrants degradation in the water. If it happens that some of them are persistent, phenomena of accumulation could occur, although the concentration of migrants themselves could remain low because they are continuously degraded.

For the middle-sized network with simple geometry ("Net 1"), the level computed in the network ranges from 0% at the waterworks up to about 50% in saturation level, when $D_{w,i} = 10^{-10}$ m^2/s, and up to almost 100% in saturation level, when $D_{w,i} = 10^{-9}$ m^2/s. The average level at the nodes investigated is believed to be governed mostly by the transport distance. Significant changes in the migrant level along the day are observed along the day for some nodes (e.g. nodes 11 and 21 with standard deviation around 5-13%, cf. Figure 27), and are most likely caused by longer transport distances induced by the elevated tank. In addition, limited variations (standard deviation around 1-3%, cf. Figure 27) are observed at all nodes, due to the variations of the water flow in the pipes. Besides, it was observed that the overall contamination is level little affected by degradation processes for the half-lives investigated (cf. Figure 28). Nevertheless it was observed that the existence of an elevated tank in the system could cause, on a local scale, a stronger influence of these degradation processes.

For the large network with complex geometry ("Net 3"), the simulations showed a behaviour generally similar than in the case study "Net 1". The migrant saturation level in the network, was computed to range from 0% at the waterworks up to about 50% when $D_{w,i} = 10^{-10}$ m^2/s

and up to almost 100% when $D_{w,i} = 10^{-9}$ m^2/s. This level is believed to be mostly governed by the transport distance. Nevertheless, it was particularly visible in this case that when this level becomes high (i.e. greater than 70%), the increase relative to the transport distance is significantly decreased, because the conditions in the water get close to saturation. Moreover and contrary to the case "Net 1", the influence of the elevated tanks in the network is much less obvious for this large network. Relatively limited changes in migrant level along the day are observed along the day (standard deviation around 1-3%, cf. Figure 36), and are likely caused by a combined effect of the presence of elevated tanks in the network and the variations of the flow rates in the pipes. Finally, simulations on this case study tend to confirm that degradation processes are not an aspect that may significantly influence the overall contamination level in large networks (cf. Figure 37), at least for the migrant half-lives investigated.

Chapter 6.
Project conclusions

EPANET 2.0. was successfully modified to enable the modelling of the release of compounds from polyethylene (PE) pipes to drinking water in distribution systems. A new version of EPANET is thus provided along with this report, which computes the contamination caused by the use of PE pipes in any EPANET network model. The modifications were made so that any parameter related to the release of compounds from the pipe can be user-defined through the existing interface of EPANET.

Various simulations were made on different network configurations and have shown that, in all investigated cases, the migrant concentration increases from the closest to furthest locations from the source(s). At the most contaminated locations, the saturation level in migrants was found to reach 50% when the diffusion coefficient of the compounds in the water ($D_{w,i}$) is 10^{-10} m^2/s and up to the saturation limit (100%) when $D_{w,i}$ equals 10^{-9} m^2/s.

It was shown that, on the scale of a network, the transport distance in the pipes is the parameter governing the most the concentration in migrant throughout the network and their variations along the day. It can thus be established that grab sampling, which is currently used, is not a valid approach to estimate the contamination potential of PE pipes to distribute drinking water. It was also seen that for common networks the residence time of the water in the system is usually smaller than the migrant half-life. Therefore, degradation was not found to be relevant in most cases. Nevertheless, some reservation should be expressed on this aspect due to the high uncertainties on the actual half-lives of the migrants. The simulations also showed that the daily variations of the contamination degree may be influenced by the network geometry. Indeed the existence of an elevated tank may sometimes increase the transport distance which leads to a higher contamination level, but it also induces higher water age, which could have the opposite effect if degradation is relevant. It was also observed that

for large networks which are continuously supplied by one or several sources, this geometry effect becomes almost negligible and that only a deviation of 1-3% is observed along the day. In addition, the simulations clearly showed that, in large networks, the flow regime remains turbulent most of the time and in most parts of the network. Laminar conditions at night or in certain area were not found to induce any decrease in the contamination level. Nevertheless, in particular cases where laminar conditions last over long periods, the contamination of the water may become severe (e.g. in networks under construction or off-season periods in summer houses areas). In such cases, degradation of the migrants may become significant, possibly leading to accumulation of by-products in the water, if some of them are persistent.

Throughout this study, the concentration of species in the network was always expressed as percentage in saturation level. As a consequence, $D_{w,i}$ is the only migrant characteristic influencing the saturation levels presented in the report. The study clearly showed that $D_{w,i}$ has a great influence on the contamination degree in the network, which calls for further research to determine more precisely this parameter for each migrant type. Other antioxidants having different concentrations in the polymer ($c_{p,i}$) or partition coefficients at the interface water / pipe ($K_{w/p,i}$) would thus give the same relative results, although the saturation concentration would be different.

The parallel between sampling and modelling, which was made in the Farum network, illustrated that measuring Non Volatile Organic Compounds (NVOC) is not a suitable approach to detect the release of compounds from PE pipes, mainly because of the large number of species that may influence the NVOC concentration. A method such as Gas Chromatography-Mass Spectrometry could be used instead, but was considered too complex within the scale of the present study. Further work with this method or an equivalent would permit the investigation of the release of specific compounds from PE pipes to water. In addition, the influence of the pipe ageing on the migration rate could be estimated. As a consequence, the modelling tool developed in this project could be precisely calibrated for specific migrants. Simulations could thus be made to assess precisely and reliably the contamination problem caused by the use of PE pipes in distribution networks and household installations for drinking water. More advanced studies could then be made to study for example the effect on the contamination degree of having PE pipes of different ages in the same network or having only a limited number of pipes made of PE in a system, while the others are for example in metal.

Chapter 7.
References

Bird, R. B., Stewart, W.E. and Lightfoot E.N. (2007). "Transport Phenomena", 2nd edition. *John Wiley & Sons*, USA.

Brocca, D., Arvin, E. and Mosbæk, H. (2002). "Identification of organic compounds migrating from polyethylene pipes into drinking water". *Water Research,* 36 (15), 3675-3680.

ChemBlink Website, Online database of chemicals (2008), available on the Internet at: http://www.chemblink.com [Accessed 15/06/2008]

Denberg, M., Arvin, E. and Hassager, O. (2007). "Modelling of the release of organic compounds from polyethylene pipes to water". *Journal of Water Supply,* 56 (6-7), 435-443.

Harris D. C. (2003). "Quantitative chemical analysis", 6th edition. *Freeman*, USA.

Mays, L.W., Koutsoyiannis and Angelakis, A.N. (2007). "A brief history of urban water supply in antiquity". *Water Science & Technology: Water Supply,* 7 (1), 1-12.

Roman aqueducts Website (2008), available on the Internet at: http://www.romanaqueducts.info/ [Accessed 24/04/2008]

Rossman, L.A. (2000). "EPANET 2 Users manual". Available on the Internet at the US-EPA webpage on EPANET (cf. reference below).

Salzman, J. E. (2006). "Thirst: A Short History of Drinking Water". *Yale Journal of Law and the Humanities*, 17 (3), 94-121.

Skjevrak, I., Due, A., Gjerstad, K. O. and Herikstad, H. (2003). "Volatile organic components migrating from plastic pipes" (HDPE, PEX and PVC) into drinking water. *Water Research*, 37 (8), 1912–1920.

US-EPA webpage on EPANET (2008), available in the Internet at: http://www.epa.gov/nrmrl/wswrd/dw/epanet.html [Accessed 14/03/2008]

Walski, T.M., Chase, D.V., Savic D.A., Grayman, W.M., Beckwith, S., Koelle, E. (2003). "Advanced Water Distribution Modeling And Management". *Haestad Press*, USA.

Wavin Website, Manufacturer of plastic pipes (2008), available on the Internet at: http://www.wavin.com/ [Accessed 24/04/2008]

Wesselinger, J.A. and Krishna, R. (2000). "Mass transfer in multicomponent mixtures". *Delft University Press*, The Netherlands.

Water Panel (2004). "Afsmitning til drikkevand fra plastrør anvendt til vandforsyningsformål - Identifikation af potentielle stoffer" (Release of material from plastic pipes, used for water supply purposes, to drinking water – identification of possible compounds). Available on the Internet at: http://www.danva.dk/sw1635.asp [Accessed on 19/06/2008]

Wurbs, R.A. (1995). "Water management models: A guide to software". *Englewood Cliffs Press*, USA.

Appendices

Appendix 1. Modifications of EPANET source code

Modified EPANET code, permitting the modelling of the compounds' release from pipes

Below is presented an extract of the source code of EPANET water quality module. Not all the code related to water quality is presented, not to overload the report, although all the functions which are relevant in the computation of the water quality value are give here.

The beginning of each function is highlighted is grey to ease the reading. Besides, in the functions that were modified to enable the modelling of the compounds' release form PE pipes, the following colour code is used:

- the blue is used to distinguish the original code that has been "commented out" and is not read by the program,
- the bold red colour is used to highlight the coding that has been added to the initial program to enable the modelling of the compounds' migration from the pipe,
- the green corresponds to the comments that concerns the modifications made to the original code.

```
double  pipereact(int k, double c, double v, long dt)

/*
**--------------------------------------------------------------
**   Input:   k = link index
**            c = current WQ in segment
**            v = segment volume
**            dt = time step
**   Output:  returns new WQ value
**   Purpose: computes new quality in a pipe segment after
**            reaction occurs
**--------------------------------------------------------------
*/
{
   double cnew, dc, dcbulk, dcwall, rbulk, rwall;

   /* For water age (hrs), update concentration by timestep */
   if (Qualflag == AGE) return(c+(double)dt/3600.0);

   /* Otherwise find bulk & wall reaction rates */
   rbulk = bulkrate(c,Link[k].Kb,BulkOrder)*Bucf;
   rwall = wallrate(c,Link[k].Diam,Link[k].Kw,Link[k].R);

   /* Find change in concentration over timestep */
   dcbulk = rbulk*(double)dt;
   dcwall = rwall*(double)dt;

   /* Update cumulative mass reacted */
   if (Htime >= Rstart)
   {
      Wbulk += ABS(dcbulk)*v;
      Wwall += ABS(dcwall)*v;
   }

   /* Update concentration */
   dc = dcbulk + dcwall;
   cnew = c + dc;
   cnew = MAX(0.0,cnew);
   return(cnew);
}
```

```
double  tankreact(double c, double v, double kb, long dt)
/*
**--------------------------------------------------------
**   Input:   c = current WQ in tank
**            v = tank volume
**            kb = reaction coeff.
**            dt = time step
**   Output:  returns new WQ value
**   Purpose: computes new quality in a tank after
**            reaction occurs
**--------------------------------------------------------
*/
{
   double cnew, dc, rbulk;

/*** Updated 9/7/00 ***/
   /* If no reaction then return current WQ */
   if (!Reactflag) return(c);

   /* For water age, update concentration by timestep */
   if (Qualflag == AGE) return(c + (double)dt/3600.0);

   /* Find bulk reaction rate */
   rbulk = bulkrate(c,kb,TankOrder)*Tucf;

   /* Find concentration change & update quality */
   dc = rbulk*(double)dt;
   if (Htime >= Rstart) Wtank += ABS(dc)*v;
   cnew = c + dc;
   cnew = MAX(0.0,cnew);
   return(cnew);
}




double  bulkrate(double c, double kb, double order)
/*
**-------------------------------------------------------------
**   Input:   c = current WQ concentration
**            kb = bulk reaction coeff.
**            order = bulk reaction order
**   Output:  returns bulk reaction rate
**   Purpose: computes bulk reaction rate (mass/volume/time)
**-------------------------------------------------------------
*/
{
   double c1;

   /* Find bulk reaction potential taking into account */
   /* limiting potential & reaction order. */

      /* Zero-order kinetics: */
      if (order == 0.0) c = 1.0;

      /* Michaelis-Menton kinetics: */
      else if (order < 0.0)
      {
         c1 = Climit + SGN(kb)*c;
         if (ABS(c1) < TINY) c1 = SGN(c1)*TINY;
         c = c/c1;
      }

      /* N-th order kinetics: */
      else
      {
         /* Account for limiting potential */
         if (Climit == 0.0) c1 = c;
         else c1 = MAX(0.0, SGN(kb)*(Climit-c));

         /* Compute concentration potential */
         if (order == 1.0) c = c1;
```

```
         else if (order == 2.0) c = c1*c;
         else c = c1*pow(MAX(0.0,c),order-1.0);
      }

   /* Reaction rate = bulk coeff. * potential) */
   if (c < 0) c = 0;
   return(kb*c);
}
```

```
double  wallrate(double c, double d, double kw, double kf)
/*
**--------------------------------------------------------------
**   Input:   c = current WQ concentration
**            d = pipe diameter
**            kw = intrinsic wall reaction coeff.
**            kw = Kwp*Cp with concentration in ug/kg
**            kf = mass transfer coeff. for 0-order reaction (ft/sec) or
**                 apparent wall reaction coeff. for 1-st order reaction (1/sec)
**   Output:  returns wall reaction rate in mass/ft3/sec
**   Purpose: computes wall reaction rate
**--------------------------------------------------------------
*/
{
   // if (kw == 0.0 || d == 0.0) return(0.0);
   // if (WallOrder == 0.0)       /* 0-order reaction */
   // {
   //    kf = SGN(kw)*c*kf;       /* Mass transfer rate (mass/ft2/sec)*/
   //    kw = kw*SQR(Ucf[ELEV]);  /* Reaction rate (mass/ft2/sec) */
   //    if (ABS(kf) < ABS(kw))   /* Reaction mass transfer limited */
   //       kw = kf;
   //    return(kw*4.0/d);        /* Reaction rate (mass/ft3/sec) */
   // }
   // else return(c*kf);          /* 1st-order reaction */


   double KwpCp, Ji, rate;

   KwpCp = kw*60*60*24/Ucf[QUALITY];  // conc. in PE must be in ug/kg
   Ji = kf*(KwpCp - c);               // mass flux through the interface
      if (d > 0) rate = 4/d*Ji;       // production rate reflecting the diffusion
   else rate = 0;


 /* The kw that is here is taken by EPANET from the location reserved in the
interface for the wall reaction coefficient. Nevertheless, the value we can get
here (kw) has already had some unit conversion by other parts of the program. kw
unit in the interface is 1/day but the program use them in 1/sec. Besides, in the
computations, EPANET works with concentrations in g/(ft^3). To have our Kwp*Cp in
ug/L, we make here the opposite conversion.*/


   /* Our study conditions */
   if (WallOrder == 0.0 && KwpCp >= 0.0 && Sc != 0.0)
   {
      /* No saturation -> production rate reflecting diffusion */
      if (KwpCp >= c)  return(rate);
      /* Saturation -> production rate = 0 */
      else return(0);
   }
   /* any other case */
   else return(pow(10,20));      // we put a big number to detect any error case
}
```

```
double piperate(int k)
/*
**--------------------------------------------------------------
**   Input:   k = link index
**   Output:  returns reaction rate coeff. for 1st-order wall
**            reactions or mass transfer rate coeff. for 0-order
**            reactions
**   Purpose: finds wall reaction rate coeffs.
**--------------------------------------------------------------
*/
{
   double a,d,u,kf,kw,y,Re,Sh;

   d = Link[k].Diam;                    /* Pipe diameter, ft */

/* Ignore mass transfer if Schmidt No. is 0 */
   if (Sc == 0.0)
   {
      if (WallOrder == 0.0) return(BIG);
      else return(Link[k].Kw*(4.0/d)/Ucf[ELEV]);
   }

/* Compute Reynolds No. */
   a = PI*d*d/4.0;
   u = ABS(Q[k])/a;
   Re = u*d/Viscos;

/* Compute Sherwood No. for stagnant flow  */
/* (mass transfer coeff. = Diffus./radius) */
   if (Re < 1.0) Sh = 2.0;                          // Kept as the original

/* Compute Sherwood No. for turbulent flow */
/* using the Notter-Sleicher formula.      */
   else if (Re >= 2300.0)
      // Sh = 0.0149*pow(Re,0.88)*pow(Sc,0.333);
      Sh = 0.026*pow(Re,0.8)*pow(Sc,0.333);       // Valid only for L/d>60

/* Compute Sherwood No. for laminar flow */
/* using Graetz solution formula.        */
   else
   {
      // y = d/Link[k].Len*Re*Sc;
      // Sh = 3.65+0.0668*y/(1.0+0.04*pow(y,0.667));
      Sh = 3.657;         // One assume fully developed laminar profile
   }

/* Compute mass transfer coeff. (in ft/sec) */
   kf = Sh*Diffus/d;

/* For zero-order reaction, return mass transfer coeff. */
   if (WallOrder == 0.0) return(kf);

/* For first-order reaction, return apparent wall coeff. */
   kw = Link[k].Kw/Ucf[ELEV];       /* Wall coeff, ft/sec */
   kw = (4.0/d)*kw*kf/(kf+ABS(kw)); /* Wall coeff, 1/sec  */
   return(kw);
}                        /* End of piperate */
```

Print screens of some parts of EPANET 2.0 interface

These print screens show the different locations where should be entered the migrants characteristics, to ensure a proper modelling of the release of compounds from PE pipes to drinking water.

As mentioned in the report, the box meant to entered the wall coefficient Kw is used in the modified version to set the factor $K_{w/p,i} \cdot c_{p,i}$. This factor can either be defined once for all pipes in the "Reactions Options" window, or separately for each pipe in the "Pipe definition" window. It is worth noting that the value entered in the "Reactions Options" window is only used when no value is entered in the "Pipe definition" window. In the case of the print screens showed below, a value of 310 µg/L is entered corresponding to the antioxidants Irganox 1010 or Irgafos 168.

The last chemical parameter relevant in the migration is $D_{w,i}$. This parameter is entered in the "Quality Options" window and must be expressed relatively to the chlorine diffusion coefficient in the water as the ratio $D_{w,i}/D_{w,Cl}$. In the case of the print screen showed below, a value of 0.830 is defined, corresponding to a diffusion coefficient of 10^{-9} $m^2.s^{-1}$.

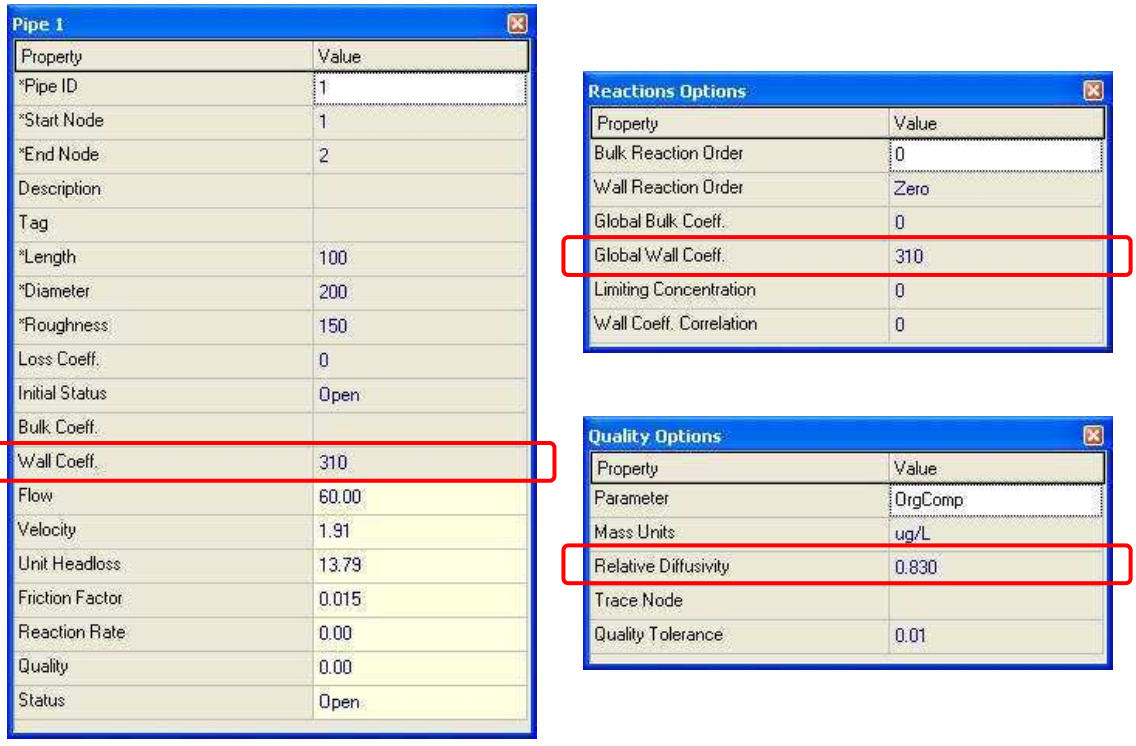

Modified EPANET code, permitting the plot of the Reynolds number in a network map

The water quality module of EPANET was modified to be permit plot of coloured network map of the Reynolds number, that were used is the report to highlight the flow regime conditions in the network (laminar or turbulent). Although the water quality module is not at all meant for this, some modifications made on the two functions presented below enable this computation. Verifications were made and proved than the Reynolds number computed in the pipes by EPANET was in accordance (2% variance) with the theoretical formula:

$$Re = \frac{\rho \cdot v \cdot d_{inner}}{\mu}$$

```
double  pipereact(int k, double c, double v, long dt)
/*
**--------------------------------------------------------------
**   Input:   k = link index
**            c = current WQ in segment
**            v = segment volume
**            dt = time step
**   Output:  returns new WQ value
**   Purpose: computes new quality in a pipe segment after
**            reaction occurs
**--------------------------------------------------------------
*/
{
//   double cnew, dc, dcbulk, dcwall, rbulk, rwall;

//   /* For water age (hrs), update concentration by timestep */
//   if (Qualflag == AGE) return(c+(double)dt/3600.0);

//   /* Otherwise find bulk & wall reaction rates */
//   rbulk = bulkrate(c,Link[k].Kb,BulkOrder)*Bucf;
//   rwall = wallrate(c,Link[k].Diam,Link[k].Kw,Link[k].R);

//   /* Find change in concentration over timestep */
//   dcbulk = rbulk*(double)dt;
//   dcwall = rwall*(double)dt;

//   /* Update cumulative mass reacted */
//   if (Htime >= Rstart)
//   {
//      Wbulk += ABS(dcbulk)*v;
//      Wwall += ABS(dcwall)*v;
//   }

//   /* Update concentration */
//   dc = dcbulk + dcwall;
//   cnew = c + dc;
//   cnew = MAX(0.0,cnew);
//   return(cnew);

   double a, d, u, Re;

   d = Link[k].Diam;
   a = PI*d*d/4.0;
   u = ABS(Q[k])/a;
   Re = u*d/Viscos;
   return(Re/Ucf[QUALITY]);

 /* The Re that is here has no unit. However, we use the Quality module to compute
it, and EPANET works with concentrations in g/(ft^3). To have our Re with no unit,
we make here the opposite conversion.*/

 }
```

```
double  tankreact(double c, double v, double kb, long dt)
/*
**--------------------------------------------------------
**   Input:   c = current WQ in tank
**            v = tank volume
**            kb = reaction coeff.
**            dt = time step
**   Output:  returns new WQ value
**   Purpose: computes new quality in a tank after
**            reaction occurs
**--------------------------------------------------------
*/
{
//   double cnew, dc, rbulk;

///*** Updated 9/7/00 ***/
//   /* If no reaction then return current WQ */
//   if (!Reactflag) return(c);

//   /* For water age, update concentration by timestep */
//   if (Qualflag == AGE) return(c + (double)dt/3600.0);
//
//   /* Find bulk reaction rate */
//   rbulk = bulkrate(c,kb,TankOrder)*Tucf;

//   /* Find concentration change & update quality */
//   dc = rbulk*(double)dt;
//   if (Htime >= Rstart) Wtank += ABS(dc)*v;
//   cnew = c + dc;
//   cnew = MAX(0.0,cnew);
//   return(cnew);

   return(0);
}
```

Appendix 2. Modelling work: details concerning the Farum network

Characteristics of the network under construction in Farum

The data presented here were used to create the EPANET model of the network investigated in Farum. These data were provided by the Farum waterworks. The number are inhabitants are based on the assumptions that in average 2 persons live in a flat and 3 persons live in a house.

Link ID	Start Node	End Node	Length (m)	Diameter (mm)
1	0	1	85	250
2	1	2	245	160
3	2	3	245	160
4	3	4	235	160
5	4	5	30	200
6	5	6	170	200
11	5	11	60	160
12	4	12	200	110
101	3	101	130	90

Node ID	Demand (L/s)	Number of inhabitants connected to the node
1	-	-
2	0.741	400
3	-	-
4	-	-
5	-	-
6	0.004	2
11	0.022	12
12	0.006	3
101	-	-

Simulations results for Farum network: effect of degradation on the migrant concentration along the day for $D_{w,i}$ = 10^{-10} m^2/s

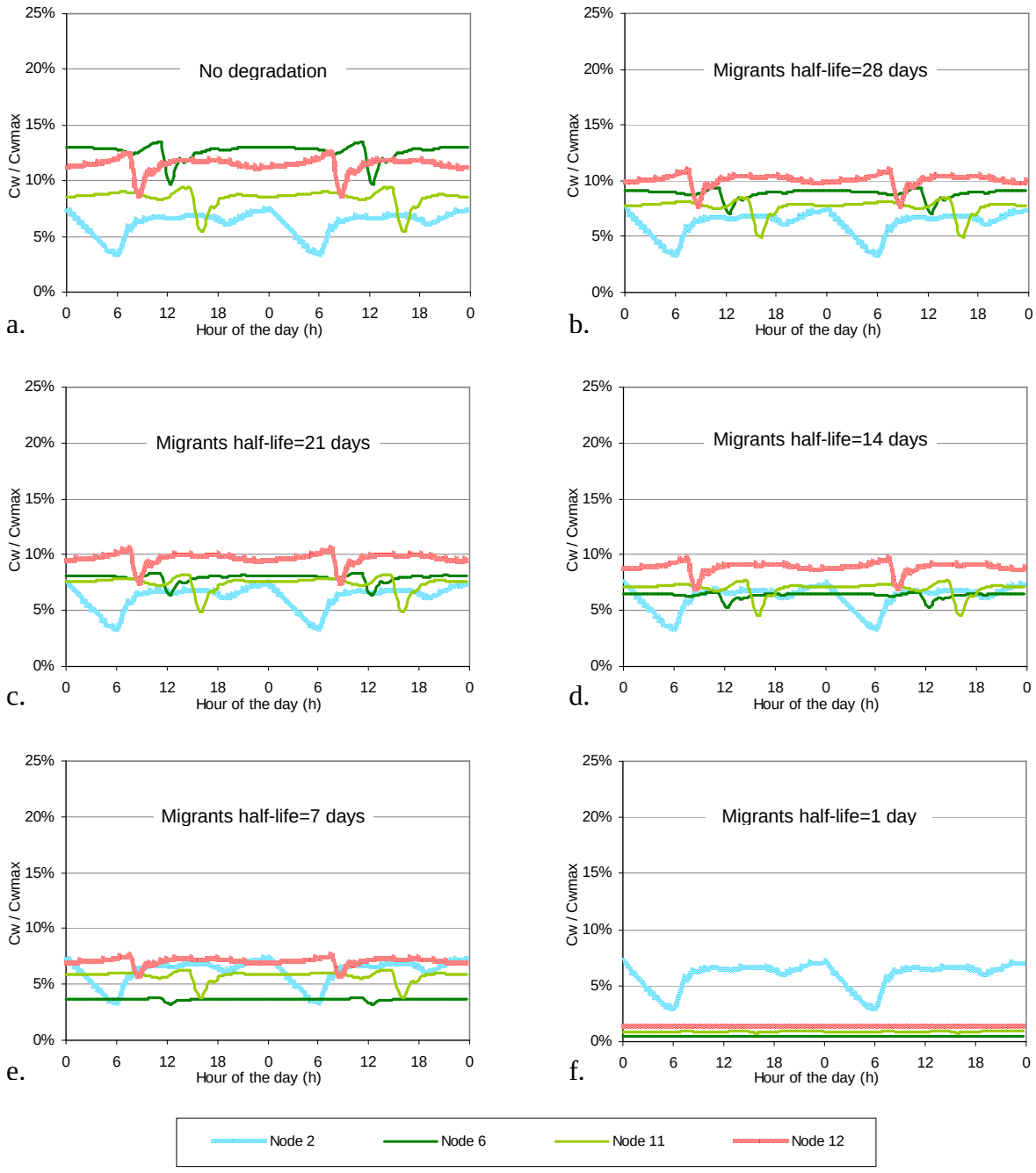

The six graphs represent the saturation level of species along the day at relevant nodes of the network and for different half-life of the species. Graph a corresponds to the case with no degradation, while graphs b, c, d, e and f show the same results with migrant half-lives of 28 days, 21 days, 14 days, 7 days and 1 day, respectively. In this case, the migrant's diffusion coefficient in the water is 10^{-10} m^2/s. If one considers antioxidants such as Irganox 1010 or Irgafos 168 then the concentration of species in the PE matrix is about 2 g/kg and their partition coefficient at the interface around $1.55*10^{-4}$, leading to a saturation concentration of 310 µg/L.

Simulations results for Farum network: effect of degradation on the migrant concentration along the day for $D_{w,i}$ = 10^{-9} m^2/s

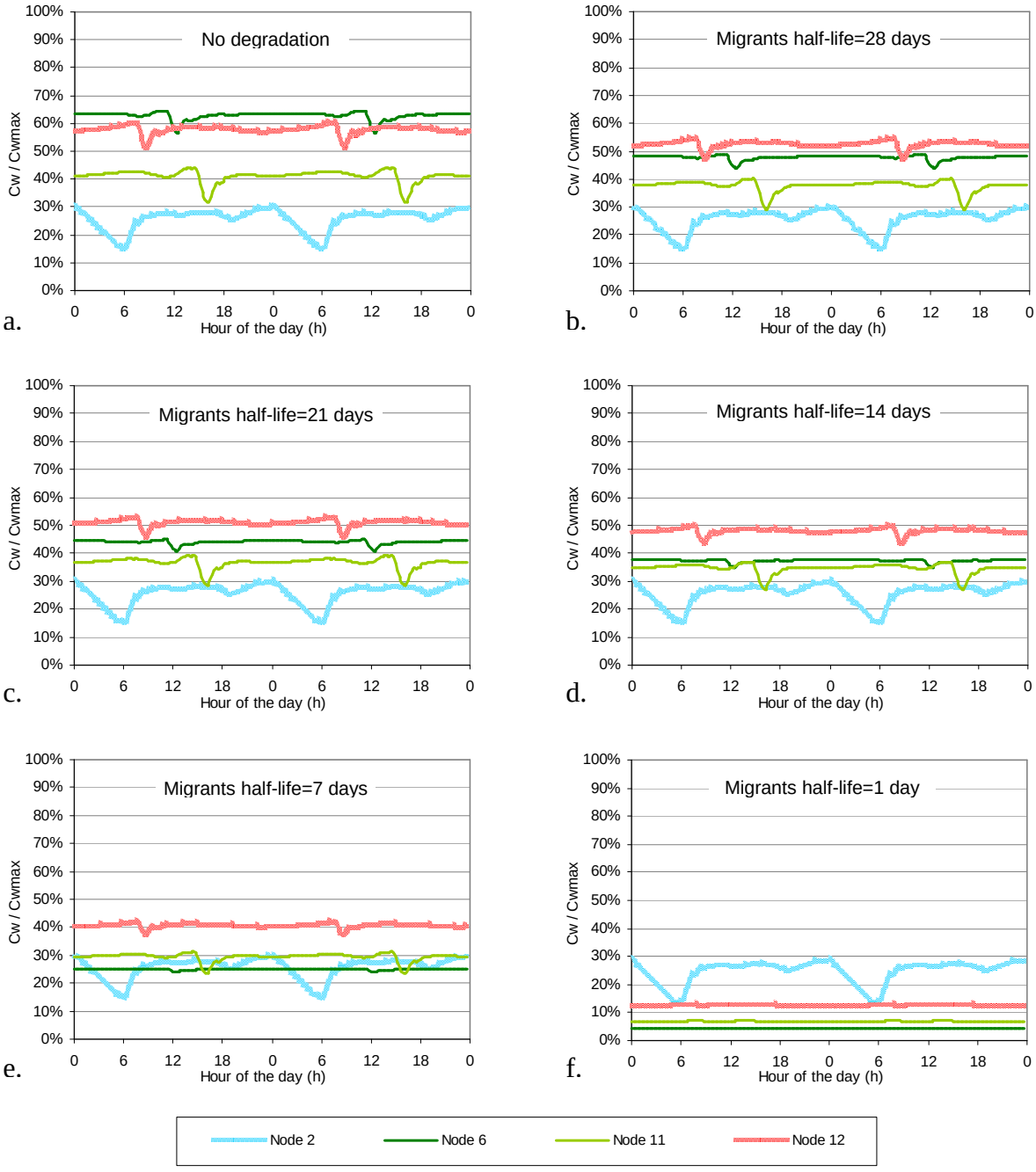

The six graphs represent the saturation level of species along the day at relevant nodes of the network and for different half-life of the species. Graph a corresponds to the case with no degradation, while graphs b, c, d, e and f show the same results with migrant half-lives of 28 days, 21 days, 14 days, 7 days and 1 day, respectively. In this case, the migrant's diffusion coefficient in the water is 10^{-9} m^2/s. If one considers antioxidants such as Irganox 1010 or Irgafos 168 then the concentration of species in the PE matrix is about 2 g/kg and their partition coefficient at the interface around $1.55*10^{-4}$, leading to a saturation concentration of 310 µg/L.

Appendix 3. Cumulative distribution function

The cumulative distribution of a set of data is a statistical distribution of these data, which corresponds to the integral of the normal (Gaussian) distribution. The cumulative distribution shows the probability that a variate will assume a value smaller or equal to x (the abscissa). The plot of the cumulative distribution always starts with an ordinate at 0% and ends with an ordinate at 100%. It is the way that the curve switches from one extremity to the other that characterizes the set of data. Basically, the mean abscissa where the curve switches is the average of the data set, while the "slope" of the curve during the switch indicates the variance in the data. During this switch from 0% to 100% in ordinate, a very steep (almost vertical) curve shows than all data are very close to each others, whereas a more gentle slope shows that some variations of the data around the average are occurring.

The normal distribution can be calculated from:

$$P(x) = \frac{1}{\sigma \cdot \sqrt{2\pi}} \cdot e^{-\frac{(x-\mu)^2}{2\sigma^2}}$$

where x is the variable studied, μ is the mean of the data set and σ its standard deviation.

The cumulative distribution function is then calculated by integration of the normal distribution, as follow:

$$D(x) = \int_{-\infty}^{x} P(x') \cdot dx' = \frac{1}{\sigma \cdot \sqrt{2\pi}} \cdot \int_{-\infty}^{x} \cdot e^{-\frac{(x'-\mu)^2}{2\sigma^2}} \cdot dx' = \frac{1}{2}\left[1 + erf\left(\frac{x-\mu}{\sigma \cdot \sqrt{2}}\right)\right]$$

where erf is the so-called error function, defined as:

$$erf(z) = \frac{2}{\sqrt{\pi}} \int_0^z e^{-t^2} \cdot dt$$

The information presented in this appendix were found in Wolfram MathWorld website (2008) and are available on the Internet at: http://mathworld.wolfram.com/NormalDistribution.html [Accessed 07/05/2008]

Appendix 4. Sampling work in Farum network

Preparation of the glassware

The glassware used to take the samples on site, as well as for the analysis in the laboratory, were prepared to minimize the risks of contamination of the water by organic compounds coming from elsewhere than the PE pipes in the network. The glassware used in the sampling work were thus:

1) subjected to a washing program with acid
2) covered separately by a lit in aluminium foil
3) placed in the oven at 220°C for at least 6 hours

This preparation of the glassware is of importance because PE is widely used for all type of plastic objects and contamination of the vials could easily occur and skew the results observed.

Procedure on site

To collect each sample on site, the following procedure was applied:

1) the aluminium lit of the collecting vial is removed
2) a steel pipe is inserted into a vial to fill it continuously from the bottom
3) the vial is flushed from the bottom for about 1 min to avoid disturbances due to sorption
4) oxygen is measured while the vial is still filled from the bottom
5) if the sample is the first or the last one of the series, then temperature, pH and electric conductivity are measured while the vial is still filled from the bottom
6) the steel pipe can be removed and two drops of nitric acid (at 37% HNO_3 in w/w) are added in the sample to inhibit degradation processes
7) the sample is covered again with its aluminium foil and brought back to the laboratory for NVOC measurements.

In this procedure, the instrument HQ10 from the Hach Company which uses the luminescent technology is used to measure the dissolved oxygen concentration. The use of a steel pipe to fill the vial continuously while oxygen is measured should permit having a better measurement. Besides, the steel pipe is previously cleaned with a burner, to minimize here again the risk of contamination by other organic compounds not coming from the sample itself.

Program of the sampling campaign in Farum (DK) on April, the 29th, 2008

The table on the next page present the program of the sampling campaign carried out in the Farum study case, but also of the operations made on the network to prepare the sampling. “Sampling point 1” corresponds to the end of an unused pipe located in the North West of the area (node 101 in the EPANET model), “sampling point 2” is the junction next to the power

plant (node 6 in the EPANET model), and "sampling point 3" is the kitchen tap of a private house in the area (node 11 in the EPANET model).

Date	Location	Description
Wednesday 23rd April	Waterworks	- **Any change of pumping well supplying water to the network was done before this date.** - **Any back washing of the waterworks filter was done before this date.**
Thursday 24th April	Sampling point 1	- **The pipes leading to sampling point 1 were flushed.** A flow meter was used to measure the flow rate during the flushing. About 1.5 m^3 of water was consumed to ensure a proper flush.
	Sampling point 2	- **The pipes leading to sampling point 2 were flushed.** A flow meter was used to measure the flow rate during the flushing. About 4 m^3 of water was be consumed to ensure a proper flush.
Tuesday 29th April	Waterworks	- **The steel pipe used to fill the bottles was cleaned with a burner.** - **11 samples of water were taken at the waterworks outlet.** For each of them the procedure described in the previous section was followed. These samples taken were used as a reference to be compared with samples from sampling points 1 and 2.
	Sampling point 1	- **The steel pipe used to fill the bottles was cleaned with a burner.** - **5 samples of water were taken at sampling point 1.** For each of them the procedure described in the previous section was followed. The objective was to study the effect of long residence time (5 days) on the concentration in migrants. - **The pipes leading to sampling point 1 were flushed:** A flow meter was used to measure the flow rate during the flushing. About 1.5 m^3 of water was consumed to ensure a proper flush. - **6 samples of water were taken at the pipe outlet.** For each of them the procedure described in the previous section was followed. The objective was to study the effect of the transport through the network on the concentration in migrants.
	Sampling point 2	- **The steel pipe used to fill the bottles was cleaned with a burner.** - **6 samples of water were taken at sampling point 2.** For each of them the procedure described in the previous section was followed. The objective was to study the effect of long residence time (5 days) on the concentration in migrants. - **The pipes leading to sampling point 2 were flushed:** A flow meter was used to measure the flow rate during the flushing. About 4 m^3 of water was consumed to ensure a proper flush. - **5 samples of water were taken at the pipe outlet.** For each of them the procedure described in the previous section was followed. The objective was to study the effect of the transport through the network on the concentration in migrants.
	Sampling point 3	- **5 samples of water were taken at sampling point 3.** For each of them the procedure described in the previous section was followed.

Method used to determine the NVOC concentration in the samples

The instrument Shimadzu TOC-Vwp is used to measure the NVOC content in the drinking water samples collect in the Farum network. Due to its high sensitivity, a rigorous cleaning procedure of all glass equipment should be used to avoid any external impact on the instrument signal. For each condition investigated in the field, at least 5 samples were taken, each samples being then divided to make duplicates for the NVOC analysis.

The method used in the instrument has the following parameters encoded: 9000 µL of injection volume, 3 injections, 0 wash, 3% of acid addition (H_3PO_4 at 6% in w/w), a sparge time of 10 min, 1 mL of UV oxidation volume (solution composed of 10.5% persulfate in w/w and 3.8% H_3PO_4 in w/w) and 1 auto dilution step.

A validation of the method was carried out, including an analysis of: the glass equipment purification method, the processed sample stability, the calibration model, the accuracy and precision, the limit of detection and the lower limit of quantification. As a result, the following table was obtained.

Parameters	Value	Unit
Detection limit	63	ppb
Quantification limit	98	ppb
Coefficient of variation	6	%

On site measurement results for Farum network (made on 29/04/2008)

Location	Sample n°	Temp ℃	pH -	Conductivity µS / m	Oxygen mg / L	Mean Oxygen mg / L	Standard Deviation (mg/L)
Waterworks outlet	1	9	6.73	486	8.86	8.95	0.03
	2				8.94		
	3				8.96		
	4				8.97		
	5				8.96		
	6				8.98		
	7				8.95		
	8				8.95		
	9				8.95		
	10	9	7.09	497	8.94		
Outlet of unused pipe (before flushing)	1	10	6.7	498	6.60	6.21	0.25
	2				6.30		
	3				6.05		
	4				5.97		
	5		7.5	486	6.11		
Outlet of unused pipe (after flushing)	1		6.9	489	8.40	8.51	0.06
	2				8.48		
	3				8.54		
	4				8.54		
	5				8.56		
	6		7.4	494	8.54		
Power plant (before flushing)	1		6.5	495	8.43	8.69	0.13
	2				8.70		
	3				8.75		
	4				8.75		
	5				8.75		
	6				8.77		
Power plant (after flushing)	1	10.3	7.09	479	8.39	8.50	0.07
	2				8.49		
	3				8.55		
	4				8.51		
	5			496	8.56		
Kitchen's tap at a private house	1	11	7	494	8.28	8.39	0.09
	2				8.32		
	3				8.48		
	4				8.40		
	5			495	8.48		

NVOC measurement results for Farum network (made in the laboratory on 30/04/2008)

Site	Sample ID	Sample name	Mean area of the triplicate (-)	Mean concentration of the triplicate (mg/L)	Mean concentration per site (mg/L)	Standard Deviation per site (mg/L)
MiliQ to rinse	1	MiliQ	40	x	x	x
MiliQ as a ref	2	MiliQ	31	x	x	x
	3	MiliQ	34	x		
Waterworks outlet	4	0.01	1877	2.98	2.985	0.044
	5	0.01	1849	2.93		
	6	0.02	1901	3.02		
	7	0.02	1919	3.05		
	8	0.03	1910	3.03		
	9	0.03	1876	2.98		
	10	0.04	1876	2.98		
	11	0.04	1882	2.99		
	12	0.05	1870	2.97		
	13	0.05	1868	2.96		
	14	0.06	1935	3.07		
	15	0.06	1861	2.95		
	16	0.07	1878	2.98		
	17	0.07	1832	2.91		
Outlet of unused pipe (before flushing)	18	1.01	1733	2.75	2.659	0.049
	19	1.01	1719	2.73		
	20	1.02	1666	2.64		
	21	1.02	1707	2.71		
	22	1.03	1670	2.65		
	23	1.03	1665	2.64		
	24	1.04	1660	2.63		
	25	1.04	1649	2.61		
	26	1.05	1645	2.61		
	27	1.05	1658	2.63		
Outlet of unused pipe (after flushing)	28	1.06	1858	2.95	2.937	0.034
	29	1.06	1807	2.87		
	30	1.07	1874	2.97		
	31	1.07	1852	2.94		
	32	1.08	1850	2.94		
	33	1.08	1870	2.97		
	34	1.09	1877	2.98		
	35	1.09	1828	2.90		
	36	1.10	1846	2.93		
	37	1.10	1845	2.93		
Power plant (before flushing)	38	2.01	1924	3.05	2.986	0.036
	39	2.01	1877	2.98		
	40	2.02	1882	2.99		
	41	2.02	1876	2.98		
	42	2.03	1843	2.92		
	43	2.03	1889	3.00		
	44	2.06	1892	3.00		
	45	2.06	1869	2.97		
Power plant (after flushing)	46	2.07	1895	3.01	2.978	0.059
	47	2.07	1870	2.97		
	48	2.08	1955	3.10		
	49	2.08	1881	2.98		
	50	2.09	1812	2.88		
	51	2.09	1846	2.93		
	52	2.10	1872	2.97		
	53	2.10	1871	2.97		
	54	2.10	1895	3.01		
	55	2.10	1868	2.96		
Kitchen's tap at a private house	56	3.01	1857	2.95	3.006	0.069
	57	3.01	1831	2.90		
	58	3.02	1889	3.00		
	59	3.02	1891	3.00		
	60	3.03	1867	2.96		
	61	3.03	1931	3.07		
	62	3.04	1941	3.08		
	63	3.04	1950	3.10		
Standard of 1ppm	64	1 ppm	629	x	x	x
	65	1 ppm	600	x		
Standard of 5ppm	66	5 ppm	3117	x	x	x
	67	5 ppm	3178	x		

The NVOC content in area unit was obtained using the Shimadzu TOC-Vwp instrument, presented previously. Then, the concentration of NVOC in mg/L is obtained using a calibration curve computed from the average of two miliQ water samples and the average of each pair of standard (1 ppm and 5 ppm). This calibration curve is given below.

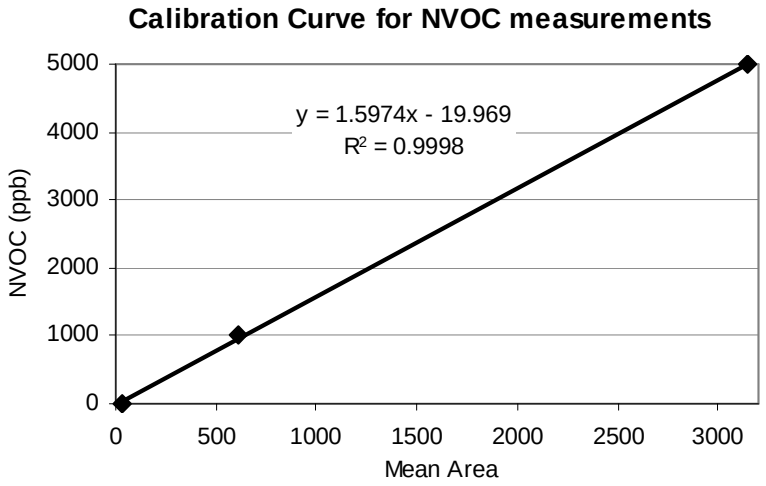

Appendix 5. Modelling work: details concerning "Net 1"

Characteristics of the study network "Net 1"

The data presented here are conversion into SI units of the data available in the EPANET model. The number of inhabitants is computed for an average consumption of 160 L/d/cap.

Link ID	Start Node	End Node	Length (m)	Diameter (mm)
10	10	11	3,210	457
11	11	12	1,609	356
12	12	13	1,609	254
21	21	22	1,609	254
22	22	23	1,609	305
31	31	32	1,609	152
110	2	12	61	457
111	11	21	1,609	254
112	12	22	1,609	305
113	13	23	1,609	203
121	21	31	1,609	203
122	22	32	1,609	152

Node ID	Demand (L/s)	Elevation (m)	Number of inhabitants connected to the node
2	-	259.1	-
9	-	243.8	-
10	-	216.4	-
11	9.5	216.4	5,110
12	9.5	213.4	5,110
13	6.3	211.8	3,407
21	9.5	213.4	5,110
22	12.6	211.8	6,814
23	9.5	210.3	5,110
31	6.3	213.4	3,407
32	6.3	216.4	3,407
		Sum	37,476

The two lines of coding below represent the control of the waterworks pump on the level in the elevated tank

```
LINK 9 OPEN IF NODE 2 BELOW 110
LINK 9 CLOSED IF NODE 2 ABOVE 140
```

Simulations results for "Net 1": effect of degradation on the migrant concentration along the day for $D_{w,i} = 10^{-10}$ m^2/s

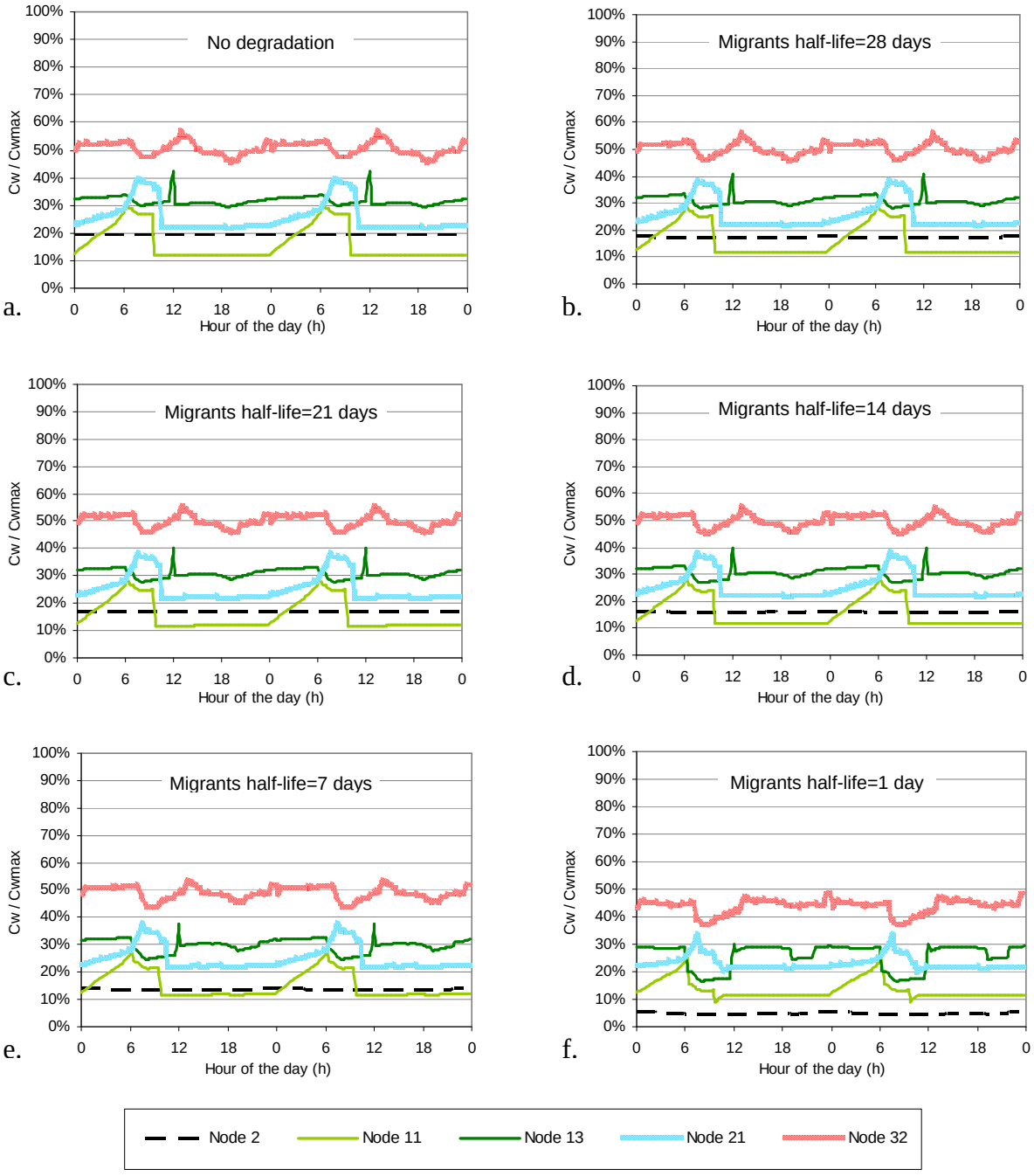

The six graphs represent the saturation level of species along the day at relevant nodes of the network and for different half-life of the species. Graph a corresponds to the case with no degradation, while graphs b, c, d, e and f show the same results with migrant half-lives of 28 days, 21 days, 14 days, 7 days and 1 day, respectively. In this case, the migrant's diffusion coefficient in the water is 10^{-10} m^2/s. If one considers antioxidants such as Irganox 1010 or Irgafos 168 then the concentration of species in the PE matrix is about 2 g/kg and their partition coefficient at the interface around $1.55*10^{-4}$, leading to a saturation concentration of 310 µg/L.

Simulations results for "Net 1": effect of degradation on the migrant concentration along the day for $D_{w,i}$ = 10^{-9} m^2/s

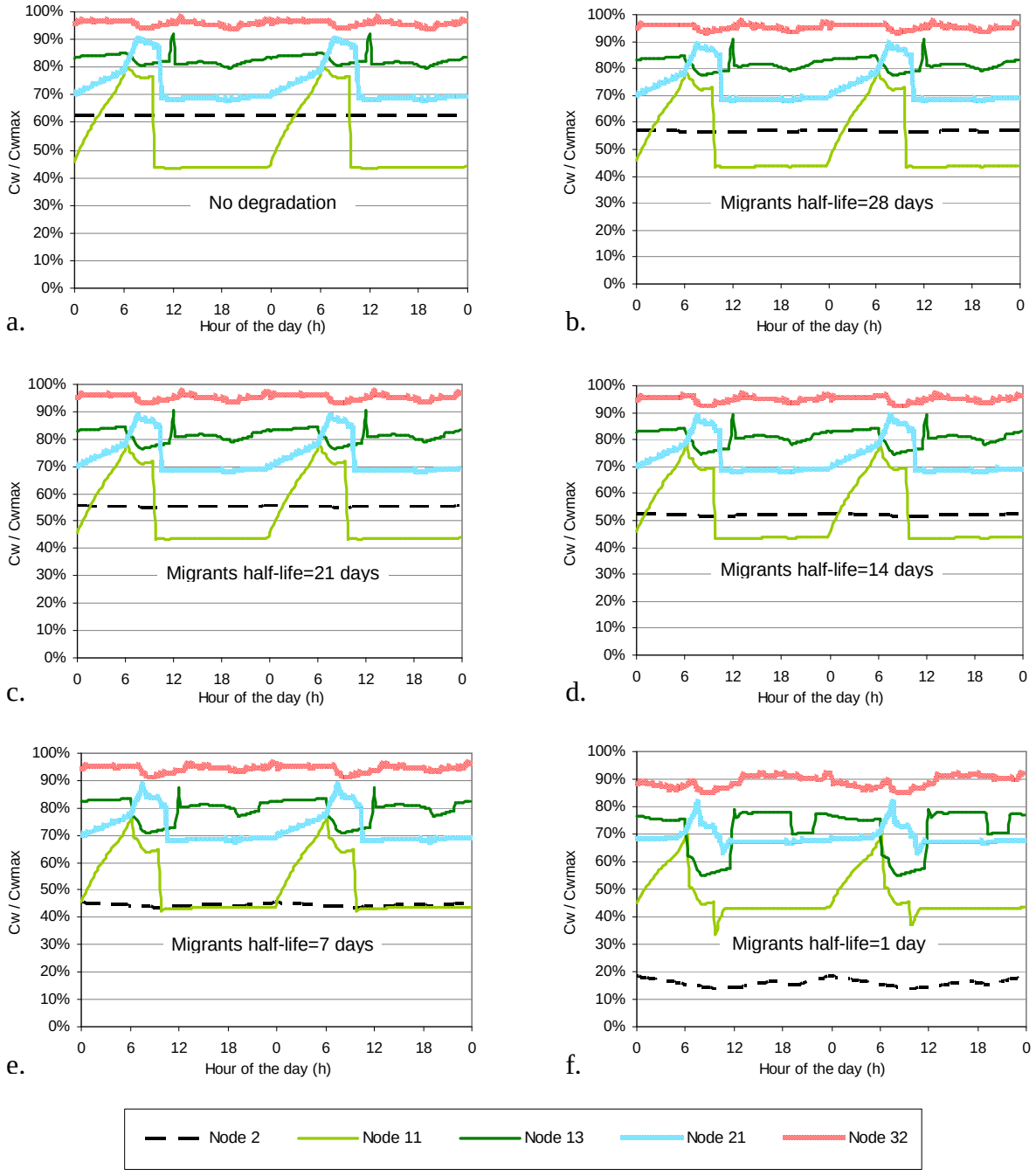

The six graphs represent the saturation level of species along the day at relevant nodes of the network and for different half-life of the species. Graph a corresponds to the case with no degradation, while graphs b, c, d, e and f show the same results with migrant half-lives of 28 days, 21 days, 14 days, 7 days and 1 day, respectively. In this case, the migrant's diffusion coefficient in the water is 10^{-9} m^2/s. If one considers antioxidants such as Irganox 1010 or Irgafos 168 then the concentration of species in the PE matrix is about 2 g/kg and their partition coefficient at the interface around $1.55*10^{-4}$, leading to a saturation concentration of 310 µg/L.

Appendix 6. Modelling work: details concerning "Net 3"

Characteristics of the study network "Net 3"

The data presented here are conversion into SI units of the data available in the EPANET model. The number of inhabitants is computed for an average consumption of 160 L/d/cap.

Link ID	Start Node	End Node	Length (m)	Diameter (mm)
20	3	20	30	2,515
40	1	40	30	2,515
50	2	50	30	2,515
60	River	60	375	610
101	10	101	4,328	457
103	101	103	411	406
105	101	105	774	305
107	105	107	448	305
109	103	109	1,201	406
111	109	111	610	305
112	115	111	354	305
113	111	113	512	305
114	115	113	610	203
115	107	115	594	203
116	113	193	506	305
117	263	105	831	305
119	115	117	664	305
120	119	120	223	305
121	120	117	570	305
122	121	120	625	203
123	121	119	610	762
125	123	121	457	762
129	121	125	283	610
131	125	127	988	610
133	20	127	239	508
135	127	129	274	610
137	129	131	1,975	406
145	129	139	838	203
147	139	141	625	203
149	143	141	427	203
151	15	143	503	203
153	145	141	1,070	305
155	147	145	671	305
159	147	149	268	305
161	149	151	311	203
163	151	153	357	305
169	125	153	1,390	203
171	119	151	1,055	305
173	119	157	634	762
175	157	159	887	762
177	159	161	610	762
179	161	163	131	762
180	163	164	46	356
181	164	166	149	356
183	265	169	180	762
185	167	169	18	203
186	187	204	30	203
187	169	171	387	762
189	171	173	15	762
191	271	171	232	610
193	35	181	9	610
195	181	177	9	305
197	177	179	9	305
199	179	183	64	305
201	40	179	363	305
202	185	184	30	203
203	183	185	155	203
204	184	205	1,381	305
205	204	185	404	305

Link ID	Start Node	End Node	Length (m)	Diameter (mm)
207	189	183	411	305
209	189	187	152	203
211	169	269	197	305
213	191	187	780	305
215	267	189	375	305
217	191	193	158	305
219	193	195	110	305
221	161	195	701	203
223	197	191	351	305
225	111	197	850	305
229	173	199	1,219	610
231	199	201	192	610
233	201	203	37	610
235	199	273	221	305
237	205	207	366	305
238	207	206	137	305
239	275	207	436	305
240	206	208	155	305
241	208	209	270	305
243	209	211	369	406
245	211	213	302	406
247	213	215	1,306	406
249	215	217	506	406
251	217	219	625	356
257	217	225	475	305
261	213	229	671	203
263	229	231	597	305
269	211	237	634	305
271	237	229	241	203
273	237	239	155	305
275	239	241	11	305
277	241	243	671	305
281	241	247	136	254
283	239	249	131	305
285	247	249	3	305
287	247	255	424	254
289	50	255	282	254
291	255	253	335	254
293	255	251	335	203
295	249	251	442	305
297	120	257	197	203
299	257	259	107	203
301	259	263	427	203
303	257	261	427	203
305	117	261	197	305
307	261	263	107	305
309	265	267	482	203
311	193	267	357	305
313	269	189	197	305
315	181	271	79	610
317	273	275	680	203
319	273	205	197	305
321	163	265	366	762
323	201	275	91	305
325	269	271	393	203
329	61	123	13,868	762
330	60	601	0	762
333	601	61	0	762

Node ID	Demand (L/s)	Elevation (m)	Number of inhabitants connected to the node
River	-	67.1	-
Lake	-	50.9	-
1	-	40.2	-
2	-	35.5	-
3	-	39.3	-
10	-	44.8	-
15	39.1	9.8	21,123
20	-	39.3	-
35	103.3	3.8	55,770
40	-	40.2	-
50	-	35.5	-
60	-	0.0	-
601	-	0.0	-
61	-	0.0	-
101	16.1	12.8	8,672
103	11.3	13.1	6,081
105	11.4	8.7	6,180
107	4.6	6.7	2,495
109	19.6	6.2	10,564
111	12.0	3.0	6,480
113	1.7	0.6	913
115	4.4	4.3	2,378
117	10.0	4.1	5,374
119	14.9	0.6	8,041
120	-	0.0	-
121	3.5	-0.6	1,900
123	-	3.4	-
125	3.9	3.4	2,082
127	1.5	17.1	806
129	-	15.5	-
131	3.6	1.8	1,951
139	0.5	9.4	269
141	0.8	1.2	450
143	0.5	-1.4	283
145	2.3	0.3	1,261
147	0.7	5.6	390
149	2.3	4.9	1,236
151	12.2	10.2	6,596
153	3.7	20.2	2,017
157	4.4	4.0	2,364
159	3.5	1.8	1,886
161	1.3	1.2	721
163	0.8	1.5	430
164	-	1.5	-
166	0.2	-0.6	119
167	1.2	-1.5	665
169	-	-1.5	-
171	3.3	-1.2	1,796
173	-	-1.2	-
		Sum	161,292

Node ID	Demand (L/s)	Elevation (m)	Number of inhabitants connected to the node
173	-	-1.2	-
177	4.9	2.4	2,656
179	-	2.4	-
181	-	2.4	-
183	-	3.4	-
184	-	4.9	-
185	2.2	4.9	1,171
187	-	3.8	-
189	9.1	1.2	4,927
191	6.9	7.6	3,739
193	6.0	5.5	3,256
195	-	4.7	-
197	1.4	7.0	778
199	10.1	-0.6	5,447
201	3.8	0.0	2,037
203	280.1	0.6	151,231
204	-	6.4	-
205	5.5	6.4	2,984
206	-	0.3	-
207	5.9	2.7	3,168
208	-	4.9	-
209	0.1	-0.6	40
211	0.7	2.1	396
213	1.2	2.1	636
215	7.8	2.1	4,209
217	2.0	1.8	1,106
219	3.5	1.2	1,886
225	1.9	2.4	1,041
229	5.4	3.2	2,930
231	1.4	1.5	752
237	1.3	4.3	713
239	3.8	4.0	2,037
241	-	4.0	-
243	0.4	4.3	198
247	6.0	5.5	3,213
249	-	5.5	-
251	2.0	9.1	1,103
253	4.6	11.0	2,489
255	3.4	8.2	1,844
257	-	5.2	-
259	-	7.6	-
261	-	0.0	-
263	-	0.0	-
265	-	0.0	-
267	-	6.4	-
269	-	0.0	-
271	-	1.8	-
273	-	2.4	-
275	-	3.0	-
		Sum	205,984

Connection between the river and the network

The river is connected to the network by a system of pipes in parallel. Either the water flows to the network directly through some pipes due to differences in water head, or the water can go through a pump that provides more pressurized water. The control of this parallel system is made by the level in the elevated tank 1, which is not far from node 169 and is thus relatively far from the river itself (cf. Figure 29). In the conditions used for this study, the water just flows by head gradient and is never pumped in the network and no impact due to the existence of this system were found on the simulations results.

Simulations results for “Net 3”: effect of degradation on the migrant concentration along the day for $D_{w,i}$ = 10^{-10} m^2/s

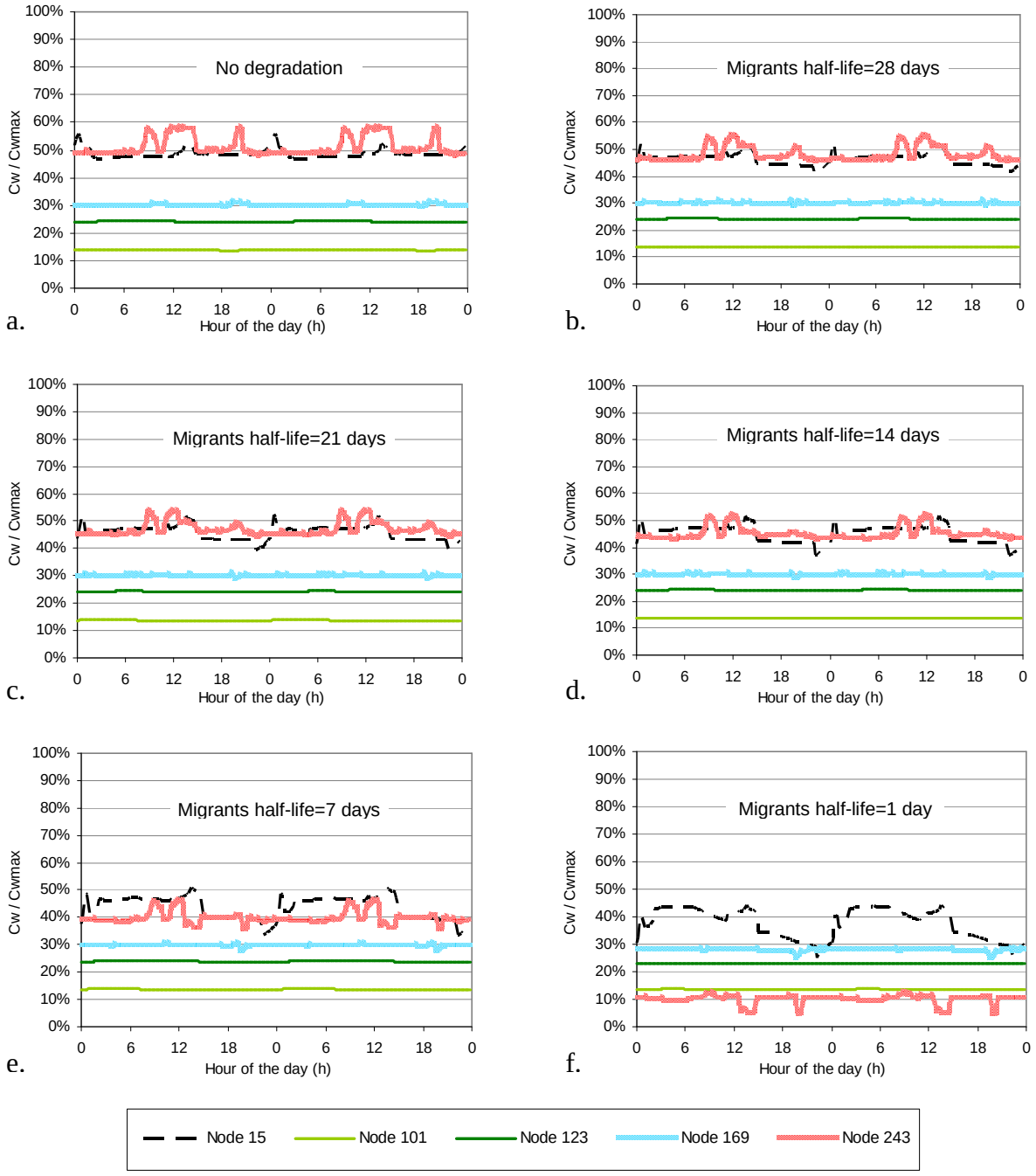

The six graphs represent the saturation level of species along the day at relevant nodes of the network and for different half-life of the species. Graph a corresponds to the case with no degradation, while graphs b, c, d, e and f show the same results with migrant half-lives of 28 days, 21 days, 14 days, 7 days and 1 day, respectively. In this case, the migrant’s diffusion coefficient in the water is 10^{-10} m^2/s. If one considers antioxidants such as Irganox 1010 or Irgafos 168 then the concentration of species in the PE matrix is about 2 g/kg and their partition coefficient at the interface around 1.55*10-4, leading to a saturation concentration of 310 µg/L.

Simulations results for "Net 3": effect of degradation on the migrant concentration along the day for $D_{w,i} = 10^{-9}$ m^2/s

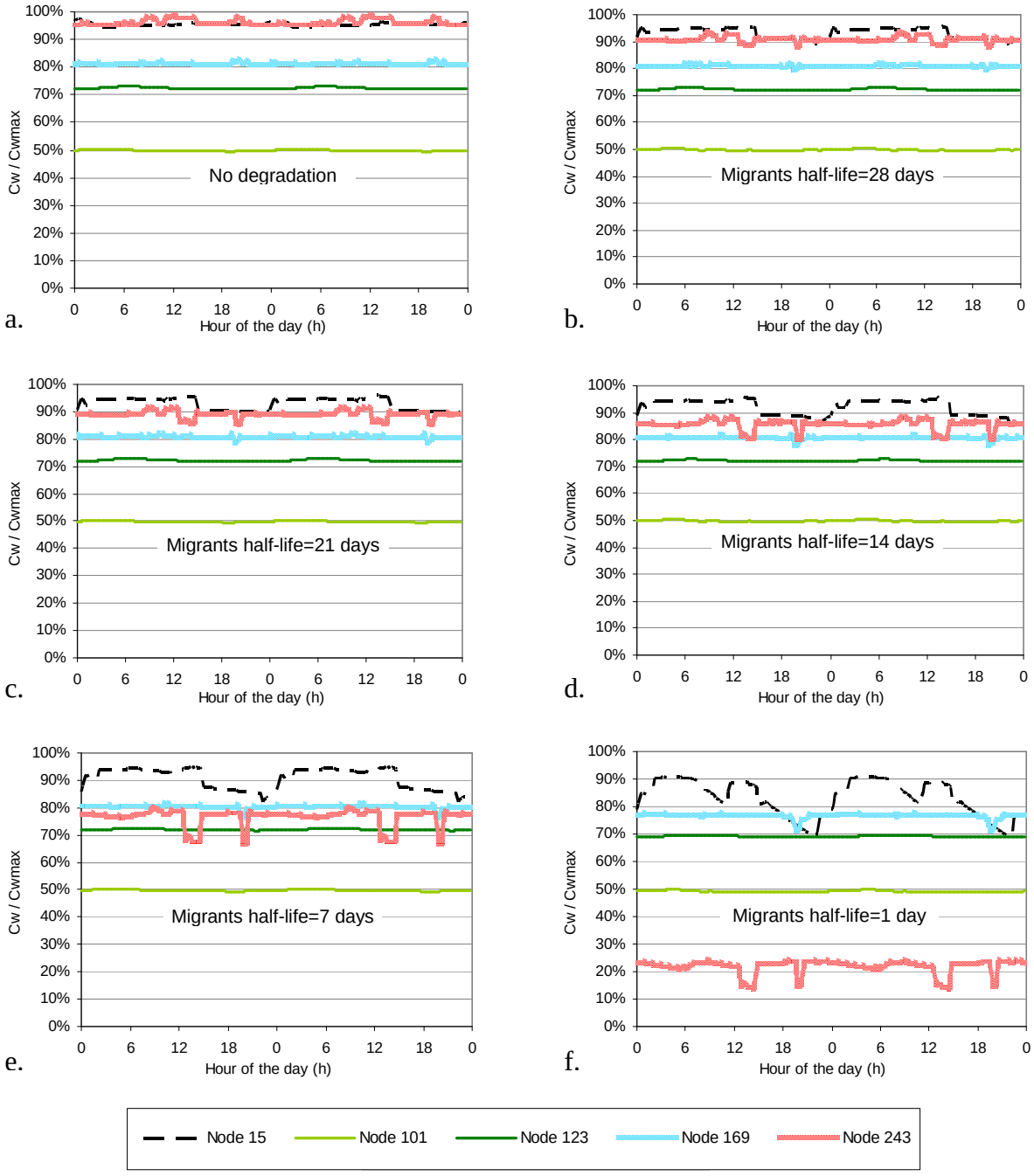

The six graphs represent the saturation level of species along the day at relevant nodes of the network and for different half-life of the species. Graph a corresponds to the case with no degradation, while graphs b, c, d, e and f show the same results with migrant half-lives of 28 days, 21 days, 14 days, 7 days and 1 day, respectively. In this case, the migrant's diffusion coefficient in the water is 10^{-9} m^2/s. If one considers antioxidants such as Irganox 1010 or Irgafos 168 then the concentration of species in the PE matrix is about 2 g/kg and their partition coefficient at the interface around 1.55*10-4, leading to a saturation concentration of 310 µg/L.